AN ABSTRACT OF THE THESIS OF

Yoji Ueda for the degree of Doctor of Philosophy in Animal Science. Presented on February 27, 2001. Title: Crystallin Proteolysis in Lens during Aging and Cataract Formation.

Abstract approved: Redacted for Privacy

Larry L. David

The major **purpose** of this research was to characterize partially degraded proteins appearing in the ocular lens during aging and cataract, and to identify the responsible proteolytic activities. This research is significant, because increased protein degradation is associated with lens opacification and cataract. Determining the sites where lens proteins become truncated and identification of the responsible proteases is important because this information could be used to develop anticataract agents, such as new protease inhibitors.

The **methods** used in this research include the application of several techniques employed in the field of proteomics. Two-dimensional electrophoresis (2-DE) was used to separate crystallins, the major proteins of the lens, and the modifications to these proteins were then determined by electrospray ionization mass spectrometry (ESI-MS). Lenses from mice of increasing age were used for these studies. Lp82 and m-calpain, the proteases hypothesized to cause the observed truncation of mouse crystallins, were purified from fetal calf lenses or expressed recombinantly, and their enzymatic properties compared. The cleavage sites produced in α-crystallin by Lp82 and m-calpain *in vitro* were then compared to truncated α-crystallins from normal rat lens, and rat lens with selenite-induced cataract.

The **results** included data showing that crystallins in mouse lenses underwent extensive truncation after 6-weeks of age that was associated with their insolubilization. Characteristics of purified Lp82 included: a lower calcium requirement for activation, a decreased sensitivity to the endogenous inhibitor calpastatin, and a greater resistance to autolysis than m-calpain. Analysis of truncated

α-crystallins isolated from both normal and cataractous rat lens indicated that Lp82 was more active in young rat lens than was m-calpain. Lp82 specifically removed 5 residues from the C-terminus of αA-crystallin. This αA degradation product was far more abundant in the lenses of young rats than was the m-calpain specific αA product missing 11 residues from its C-terminus.

In **conclusion**, this study showed that insolubilization of crystallins and cataract may result in animal lenses from uncontrolled crystallin degradation by the protease Lp82. This has led to a fundamental change in our view of experimental cataract formation, since activation of the protease m-calpain was previously believed to cause cataract.

Crystallin Proteolysis in Lens during Aging and Cataract Formation

By

Yoji Ueda

A THESIS

submitted to

Oregon State University

in partial fulfillment of
the requirements for the
degree of

Doctor of Philosophy

Presented February 27, 2001
Commencement June 2001

Doctor of Philosophy thesis of Yoji Ueda presented on February 27, 2001

APPROVED:

Redacted for Privacy

Major Professor, representing Animal Sciences

Redacted for Privacy

Chair of Department of Animal Sciences

Redacted for Privacy

Dean of the Graduate School

I understand that my thesis will become part of the permanent collection of Oregon State University libraries. My signature below authorizeds release of my thesis to any reader upon request.

Redacted for Privacy

Yoji Ueda, Author

Acknowledgement

I would like to express my sincere appreciation to my major professor, Dr. Larry L. David, for his generous support. The expertise I gained in his lab will allow me to pursue my career in the new field of proteomics.

I would also like to thank Dr. Neil E. Forsberg, Dr. Philip D. Whanger, Dr. Jeffrey J. Widrick, Dr. Gary E. DeLander, and Dr. J. Boone Kauffman for their advice and suggestions while serving on my committee.

I am grateful for the help and encouragement of my colleagues and friends: Dr. Thomas Shearer, Dr. Kirsten Lampi, Dr. Hong Ma, Dr. Chiho Fukiage, Deborah Kapfer, Majorie Shih, and Yung-Hae Kim.

I would like to recognize the Department of Animal Sciences of Oregon State University, and to the Department of Oral Molecular Biology at Oregon Health Sciences University for allowing me to learn and perform research in their excellent facilities.

Contribution of Authors

Marjorie Shih assisted preparation of rat lens proteins and contributed in electrophoresis separations. Dr. Melinda Duncan contributed in preparing mouse lenses, and writing of a manuscript. Recombinant Lp82 was cloned, expressed, and purified by Dr. Chiho Fukiage. Dr. Thomas Shearer was involved in writing of manuscripts.

Table of Contents

		Page
Chapter 1	Introduction	1
	Eye lens	1
	Crystallins	1
	Cataract	7
	Age related changes in human lens	8
	Animal models in lens research	10
	Calpain isoforms	14
	Lens protein breakdown by calpain	16
	Crystallin insolubilization	17
	Lens crystallin proteomics	18
	Basic proteomic approach	20
	Overview of manuscripts in chapters 2-4	22
Chapter 2	Lens Proteomics: The Accumulation of Crystallin Modifications in the Mouse Lens with Age	24
	Structured Abstract	25
	Introduction	26
	Methods	27
	Results	31
	Discussion	51
Chapter 3	Purification and Characterization of Lens Specific Calpain (Lp82) from Bovine Lens	56
	Summary	57
	Introduction	57

Table of Contents (*Continued*)

		Page
	Experimental Procedures	59
	Results	66
	Discussion	76
	Acknowledgement	80
Chapter 4	Comparison of the *In Vitro* and *In Vivo* C-terminal Cleavage Sites Produced by m-Calpain and Lp82 on Rat α-Crystallins	81
	Abstract	82
	Introduction	83
	Methods	84
	Results	88
	Discussion	102
	Acknowledgement	107
Chapter 5	Conclusions	108
	Bibliography	114

List of Figures

Figure		Page
1.1	Ribbon diagrams of typical β- and γ-crystallins.	5
2.1	Two-dimensional electrophoresis (2-DE) map showing the identities of the major soluble proteins in whole lenses of 1.5-week-old mice.	34
2.2	Changes in relative abundance of the major proteins of mouse lens during maturation.	35
2.3	Accumulation of modified crystallins in mouse lens during aging.	39
2.4	Identification of modified crystallins appearing with age in mouse lens.	39
2.5	Masses of phosphorylated α-crystallins appearing with maturation and increasing age in mouse lens.	46
2.6	Comparison of soluble lens protein profiles from two mouse strains by 2-DE.	50
3.1	Purification of m-calpain and Lp82 from fetal bovine lens.	63
3.2	SDS-PAGE of purification steps and immunoblot of purified m-calpain and Lp82.	64
3.3	Comparison of m-calpain and Lp82 enzymatic properties.	67
3.4	SDS-PAGE of lens crystallins incubated with m-calpain or Lp82.	71
3.5	Mass determination of cleaved crystallins by liquid chromatography/mass spectrometry.	72
3.6	Identification of truncated αA-crystallin *in vivo*.	75
4.1	Two-dimensional electrophoresis of soluble α-crystallins.	89

List of Figures (*Continued*)

Figure		Page
4.2	Deconvoluted mass spectra of unique αA-crystallin fragments produced *in vitro* by incubation with m-calpain and Lp82	92
4.3	Two-dimensional electrophoresis of insoluble protein from the nucleus.	95
4.4	Deconvoluted mass spectra of αA-crystallin fragments found in spot 1 and 2 of Fig. 4.3.	100
4.5	Calcium required for proteolysis of casein by recombinant Lp82 and m-calpain.	101

List of Tables

Table		Page
2.1	Mouse lens crystallin theoretical and measured mass.	32
2.2	Changes in % abundance of mouse crystallin subunits during lens maturation	37
2.3	Changes in % abundance of unmodified mouse crystallin subunits during lens aging	42
2.4	Identification of modified crystallins in 51-week-old mouse lens	43
4.1	Masses and identities of truncated α-crystallins produced by incubation with Lp82 or m-calpain	91
4.2	Masses and identities of truncated α-crystallins found in the insoluble fraction of rat lens nucleus.	97

Dedication

This dissertation is dedicated to my wife, Shiomi, who gave me her constant love and support, and to our children, Akeno Andrea and Alexander Ryo, for their trust in me.

Crystallin Proteolysis in Lens During Aging and Cataract Formation

Chapter 1

Introduction

Yoji Ueda

Department of Animal Sciences

Eye lens

The eye lens is located behind the iris, separating the anterior and posterior chambers of the eye. The lens has an important role in providing a proper refraction to focus images from the outside world to the retina. A well organized cellular and subcellular lens structure is critical to maintain the clear transparency of the lens.

The lens is composed of two main cell types. A single layer of epithelial cells covers the anterior surface. Epithelial cells are mitotically active and continually grow toward equatorial region of the lens where the cells elongate to form fiber cells. Fiber cells form the bulk of the eye lens and do not contain organelles such as cell nuclei, mitochondria, and ribosomes. The lack of these organelles likely prevents the synthesis of new protein, but allows light to pass through these cells without scattering it. Newly formed fiber cells are laid on top of older fiber cells, which do not turnover. Therefore, the fiber cells found in the most inner core of the lens were produced before the birth of the individual.

The fiber cells contain a high concentration of proteins, and 90% are the structural proteins called crystallins (Bloemendal, 1982). The structural formation and alignment of crystallins are the key to maintaining the proper refractive index and transparency of the lens.

Crystallins

Crystallins in the mammalian lens have been classified as α-, βH-, βL-, and γ-crystallins based on their separation by gel filtration chromatography (Harding, 1984). Of these, βH- and βL-are essentially comprised of the same proteins, and β- and γ-crystallins belong to the same superfamily, sometime referred to as βγ-crystallins (Piatigorsky, 1984).

α-crystallins

There are two α-crystallin genes situated on different chromosomes producing the subunits αA- and αB-crystallins. These crystallins have 57% sequence homology, and each have approximately 20 kDa mass. An alternative RNA splicing variant of αA has been found in rodent, but not in human, bovine or other mammalian species. This variant, called αA_{insert} contains an extra 23 amino acid residues (Hendriks et al., 1988). α-Crystallins in lens form large heterogeneous multimeric aggregates with an average mass of between 600 kDa to 900 kDa. Consisting of both αA- and αB-subunits, with the occasional presence of αA_{ins} subunit in rodent α-crystallin aggregates. The aggregate is made up of approximately 40 – 50 crystallin subunits, but its exact quaternary structure is still under heated discussion. A number of models suggest that the aggregate is three-layered, with variations in how each layer is formed (Groenen et al., 1994). Yet, other models propose a flexible micelle structure with the N-terminal region of each subunit situated close to the center of the aggregate (Augusteyn, 1998). It is also suggested that each native α-crystallin complex is made up of both αA and αB subunits with the ratio of approximately 3:1, respectively (Horwitz et al., 1999). This ratio may increase the stability of the α-crystallin complex.

α-Crystallin was thought to have a role only as a structural protein in lens until its sequence similarity to the small heat shock protein (sHsp) family was discovered (Ingolia and Craig, 1982). Also, identification of αB-crystallin (Bhat and Nagineni, 1989), followed by αA-crystallin (Kato et al., 1991) outside of the lens indicated that α-crystallins may also have extra-lenticular functions. In 1992, α-crystallin was shown to possess molecular chaperone activity common to sHsp family proteins (Horwitz, 1992). α-Crystallin was effective at preventing thermally induced aggregation of β- and γ-crystallins. Therefore, α-crystallin is considered to function as a house keeping protein in lens.

One major reason for the poor understanding of quaternary structure of α-crystallins is because of the heterogeneity of each α-crystallin subunit forming the aggregate. This has prevented crystallization of α-crystallin and analysis by x-ray diffraction. α-Crystallin subunits are known to undergo various post-translational modifications, such as phosphorylation, deamidation, glycation, oxidation, and proteolysis (reviewed by Groenen et al., 1994). α-Crystallin oligomers constantly undergo subunit exchange (Bova et al., 1997), thus readily incorporating modified crystallins. Although the effect of most of these protein modifications are unknown, proteolysis has been shown to decrease the chaperone activity of α-crystallins (Kelley et al., 1993; Takemoto, 1994). The C-terminus of α-crystallins is especially susceptible to the truncation since it is solvent exposed (Carver et al., 1992).

β/γ-crystallins

The 7 different subunits of β-crystallins are classified into two subfamilies: βA (acidic) and βB (basic), categorized as βA1, βA2, βA3, βA4, βB1, βB2, and βB3. βA1 and βA3 are derived from the same gene product and translated from the same mRNA but using different AUG initiation sites, leading to an extra 17 amino acids on the N-terminus of βA3. This results from the "leaky ribosomal scanning" mechanism triggered by the shortness of the 5' leader sequence on the βA1/A3 mRNA (Werten et al., 1999b). β-crystallin subunits are found in most mammalian lenses, though the expression level of each subunit depends on the species and age. For example, βA2-crystallin has not been found in human (Lampi et al., 1997). β-crystallins are found in lens as both homodimers and heterodimers, or oligomers of 50 kDa (βL-) to 200 kDa (βH-) (Slingsby and Bateman, 1990). This is in contrast to the closely related γ-crystallins which remain monomers.

The key to the transparency of the lens is that all β-subunits have similar structure and form symmetrical oligomers, allowing light to pass through the array of crystallins. Unlike α-crystallins, members of the β/γ family have been crystallized

and their structure determined (Bax et al., 1990). Each β- and γ-crystallin subunit consists of four "Greek Key" motifs made up of beta-sheet folds. Two motifs form one domain, thus each crystallin consist of two domains (Lubsen et al., 1988). The main difference between β- and γ-crystallin structure is the length of the peptide connecting the two domains. For β-crystallins, the connecting peptide is long, thus motifs are arranged so that two domains resemble heads of a "dumbbell". In β-

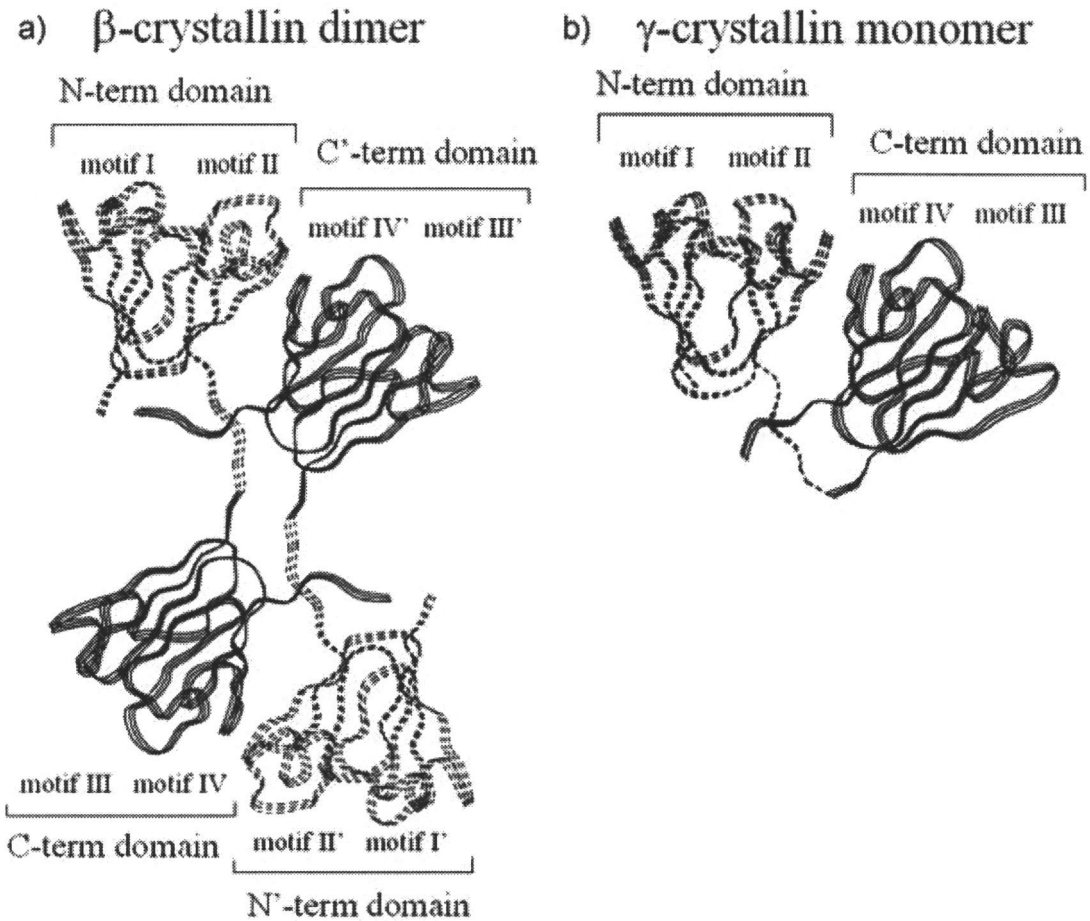

Figure 1.1. Ribbon diagrams of typical β- and γ-crystallins. N-terminal domains are shown as dashed lines, C-terminal domains as continuous lines. a) Dimeric βB2-crystallin. b) Monomeric γB-crystallin. Figure adapted from Kroone et. al. (1994).

crystallin dimmers, each N-terminal domain interacts with a C-terminal domain of its partner (Figure 1.1a;Lapatto et al., 1991). In contrast, the short connecting peptide in γ-crystallins result in the N-terminal domain of each protein interacting with its C-terminal domain intramolecularily (Figure 1.1b). Thus, a line bisecting a β-dimer through the connecting peptides would produce two γ-like structures.

All β-crystallins have N-terminal extensions of various length, but only basic β-crystallins have C-terminal extensions (Berbers et al., 1984). The interaction between β-crystallin subunits may also be stabilized by their N- and/or C-terminal extensions. These terminal extensions are susceptible to post-translational modifications, especially proteolytic truncations. When β-crystallins from rodents lose their N-terminal extensions, they become water insoluble (David and Shearer, 1993), suggesting that the extensions are required to maintain their native state.

There are 7 different forms of γ-crystallins: γA, γB, γC, γD, γE, γF, and γS, each coded for by separate genes. The mass of γ-crystallins range from 20 to 22 kDa. As described above, unlike α- and β-crystallins, these proteins exist as monomers in lens. γB-crystallin was the first crystallin whose three-dimensional structure was studied using X-ray crystallography (Blundell et al., 1981). γ-crystallins are found at high concentration in the nucleus (center) of the lens. Thus there is a developmental shift in crystallins gene expression during lens growth (Goring et al., 1992).

A unique γ-crystallin aggregation is triggered by lowering the temperature of lens, a phenomenon called cold cataract. When the lens is placed below body temperature, the nuclear region of the lens turns white due to phase separation of γ-crystallins (Siezen et al., 1985). Upon returning to normal room temperature, the cold cataract disappears. Although all γ-crystallins have relatively high sequence homology (49% - 90%), each subunit has different susceptibility to cold cataract. γS-crystallin, for example, may play an important role in suppressing the phase separation (Liu et al., 1998).

Unlike α- and β-crystallins, γ-crystallins do not have N- or C-terminal extensions. Thus, truncated forms of γ-crystallins are rare. However, Srivastava and Srivastava (1998) have reported age-related truncation of γ-crystallins due to cleavage with the connecting peptide, resulting in separation of the two domains. The significance and mechanism of this truncation have yet to be determined. It is likely that γ-crystallins also undergo other modifications. For example, their high sulfhydryl content makes γ-crystallins subject to oxidation, making them more susceptible to subsequent chemical attack (Kono et al., 1990).

Cataract

Cataract is generally defined as opacity in the lens. It becomes clinically significant when visual acuity is affected. A number of causes can lead to cataract, such as radiation, drugs, or nutritional imbalance. However, age-related cataract, termed senile cataract, is by far the leading cause of cataract in human. Cataract, if not surgically removed, is the leading cause of blindness in the world. Cataract removal is the most frequently performed surgery among persons over age 60 in the United States, and cost $3.4 billion each year (National Advisory Eye Council). More people will also develop cataract as the life expectancy increases.

Current cataract research mainly focuses on understanding cataract pathogenesis at the cellular and molecular level. Determination of the causes and mechanism of cataract formation may lead to development of an effective drug or method to prevent or delay cataract development. Determining the developmental mechanism of human senile cataract is especially difficult due to the confounding factors involved during the life-time of the individual. These include social status, life style, environmental conditions, and general health conditions of the individual (Taylor, 1999). However, the end results are similar: disturbed protein organization causing loss of lens transparency. Therefore, understanding of changes in lens

proteins due to post-translational modifications during cataract development is a crucial step in elucidating the mechanism of the disease.

Age related changes in human lens

Though the exact cause of senile cataract has not been pinpointed, two major changes occur in the cataractous lens: an increase in oxidation, and proteolysis of crystallins.

Oxidative damage is thought to be one of the major initial events leading to human senile cataract. Although the source of the oxidant is still unclear, H_2O_2 in conjunction with a loss of UV-filter compounds has been suggested to be the primary oxidant in aged lens (Spector and Garner, 1981; Truscott, 2000). Another factor in relation to oxidative damage is the decrease of reduced glutathione (GSH) in the aging lens (Rao et al., 1983). Glutathione is an antioxidant and reduces H_2O_2 and other reactive oxidative agents. In turn, oxidized glutathione (GSSG) is reduced by glutathione reductase. Therefore, either limited glutathione synthesis or loss of glutathione reductase activity can cause increased oxidative damage in lens. There is less glutathione reductase activity in the older fibers of the lens nucleus, than in cortex (outer region) (Zhang and Augusteyn, 1994). This may explain why nuclear opacity often occurs in aged lenses. Another mechanism that may explain the senile nuclear cataract is that a barrier develops between the cortex and nucleus of the aged lens, preventing transport of glutathione from the metabolically active epithelium/cortex to the nucleus (Truscott, 2000). The crystallin that may be most influenced by increased level of oxidative material is γ-crystallin due to its high cysteine content. γ-crystallin was shown to associate with membrane proteins in cataractous human lens (Kodama and Takemoto, 1988). This is presumably due to the disulfide interaction between γ-crystallin and membrane proteins during cataractogenesis.

The initial site for oxidative damage in lens may be the cell membranes of the lens epithelium. The lens epithelium is responsible for the majority of ion pumping in

lens (Delamere et al., 1998). Oxidative damage to epithelial membranes may lead to loss of ionic homeostasis, especially unregulated cellular calcium levels, which lead to further damage in lens fiber cells (Hightower, 1985).

A comparison of young and old human lens nuclear protein profiles by gel filtration chromatography shows specific changes in the crystallin composition. First, α-crystallin is reduced and there is an increase high molecular weight (HMW) protein. Second, there is a reduction in the γ-fraction, and third, a loss of resolution in the two β-crystallin peaks occurs (Pereira et. al., 1994; Ma et. al., 1998). α-Crystallin is the main component of the HMW fraction, although β- and γ-crystallins are also present (McFall-Ngai et al., 1985). Therefore, the HMW fraction may represent a transitional intermediate of denatured crystallins that are bound to α-crystallin due to its chaperone activity (Boyle and Takemoto, 1994). Srivastava et. al. (1996) determined that the HMW fraction consists of both intact and degraded α-, β-, and γ-crystallins. The same study also found that as much as 27% of the HMW fraction in the 60 – 80 year old lenses is composed of degraded crystallins. Once this HMW fraction forms it may eventually become water-insoluble and form aggregates large enough to scatter light and cause cataract.

Additional evidence also supported the hypothesis that fragmentation of crystallins may lead to cataract. A series of recent studies by Ma et. al. (1998c) and Lampi et. al. (1998) found extensive changes in the molecular weights of βB1 and βA3/βA1, indicating that these crystallins are truncated with age. One of the earliest truncation was seen in βB1 and βA3/A1, resulting in the removal of 15 and 22 residues from their N-termini, respectively. Interestingly, these cleavages of the N-termini of βA3/βA1- and βB1-crystallin occurred between amino acids N and P within the consensus site NPXP, indicating possible cleavage by the same protease. Two-dimensional SDS-PAGE gel also indicated increased deamidation of βB1, βB2, βA3/A1, and βA4-crystallins. Acidified forms of αA, and αB-crystallins also increased as the lens aged, as a result of both deamidation and phosphorylation. However, truncated forms of α-crystallins were not seen in the water-soluble fractions

of lens, possibly due to their insolubilization following truncation (Lund et al., 1996). Although, identification of modifications to γ-crystallins were limited to deamidation of γS-crystallin, Ma et. al. (1998c) suggested that the broadening of the γ-fraction during HPLC separation was due to both deamidation and disulfide cross-linking. A similar extensive analysis of the human lens water insoluble fraction remains to be performed. It is hypothesized that the major modification found in the soluble fraction of the lens are more extensive in the insoluble fraction. In Chapter 2, we have tested this hypothesis by showing accumulation of truncated crystallins in insoluble fraction rather than in soluble fraction of aged mouse lens.

Post-translational modifications of crystallins are part of normal aging process of human lens. The key question remaining to be answered in human senile cataract research is what are the differences between the post-translational modification in normal transparent aged lenses, and aged lens with cataract. These studies are difficult, because of the complexity of the post-translational modifications in human lens, and the scarcity of cataractous human lens tissue. Cataractous lenses are destroyed during cataract surgery. Although there is no animal model exactly mimicking human senile cataract, the use of animal lenses has been a great tool to gain insight into the mechanisms causing human cataract.

Animal models in lens research

Animal cataract models are important to obtain reproducible data and to perform tests that cannot be done with human subjects. A summary of different animal models of cataract are given below.

Lens studies using non-laboratory animals

Congenital cataracts in domestic animals used for agricultural purposes are uncommon. Experimentally induced cataract eyes from animals such as sheep

(Michaeli-Cohen et al., 1998), goat (Dada and Sindhu, 2000), and pig (van Vreeswijk and Pameyer, 1998) are primarily used as training models for cataract surgery by physicians or veterinarians. Bovine lenses are an excellent source of lens crystallins and other cellular components, because of their large size and routine availability. Bovine lenses have also been used in a number of studies investigating age-related changes in lens. Using 24 bovine lenses ranging in wet weight from 0.17 g to 3.0 g (corresponding to about 7 month prenatal gestation and 190 month postnatal, respectively), Pierscionek and Augusteyn (Pierscionek and Augusteyn, 1988) were able to investigate the detailed developmental and aging changes of lens proteins. In their study, α-crystallin consistently represented 50% of the protein synthesized by the fiber cells, though the major portion of α-crystallin found in insoluble fraction was post-translationally modified. γ(A-F)-crystallins synthesis was found to be active before birth, however it ceased shortly after birth, at which time γS-crystallin synthesis increased. They also observed increased expression of a β-crystallin, presumably βB2, after birth. In a different study, bovine lens proteins were used to demonstrate that the water-insoluble protein aggregate found in the lens was not an artifact produced by homogenization (Ortwerth and Olesen, 1989). Two-dimensional SDS-PAGE gel analysis of bovine β-crystallins from young and old lenses showed a similar breakdown pattern to that occurring in human crystallins (Shih et al., 1998).

Cataracts have also been studied in common household animals. Feline cataract is very rare in domesticated cats, but congenital cataract is commonly seen in pure bred canines. Pathophysiological studies of the development of hereditary cataracts in number of pure bred dogs was studied in the 80's (Narfstrom, 1981; Barnett and Startup, 1985). Dogs can also develop cataract due to a high sugar diet, due to the activity of lens aldose reductase and accumulations of sugar alcohols in lens (Sato et al., 1998). Small animals such as guinea pigs and rabbits are also frequently used in cataract research, however rats and mice are by far the most used lab animals for cellular and molecular cataract research.

Mouse cataract models

The mouse is an especially useful species to study cataract due to its ease of genetic manipulation. In addition to several strains of mice known to develop congenital cataract due to spontaneous mutations, genetic manipulation techniques have also allowed production of numerous mouse strains developing cataract. Some of the genes that have been altered for lens research include: SPARC (Gilmour et al., 1998) and alpha 3 connexin (Gong et al., 1999) knockout mice, as well as transgenic mice over-expressing a large variety of proteins including truncated fibroblast growth factor receptors (Stolen and Griep, 2000), ΔfosB (Kelz et al., 2000), and HIV protease (Mitton KP, 1996). Mice carrying mutations in transcription factors are especially useful tool in developmental biology. Since some of these mutants develop cataract as the result of interference in the transcription of certain developmentally regulated genes (Duncan et al., 2000), they are useful model for human congenital cataract. For example, mutations in the genes coding for the transcription factors Pax 6 and *Shh*, cause ocular deformities that are also found in human (Jordan et al., 1992; Belloni et al., 1996).

Mutations to single crystallin genes are sufficient to induce cataract formation. For example, the mutation causing cataract in the spontaneous mutant mouse *lop18* was localized to a missense mutation in αA-crystallin gene (Chang et al., 1999). This mutation causes severe opacification of the lens at about three weeks of age, but it does not effect eye development. The exact mechanism of how the replacement of one amino acid in αA-crystallin leads to cataract formation is still unclear, however, the mutation may affect the tertiary and quaternary structure of αA-crystallin and effect its chaperone function. Another strain of mice containing mutant crystallin, called the Philly mouse, develops cataract approximately 6 weeks after birth. This mouse carries a mutation that causes abnormal βB2-crystallin to be accumulated in HMW fraction instead of β-fractions (Russell and Chambers, 1990). The mutation resulted from a deletion in βB2-crystallin mRNA, leading to a loss of 4 amino acids

near the C-terminus (Chambers and Russell, 1991). This deletion causes an unstable βB2 tertiary structure, and inappropriate interaction with other crystallins, causing aggregation. Genetic analysis of another mouse cataract mutant (Cat2), with three variant forms, showed mutations in three different γ-crystallin genes (Klopp et al., 1998). One mutation lead to a single amino acid substitution in γA-crystallin. The other mutations caused premature termination of γB- and γE-crystallin synthesis, resulting in proteins over 30 amino acids shorter than the wild type. Analysis of mutant mice indicates the importance of intact crystallins in maintaining lens transparency. Modifications to many crystallin appears sufficient to cause lens opacifications.

As noted before, mouse is an excellent model to study protein function, especially during development. Genetic alteration allows pinpointing functional sites of proteins by deletion of certain regions of the genes.

Rat cataract model

There are numerous ways to induce cataract in rat lens. These include radiation, free radicals, nutritional deficiency, chemical exposure, and antibiotics (Bloemendal et al., 1996). These experimentally induced cataract rat lenses are especially useful in identifying common biochemical events, or post-translational modifications, leading to cataractogenesis.

Selenite cataract has been used many years as a model for nuclear cataract. Selenite cataract is usually produced by a single subcutaneous injection of sodium selenite into rats of 10 – 14 days of age. A nuclear cataract usually forms within 4-6 days after injection. A detailed mechanism of selenite induced cataract formation has been elucidated (Shearer et al., 1997). Briefly, the outer most lens cell layer, the epithelium, undergoes various metabolic changes following selenite injection. One such change is the loss of calcium homeostasis, possibly due to oxidative damage to the calcium ATPase pump or ion channels caused by direct interaction with selenite.

Selenite is known to catalytically oxidize sulfhydryl groups (Tsen and Tappel, 1958). Interestingly, the free calcium level increases mainly in the nucleus, reaching concentrations over 100 μM (Hightower et al., 1987). This level of calcium is sufficient to activate the calcium-dependent protease m-calpain which truncates the C- and N-terminal extensions of α- and β-crystallins, respectively (David et al., 1993; Kelley et al., 1993). Truncated crystallins may have unstable quaternary structure which lead to their insolubilization and precipitation (Shearer et al., 1995).

Calcium activated proteases are involved in not only selenite induced cataract, but a number of other experimentally induced cataracts in rats. These include the cataracts induced by galactose (Azuma et al., 1990), diamide (Azuma and Shearer, 1992), the hypocholesterolemic drug U18666A (Chandrasekher and Cenedella, 1993), and the hereditary Shumiya cataract (Inomata et al., 1997).

Thus, it is hypothesized that opacification of lens occurs by a common pathway regardless of the initiating factor. One of the last steps of opacification may be crystallin breakdown and insolubilization which leads to opacification.

Calpain isoforms

Calpains are cysteine proteases and the name originally indicated their calcium requirement for activation. Two major classes of calpains are known: ubiquitous calpains and tissue specific calpains. Ubiquitous calpains are widely distributed in animal tissues. Two major isoforms of ubiquitous calpains found in mammalian tissues are μ- and m-calpains, initially differentiated by their requirement for micromolar and millimolar amounts of Ca^{2+} for activation (Mellgren, 1980). Both isoforms are composed of a 80 kDa catalytic subunit (large subunit) and a common 30 kDa subunit (small subunit). The large subunit is divided into four structures designated as domains I, II, III, and IV. Domain II is the protease domain shearing significant homology with other cysteine protease families (Berti and Storer, 1995). Domain IV is also called "the calmodulin-like" domain and contains EF-hand

structures for calcium binding. Domains I and III are not highly conserved and their functions are still unclear. However, autolysis of domain I (N-terminal region) is found to increase the Ca^{2+} sensitivity (Suzuki et al., 1981). The small subunit is divided into domains V and IV'. Domain V is suggested to be the binding site for phospholipid, which is an important cofactor activating calpains (Imajoh et al., 1986). Domain IV' is thought to be responsible for the interaction with the large subunit (Imajoh et al., 1987).

Skeletal muscle specific calpain, p94, was the first tissue specific calpain discovered (Sorimachi et al., 1989). Other than being tissue specific, p94 has a number of unique features: 1) It does not associate with a 30 kDa subunit, 2) it does not require elevation of calcium for its activation, 3) it contains three inserted sequences, NS, IS1, and IS2, that are not found in μ- and m-calpains, and 4) it autolytically degrades rapidly and loses catalytic activity. The last feature is suspected to result from the presence of the inserted sequences (Sorimachi et al., 1993b). Because the enzyme is lost rapidly as soon as it is translated in muscle, it was thought for sometime to have no function. However, p94 was the first calpain isoform to be associated with human disease. Mutation in p94 are associated with limb-girdle muscular dystrophy type 2A, also known as LGMD2A (Richard et al., 1995). DNA sequence analysis of LGMD2A patients strongly suggest that the loss of p94 function is responsible for the disease. However, because of the rapid autodegradation of p94, characterization has been only possible using recombinantly expressed inactive p94.

Following the discovery of p94, several other tissue specific calpains were identified in the last decade. Some of these include stomach-specific calpains (nCL-2 and 2')(Sorimachi et al., 1993), digestive organ-specific calpain (nCL-4)(Lee et al., 1998), and lens specific calpain called Lp82 (Ma et al., 1998a). Lp82 is actually a splice variant of p94, containing an alternative exon 1 resulting in an unique N-terminus, and missing IS1 and IS2 sequences. Although the significance of the alternative N-terminus is unknown, the absence of insertion sequences likely contributes to the stability of Lp82. Lp82 can be detected by immunobloting in young rat lens, and the enzyme has been partially purified from this tissue (Ma et al., 1998b).

The expression of Lp82 at both the mRNA and protein levels are higher than that of m-calpain in young mouse lenses and nearly equal in young rat lens (Shearer et al., 1998; Ma et al., 1999). Although μ-calpain is present in lens, its activity is considered to be very low in rodents and other species (Yoshida, 1985). Therefore, Lp82 is likely to have a role in lens, but its enzymatic characteristics are yet to be determined. For example, Lp82 appears to be calcium activated, but its minimum requirement remains unknown.

Lens protein breakdown by calpain

There are number of proteases that have been identified in the lens. Some proteases are specifically expressed in epithelial cells. For example, caspases are expressed mainly in epithelial cells, assisting in cell differentiation (Ishizaki et al., 1998). Proteasome is also expressed in lens epithelial cells and is involved in lens development and differentiation (Andersson et al., 1998; Cai et al., 1998), but it is unlikely to have an active role in fiber cells. In fiber cells, a number of aminopeptidases are found to retain their proteolytic activity (Sharma and Kester, 1996). These exopeptidases are important in clearing peptide fragments from the lens cells. Additional proteases have recently been identified in the lens, but their identities and functions have yet to be clarified (Sharma et al., 1996; Srivastava et al., 1999), leaving calpain as the only well defined endopeptidase in fiber cells.

Ever since its discovery in the lens, m-calpain has been considered to be a major player in the development of cataract (Yoshida et al., 1984b). Increases in free calcium levels during selenite-induced cataract activate m-calpain (Hightower et al., 1987), and cataract formation was reduced by the synthetic calpain inhibitor E64 *in vitro* and *in vivo* (Azuma et al., 1991). Although, a number of experiments showed a similar breakdown pattern in crystallin fragments produced by m-calpain *in vitro* and crystallin fragments in cataract lens (David et al., 1993; Kelley et al., 1993), there are two factors that make m-calpain activation in lens questionable. First, m-calpain

requires at least 0.1 mM calcium to be activated where as the normal lens cytosolic calcium concentration is below 0.2 μM. Second, calpastatin, the endogenous inhibitor of calpain, interferes with both m- and μ-calpain activity. The discovery of Lp82 suggest that this calpain isoform may be more active than m-calpain in lens. It is possible that previously reported *in vivo* crystallin breakdown related to maturation and cataract formation may be the result of Lp82 instead of m-calpain. Thus, a closer examination is necessary to determine which proteolytic activity predominates in the lens. It is hypothesized that there are enzymatic differences between Lp82 and m-calpain which will allow identification of the active protease. Unfortunately, Lp82 is not present in human lens (Fougerousse et al., 2000), however, the basic mechanism of protein insolubilization triggered by protease activation could still be a key event leading to cataract in humans. As yet undiscovered isoforms of calpain may be responsible for crystallin fragmentation in human lens.

Crystallin insolubilization

One model for insolubilization of crystallins is that their proteolysis leads to aggregation and precipitation. As mentioned before, the terminal extensions of α- and β-crystallins have a critical role in keeping these proteins stabilized and soluble. Degradation of C-terminal extensions of α-crystallins results in a decrease in their chaperone activity that protects other crystallins from denaturation (Kelley et al., 1993; Takemoto, 1994). For β-crystallins, the terminal extensions may have two functions. One function is to maintain the solubility of β-crystallins (David and Shearer, 1993), the other is to facilitate oligomer formation (Hope et al., 1994; Werten et al., 1999a).

Direct evidence for proteolysis of crystallins causing precipitation was shown by Shearer et. al. (1995). In that study, light scattering of lens protein homogenates from rats was induced by activation of endogeneous calpain through the addition of excess calcium. Accumulation of truncated α- and β-crystallins in the insoluble

protein fraction was shown by two-dimensional gel electrophoresis (2-DE). Light scattering induced by calpain degradation of α- and β-crystallins was also later shown in mouse (Fukiage et al., 1997), and guinea pig lens crystallins (Fukiage et al., 1998). Thus, these experiments showed proteolysis of crystallins induces protein precipitation in rodent species. However, precipitation of calpain treated crystallins from rabbit, cow, and human lens was not successful. The reason they were not susceptible to precipitation in these species is unknown, since the extent of crystallin breakdown was similar to that of mouse and rat. The lack of precipitation may be related to the proportion of individual crystallin subunits in each species. It may also be possible that slight differences in their amino acid sequences between species leads to increased solubility of β-crystallins following their proteolysis by calpain. Crystallins from various species may also be cleaved differently by calpains. Thus, analysis of crystallins present in different species, to determine their relative proportions, comparison of their breakdown patterns *in vivo*, and measurement of their calpain cleavage sites *in vitro* would be useful.

Lens crystallin proteomics

To understand the organization and function of any cell in the body, the study of gene expression and protein content is vitally important. This is especially true when a researcher is assessing the cells' response to certain chemicals or environmental changes. Although analysis is possible by measuring mRNA expression, the correlation between mRNA expression and protein abundance can be low (Gygi et al., 1999). Additionally in the lens, proteins are only actively synthesized in epithelial cells and the outer layers of fiber cells, leaving the bulk of lens cells without active protein synthesis. Thus, correlation between mRNA levels and protein content in whole lens would be very low. Furthermore, post-translational modifications to crystallins would not be predicted by analysis of gene expression.

Therefore, protein analysis is essential in lens research, and introduction of a proteomic approach will greatly enhance progress in this field.

The word "proteome" refers to the PROTEins expressed by the genOME of a cell or tissue (Wilkins et al., 1996). The primary aim of genome projects is sequencing the entire genome of organisms. The initial goal of proteome projects is to catalogue all proteins expressed by a cell or tissue. While the genome of an organism is static, the proteome of an organism is dynamic and constantly changing depending on the tissue, stage of development, or environmental stress, etc. Thus, proteomics is much more complex than genomics. A "standard" profile of the given cell or tissue is always changing.

Although the term proteomics is relatively new, the techniques routinely used today are the result of improvements in techniques that have existed for at least 25 years, such as two-dimensional protein gel electrophoresis (2-DE)(O'Farrell, 1975) and biological mass spectrometry (Shemyakin et al., 1966). The key improvements to these techniques include: reproducibility of 2-DE, increased accuracy of mass analysis, the availability of DNA and protein sequence databases, and automation. These modifications are continually being advanced, helping researchers obtain more data in less time.

In lens research, the 2-DE technique has been especially useful. Since more than 90% of mammalian lens protein is composed of 17 crystallins, the 2-DE protein profile would be expected to be relatively simple (Voorter et al., 1990). However, the accumulation of numerous post-translational modifications in crystallins causes the appearance of many new species on 2-DE gels (Huang et al., 1990). Standard techniques, such as column chromatography, are incapable of resolving these species. So far, 2-DE provides the only practical mean to simultaneously resolve all these species.

Once modified crystallins are resolved by 2-DE the only way to confirm the identity of modified crystallin and determine their specific protein modifications was by either immunoblotting (Chandrasekher and Cenedella, 1993), or Edman sequencing of proteins transferred to membranes (Datiles et al., 1992). The determination of

molecular weight was limited to the nearest 1000 mass units through the use of protein standards of known mass run simultaneously on the same gel.

Mass spectrometry does not have this limitation, because it is capable of determining the mass of a protein with an accuracy of 0.01% or better. The technique has become a powerful tool in lens research over last 10 years. It has been especially useful in rapidly identifying lens proteins and confirming their sequences (David et al., 1996; Ma et al., 1998c). Mass spectrometry is also a powerful method to determine modifications such as disulfide bonds, deamidation, and methionine oxidation.

Recently, the 2-DE and mass spectrometric techniques have been merged together. The extreme sensitivity of mass spectrometric analysis allow analysis of proteins separated by 2-DE (Lampi et al., 1998; Lampi, 2000; Colvis et al., 2000). Still, lens proteomics is in its initial stage, requiring more fundamental work, such as producing standard lens 2-DE databases, actively exchanging data between laboratories, and developing better methods to detect modifications of crystallins separated by 2-DE.

Basic protemic approach

The first step in proteome analysis is to separate the complex mixture of proteins in cells. 2-DE is by far the most practical, commonly available method to separate thousands of protein at once. Until recently, 2-DE gels were more art than science and were virtually non-reproducible between individual laboratories. Recent advances in the application of immobilized pH gradient gels in the first dimensional separation of 2-DE contributed to the production of more reproducible 2-DE gels (Fichmann, 1999). Traditionally, Coomassie blue staining has been used to visualize proteins on 2-DE gels, but more sensitive stains such as silver stain, zinc-immidazole negative stain, and fluorescent stain are now available (Steinberg et al., 1996; Matsui et al., 1999; Rabilloud, 1999). Once protein spots are visualized, each spot is cut out and the protein digested by a protease, such as trypsin, directly in the gel. Then, the

fragmented peptides diffuse out of the gel matrix and are available for mass analysis by mass-spectrometry (MS).

Although a number of different ionization methods for peptide mass analysis are available, electrospray ionization (ESI) was used in the present study. One of the biggest advantage of ESI-MS is that it allows on-line analysis of samples separated by high performance liquid chromatography (HPLC). Thus, tryptic peptides produced from in-gel digest are first separated by HPLC and analyzed by MS as they elute from the chromatography column. The masses of ionized peptides are then recorded for further analysis.

After cataloging the peptide masses, unknown proteins are identified by comparing the measured peptide masses with the theoretic masses of tryptic peptides of proteins in databases available online. It is possible, but unlikely, that more than two unrelated proteins share tryptic peptides with similar masses. In this case, further detailed information is obtained from each peptide using tandem mass spectrometry that is capable of producing amino acid sequence data for each peptide. The amino acid sequence data then unambiguously identifies the protein.

Mass spectrometry not only identifies the unknown proteins, it is also a powerful tool to determine post-translational modifications in proteins. Any change in the mass of certain peptides indicates a modification has occurred. However, unless recovery of peptide fragments is complete peptides containing the modification may be missed. Therefore, a useful alternative strategy to determine the post-translational modification of the protein is measuring its whole mass. However, current methods for eluting protein out of 2-DE gels are limited due to poor recovery, resulting in insufficient material to analyze by mass spectrometry (le Maire et al., 1993; Nakayama et al., 1996). Improvements in the efficiency of recovering whole proteins from 2-DE gels would greatly facilitate the analysis of post-translational modification in proteins.

Overview of manuscripts in chapters 2-4

Although cataract is not life-threatening in nature, its emotional and economical impact is enormous. Understanding the basic mechanism of protein insolubilization associated with crystallin degradation is one of the many steps in finding a way to prevent or delay cataract development. There is currently no effective drug treatment to slow cataract development.

Animal cataract models have provided evidence that crystallin truncation may lead to cataract. However, the time course that these truncations occur during aging of common species used in cataract models, the specific sites crystallins become truncated, and the proteases responsible for this truncation need to be clarified. The results presented in the manuscripts in chapters 2-4 provide this information.

In chapter 2, detailed proteome maps were created for mouse lens. A series of 2-DE gels of proteins from mouse lenses of increasing age were produced. The effect of lens aging on protein composition was investigated by identifying each protein spot by mass spectrometry, and performing image analysis to determine their relative abundance. Evidence for extensive truncation of α- and β-crystallins was determined, and these truncated crystallins were selectively found in the water insoluble fraction of the lens. The mouse lens 2-DE maps produced in this study will benefit other lens researchers, who can use them as baseline data to identify modified crystallins unique to cataracts. The project presented in chapter 3 is a logical extension of the work in chapter 2. We next focused on determining the characteristics of Lp82, the enzyme likely responsible for the degradation of crystallins observed in mouse lens.

In animals, especially rodents, m-calpain has been implicated as the primary protease involved in aging and cataract formation. However, the recent discovery of the lens specific protease Lp82 suggested that this protease may be more active in lens than m-calpain. Therefore, the enzymatic properties of both Lp82 and m-calpain were compared. Chapter 3 describes the very first purification of Lp82 using bovine lenses as a tissue source. Detailed comparisons of Lp82 and m-calpain were performed to determine calcium requirements for activation, susceptibility to various inhibitors, and

substrate specificity. We found that Lp82 degraded the endogenous substrate αA-crystallin at a site identical to where the protein is cleaved *in vivo*. These results not only produced a new protocol that other investigators can use to purify Lp82, they also provided direct evidence that Lp82 is more active in lens than m-calpain. This finding led to the final project of thesis, which was a more detailed examination of the cleavage site specificity of Lp82 and m-calpain and comparison to *in vivo* cleavage sites in α-crystallins.

In chapter 4, the role of m-calpain and Lp82 in the *in vivo* production of α-crystallin fragments was investigated. This project required the development of a novel protocol to isolate proteins from 2-DE gels so that their masses could be accurately measured. The resulting data not only produced the most detailed analysis of α-crystallin modification to date, it provided strong evidence that Lp82, and not m-calpain, is responsible for producing the majority of fragmented crystallins in young rodent lenses.

These data have produced a significant change in the mechanism for cataract formation in experimental animals. They have altered the previous hypothesis that m-calpain is responsible for crystallin fragmentation and opacity in rodent lenses, and replaced it with the hypothesis that Lp82 is instead responsible.

Chapter 2

Lens Proteomics: The Accumulation of Crystallin Modifications in the Mouse Lens with Age

Yoji Ueda; Melinda K. Duncan; and Larry L. David

Department of Animal Sciences

Structured Abstract

Purpose: To identify modified crystallins associated with aging of lens and produce two-dimensional electrophoresis (2-DE) proteome maps of crystallins in mouse lens. Methods: Lens proteins from mice of increasing age or different strains were separated by either chromatography or 2-DE. Masses of whole proteins or tryptic peptides were analyzed by mass spectrometry. Changes in the abundance of individual crystallins were determined by image analysis of 2-DE gels.

Results: The measured masses of all known mouse crystallins, with the exception of γD and γF, matched the masses calculated from their reported sequences. Analysis by 2-DE indicated that most post-translational modifications took place after 6 weeks of age. Partially degraded crystallins, including βB1, βB2, βB3, βA3, αA, and αB, were found in greater proportion in the insoluble fractions. γ-crystallins A-F also became insoluble during aging. However, insolubilization of γ-crystallins was associated with a decrease in pI. Aging was also associated with increased phosphorylation of soluble αA and αB-crystallins, confirmed by mass measurements of these proteins eluted from 2-DE gels. Comparison of protein profiles between several strains of mice used to produce transgenic or knockout models of cataract indicated few differences, except for an additional acidic form of a γ-crystallin, possibly due to a polymorphism. Conclusions: These results suggest that partial degradation of α- and β-crystallins and increased acidity of γ-crystallins may cause insolubilization during aging. The 2-DE proteome maps of mouse lens proteins created here using immobilized pH gradients will be useful for comparison to maps of lens proteins of mice with cataracts so that cataract specific modifications may be identified.

Introduction

The transparency of eye lens is largely determined by the properties of crystallins, the structural proteins of the lens. Aging of normal lens leads to the accumulation of post-translationally modified proteins, because crystallins undergo very little turnover following synthesis (Young and Fulhorst, 1966). We hypothesize that these modifications may contribute to cataract by causing aggregation and insolubilization of crystallins. However, studying the role of crystallin modification in lens is complex, because many modifications are part of the normal maturation process. For example, site-specific proteolysis of β-crystallins in young lens may serve to initiate tighter packing of crystallins during lens maturation (David et al., 1994a; Lampi et al., 1998; Werten et al., 1999a). Evidence from experimental cataracts in young rats also suggests that opacity may result when this process becomes unregulated (David et al., 1994a). In contrast, cataracts in mature lenses may result from unique modifications that are not found in normal age-matched lenses.

The mouse is an especially useful species to test the role of crystallin modification in cataracts, because a large number of transgenic and knockout strains have been produced that develop cataracts. These include: the αA-crystallin (Brady et al., 1997), SPARC (Gilmour et al., 1998), alpha 3 connexin (Gong et al., 1999) knockout mice, as well as transgenic mice over-expressing a large variety of proteins including truncated fibroblast growth factor receptors (Stolen and Griep, 2000), transcription factors such as PAX6 (5a) (Duncan et al., 2000) or ΔfosB (Kelz et al., 2000), HIV protease (Mitton KP, 1996) and structural proteins (summarized by Bloemendal et al., 1996). In addition, a number of spontaneous mutant mouse strains have been identified that develop cataract. See the recent review by Graw for further information on murine models of congenital cataract (Graw, 1999).

Many studies have used two-dimensional electrophoresis (2-DE) to study protein modifications that take place in the mouse lens during aging and/or during cataractogenesis (Garber et al., 1984; Calvin et al., 1996; Mitton KP, 1996; Jungblut et al., 1998). However, the interpretation of the available data is hampered by the lack of

standardized 2-DE protein maps comparing mice of different ages. Furthermore, the precise protein modifications that occur with normal aging have not been systematically explored. Thus, in this study, reproducible mouse lens 2-DE maps were created for lenses of increasing age, and of different strains to serve as reference maps. Further, the molecular identity of the separated proteins was confirmed by mass spectrometry and a number of post-translational modifications were identified. In future studies, these data will facilitate the identification of specific modifications in cataractous lenses of mice.

Methods

Preparation of mouse lens

FVB/N mice (Taketo et al., 1991) were generated in house from a breeding stock obtained from Taconic Laboratories (Germantown, New York). C57BL/6 and ICR mice were obtained from Harlan-Spraque Dawley (Indianapolis, IN). CB6F1 mice were obtained from Charles River Labs (Wilmington, MA). The FVB/N and C57BL/6 strains were analyzed because they are derived from mice with widely different genetic backgrounds (Beck et al., 2000), and cells from these strains are commonly used to produce transgenic mice to study lens biology (Wawrousek et al., 1990; Reneker et al., 2000; Stolen and Griep, 2000). Descriptions of these and other inbred strains of mice can be obtained at a web site maintained by the Jackson Laboratory (Bar Harbor, Maine; <http://www.informatics.jax.org/mgihome/genealogy/>). Mice were sacrificed, and then the lenses were dissected and flash frozen until use. All experiments utilizing animals were approved by the University of Delaware institutional review board and conform to the ARVO Statement for the Use of Animals in Ophthalmic and Vision Research.

Isolation of lens crystallins for mass determination

Six lenses of 6-week-old FVB/N mice were homogenized in 200 µl of lysis buffer, containing 20 mM sodium phosphate (pH 7.0), 1 mM EGTA, 100 mM NaCl, and 1 tablet of protease inhibitor (Complete Mini Protease Inhibitor Cocktail, Boehringer Mannheim, Indianapolis, IN) dissolved at 10 ml lysis buffer/tablet. Lens homogenates were centrifuged at 20,000 xg for 45 minutes at 4 °C and supernatants were removed for further crystallin purification.

Crystallin aggregates and monomers were fractionated by gel filtration on a 10 x 250 mm Superose 6HR 10/30 column (Amersham Pharmacia Biotech, Piscataway, NJ) equilibrated with lysis buffer at a flow rate of 0.2 ml/min. This resolved the α-, βH-, βL-aggregates of approximately 600, 150, and 60 kD, respectively; and the γ-crystallin monomers of approximately 20 kD molecular weight, which were further separated by ion exchange or reverse phase chromatography. Beta heavy-aggregates, containing a complete compliment of individual β-subunits, were deaggregated in 6 M urea and individual subunits isolated by DEAE chromatography as previously described (Lampi, 2001). γ-crystallin monomers were separated by SP chromatography, as previously described (Siezen et al., 1988) except using a 7.5 x 150 mm SP 5-PW column (TosHaas, Montgomeryville, PA) and 20 mM histidine (pH 6.0), 1.0 mM EGTA, 2 mM DTT mobile phase, and 0.1 M NaCl gradient over 60 minutes.

Mass measurement of intact crystallins

Approximately 5 µg samples of whole α-crystallin aggregate or isolated β-crystallin and γ-subunits were injected onto a 1.0 x 250 mm C4 column (214 MS C4, Vydac, Hesperia, CA) and masses determined by on-line analysis of eluents by electrospray ionization mass spectrometry (ESI-MS) on a model LCQ iontrap (ThermoQuest, San Jose, CA). The column used a 25 µl/min flow rate and linear gradient of 10-50% acetonitrile over 30 min in a mobile phase containing 0.1% acetic acid and 0.025%

trifluoroacetic acid. Crystallin masses were then calculated as previously described (Lampi, 2001).

Two-dimensional electrophoresis and identification of lens proteins

Four lenses from identical aged mice were homogenized in 200 µl of lysis solution containing protease inhibitors followed by centrifugation as described above. The supernatant containing the soluble protein was removed, and the pellet (insoluble protein) was washed once. The insoluble protein was then resuspended in 0.5 ml lysis buffer by sonication, and the protein content in both soluble and insoluble fractions were measured by the BCA assay (Pierce Chemical Co., Rockford, IL) using bovine serum albumin as a standard. Both fractions of lens proteins were aliquoted into 400 µg portions and stored at –70 °C.

Isoelectric focusing was performed using immobilized pH gradient (IPG) gel strips (18 cm, pH 5-9), followed by second dimension electrophoresis using 12% SDS-PAGE gels as previously described (Lampi, 2001). The Coomassie blue stained gel images were captured and image analysis performed to determine the % that each spot contributed to the total protein on the gel. The relative pIs of proteins on 2-DE gels were determined based on the calculated pIs of unmodified αA, βA2, and γB.

Protein identification and mapping on 2-DE gels was performed using soluble protein from pooled lenses of 6-weeks-old mice (FVB/N strain). Similarly, mapping of identities of insoluble proteins was performed by pooling protein from 6-51 week-old mice. Gel slices from negatively stained gels containing protein spots were washed, dried, and in-gel digested with trypsin as described by Courchesne and Patterson (Courchesne and Patterson, 1999). Proteins in gel spots were then identified by LC-MS/MS analysis of digests to determine the amino acid sequences of peptides as previously described (Lampi, 2001).

Mass measurement of proteins isolated from 2-DE gels

Protein masses were determined after recovery from 2-DE gel spots either by elution using a custom electroelution device or by passive diffusion. Two-DE gels of soluble protein from 10-week-old mice were prepared as above, and then negatively stained (Matsui et al., 1999). Excised spots from 3 gels were pre-incubated twice for 15 min at room temperature by rotation in 1 ml of elution buffer (25 mM Tris, 192 mM glycine, and 1 mM thioglycolic acid, pH 8.8) supplemented with 0.1% SDS. For electroelution, the gel piece was minced to approximately 2 mm cubes, then placed into a 250 µl disposable pipette tip plugged with 4 µl of 4% polyacrylamide gel and filled with 150 µl of elution buffer. The pipette tip was then placed into a 200 µl microtiter plate well (Cat. No. 3690, Costar, Cambridge, MA) filled with 130 µl elution buffer and protein electroeluted into the microtiter plate well. Current was applied by placing platinum wires into both the elution buffer contained in the upper 250 µl pipette tip and the lower microtiter plate well. The protein was eluted for 1.5 hours at 100 v with the apparatus inside a 4°C cold room.

Alternately, proteins were recovered by passive diffusion using a modification of the method of Castellanos-Serra et. al. (1996). Following pre-incubation as above, excised protein spots were dispersed into 20 µM particles by forcing them through a 20 µm porous metal frit (Cat. No. A-120X, Upchurch Scientific, Oak Harbor, WA) placed at the bottom of a 500 µl air tight glass syringe. This required removal of the plastic ring surrounding the frit. The gel particles remaining in the syringe were collected by passing 100 µl of elution buffer containing 0.1% SDS through the syringe. Proteins were then allowed to diffuse from the gel particles by incubation for 30 min at 37°C in an ultrasonic bath. The slurry was then filtered using a 0.22 µm micro-centrifuge filter (Micropure-0.22; Amicon, Beverly, MA).

Masses of proteins recovered by both of the above methods were then determined by on-line LC-MS as described above in the section on mass measurement of intact

crystallins. The approximately 100 μg of SDS present in each sample did not interfere with chromatography or mass measurement of the eluted protein.

Results

Crystallin mass determination

To compare the actual masses of mouse crystallins and calculated masses based on the reported cDNA sequences, the masses of individual HPLC separated or gel eluted crystallins from 6-week old mice were measured by ESI-MS (Table 2.1). The measured masses of all HPLC purified α- and β-crystallins matched the theoretical masses derived from published cDNA sequences within an instrumental error of 3 mass units. This suggested that the reported sequences of these crystallins matched the sequences found in FVB/N mice. βA1-crystallin was not obtained in sufficient purity by HPLC to determine its mass. However, the mass of βA1 eluted from 2-DE gels differed by only 0.8 mass units from the theoretical mass (Table 2.1), again suggesting that the reported sequence was identical.

When purified γ-crystallins were similarly analyzed by ESI-MS, proteins matching the predicted masses of mouse γA, B, C, E, and γS-crystallins were identified. However, the measured mass of 20,958.5 for γD was 81.2 mass units higher than the theoretical mass. This mass of HPLC purified γD was confirmed by analysis of γD eluted from 2-DE gels. Due to alkylation, gel purified γD had a mass of 21,357.8. Since γD reportedly contains 7 cysteines, the corresponding non-alkylated mass was 20,958.1, which closely matched the mass of HPLC purified γD. These data indicated that the sequence of γD crystallin in FVB/N mice was different than the previously reported murine γD sequence (P04442). A protein matching the theoretical mass for γF-crystallin was not detected by either method. However, in HPLC fractions, the identity of two species with masses of 20,916 and 20,974 could not be determined.

Table 2.1. Mouse lens crystallin theoretical and measured mass

crystallin	accession*	theoretical mass†	measured mass	difference
αA	P02490	19,834.1	19,835.9	+1.8
αAinsert	P24622	22,531.3	22,533.6	+2.3
αB	P23927	20,110.8	20,112.0	+1.2
βA1	P02525	23,586.2‡	23,587.0§	+0.8
βA2	CAB75585	22,147.4	22,148.6	+1.2
βA3‖	CAB52418	25,248.2	25,249.2	+1.0
βA4	CAB75586	22,379.6	22,379.8	+0.2
βB1	AAD42048	27,913.3	27,914.5	+1.2
βB2	P26775	23,291.8	23,294.0	+2.2
βB3	CAB75587	24,201.9	24,205.0	+3.1
γA	P04345	21,017.6	21,019.8	+2.2
γB	P04344	21,007.6	21,009.8	+2.2
γC	Q61597	20,785.4	20,787.4	+2.0
γD	P04342	20,877.3	20,958.5¶	+81.2
γE	P26999	21,093.5	21,096.2	+2.7
γF	Q03740	21,132.6#	-	-
γS	AAC53579	20,761.2	20,762.6	+1.4

*SWISS-PROT accession numbers start with P or Q, otherwise GenBank accession numbers are given. †Theoretical masses were determined by removing the N-terminal methionine from all sequences, except for αA, αAinsert, αB, and βA3. A mass of 42 was also added to the mass of all crystallins, except γA-F, due to N-acetylation. ‡Alkylated protein mass, adding 57.1 mass units to each cysteine residue. §Mass determined following alkylation and elution from 2-DE gels. ‖Mass for βA3 missing 11 amino acid of N-termini was also identified (theoretical 23,860.7, measured 23,858.8). ¶This mass was also confirmed by elution of γD from 2-DE gels (see text). #The theoretical mass of γF could not be confirmed. Its mass may match one of the remaining non-assigned masses of the γ-fraction (20,915.9 and 20,974.5).

Composition of soluble proteins in young mouse lens

To determine the identities and relative abundance of crystallin subunits, the time course of post-translational modifications, and variation between the water-soluble and insoluble fractions in mouse lens, 2-DE was performed and spots identified by in-gel trypsin digestion and LC-MS.

A 2-DE gel of lens soluble protein from 1.5-week old FVB/N mice is shown in Fig. 2.1, with the identities of major proteins indicated. All crystallins previously reported in a 2-DE map of 33-51 week old mouse lens were identified (Jungblut et al., 1998), in addition, we were able to confirm the presence of γF-crystallin by identifying a γF specific peptide within the digest of the co-migrating γE/F spots. Similarly, γB/C did not separate from one another, but peptides unique to each protein were identified in the digest. The majority of crystallins in the lenses of these young animals migrated to their expected relative isoelectric points, except γE-crystallin, which based on its expected pI of 7.7, should have been the most basic crystallin subunit. Since it was unlikely that γE was modified in lenses from these very young animals, the result suggested that the reported sequence (Swiss Prot P26999) was different than the γE sequence in the FVB/N strain. This result was unexpected, since a γ-crystallin was found with a mass only 2.7 units different from the expected mass of γE (Table 2.1). A non-crystallin protein was also identified in the soluble fraction of mouse lens with a concentration at 1.5-weeks of age similar to the less abundant crystallins (~1.2% of soluble protein). This species, identified as a fatty acid binding protein, has been previously described in both rat and cow lens, and is a marker for differentiation of fiber cells (Wen et al., 1995) (Jaworski and Wistow, 1996). Since the cDNA sequence for the mouse lens gene is unknown, it was not possible to determine whether this is a novel gene product or identical to the gene expressed in mouse keratinocytes (Swiss Prot Q05816).

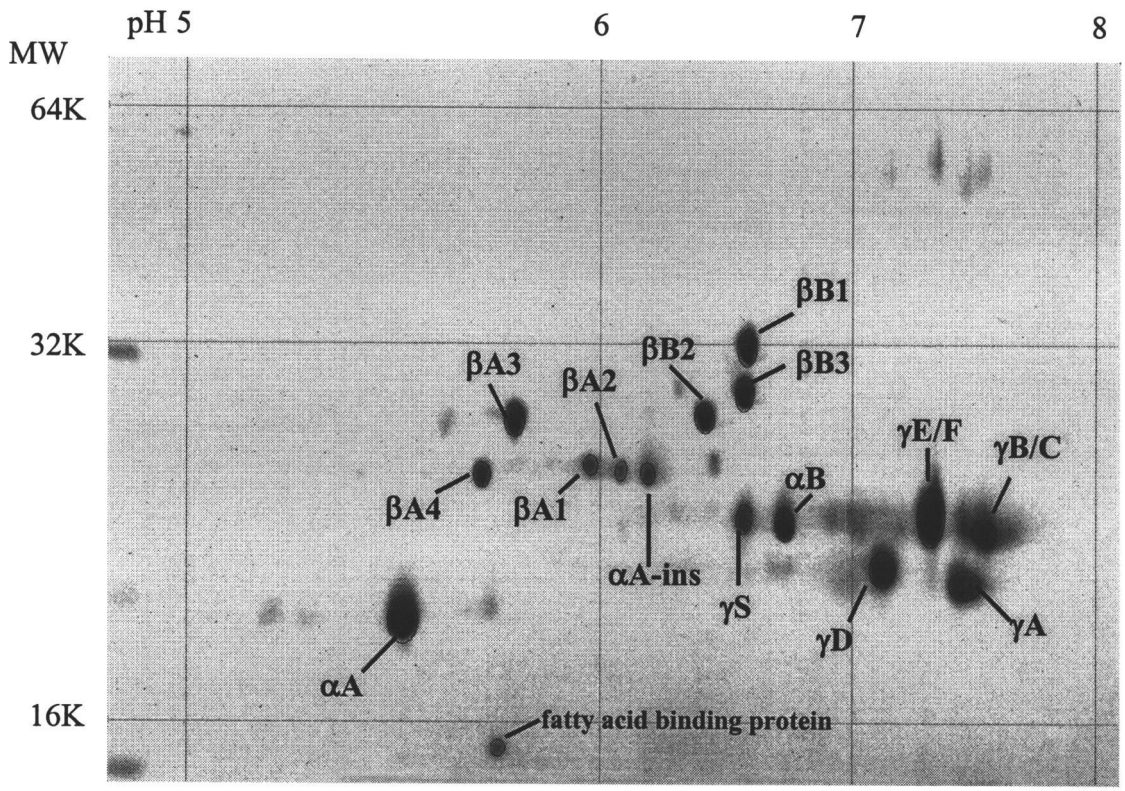

Figure 2.1 Two-dimensional electrophoresis (2-DE) map showing the identities of the major soluble proteins in whole lenses of 1.5-week-old mice. Protein spots were detected and quantified within circled regions by 2-DE image analysis software and identified by MS/MS analysis of in-gel tryptic digests. Approximate molecular weight and pH range of the gel were determined by reference to molecular weight markers and calculated pIs of selected crystallins, as described in methods. Only the lower molecular weight region of the gel is shown, which contained all crystallin subunits and fatty acid binding protein. As in all gels shown in this manuscript, staining was performed by Coomassie blue, and 400 μg of protein was applied.

Figure 2.2 Changes in relative abundance of the major proteins of mouse lens during maturation. Two-DE gels of soluble proteins of (a) newborn, (b) 1.5-week-old, and c) 6-week-old mouse lens are shown. Protein spots undergoing changes in relative abundance during lens maturation are labeled. Unlabeled spots can be identified by reference to Fig. 1. The relative abundance of each protein spot was determined by image analysis as shown in Table 2.

a) Newborn

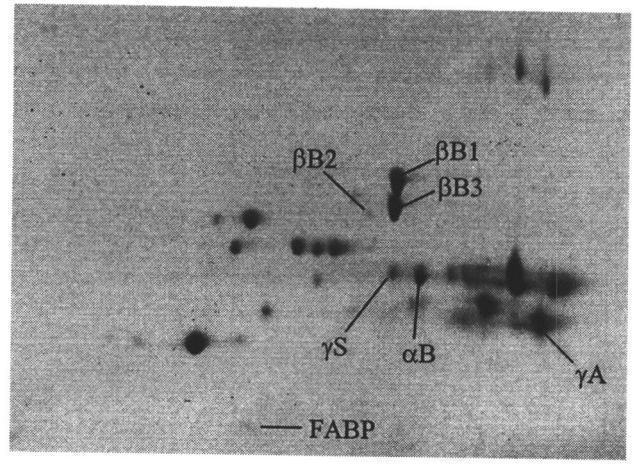

b) 11-day-old

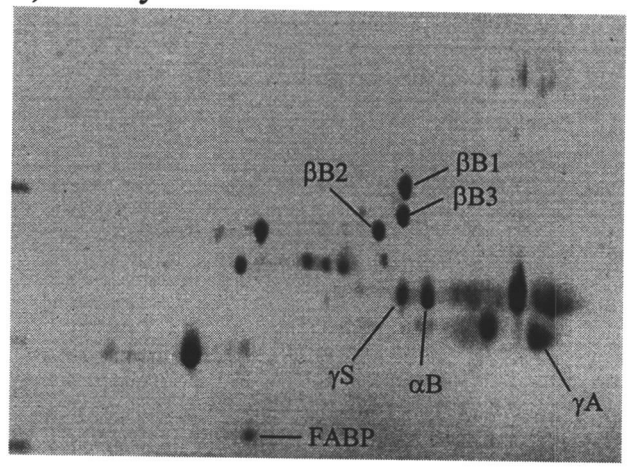

c) 6-week-old

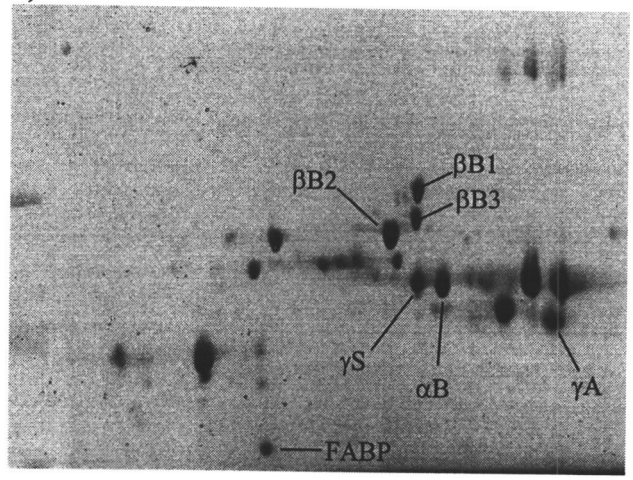

Figure 2.2

Table 2.2. Changes in % abundance of mouse crystallin subunits during lens maturation.

Crystallin*	newborn	1.5 w	4 w	6 w	% change
βB1	8.5[†]	6.1	4.0	4.4	-48.[‡]
βB2	0.2	5.0	9.8	10.3	+5100.
βB3	8.2	5.8	3.5	3.9	-52.
βA1	2.2	1.4	2.2	1.7	-23.
βA2	1.6	1.2	1.9	1.4	-12.
βA3	4.1	5.4	4.1	4.3	+5.
βA4	1.6	2.9	2.4	2.3	+44.
αAins	2.8	1.5	2.1	1.4	-50.
αA	14.0	12.2	11.7	12.9	-8.
αB	3.8	6.1	7.5	7.2	+89.
γA	7.7	8.6	2.8	3.7	-52.
γB/C	4.0	7.1	8.2	6.3	+57.
γD	7.5	8.7	9.0	8.5	+13.
γE/F	15.8	16.3	12.7	14.1	-11.
γS	0.8	3.2	5.4	4.8	+500.
(fatty acid binding protein)	0.1	1.2	1.5	1.3	+1200.

*Identified by MS analysis of in-gel digests. [†]% relative abundance of each crystallin subunit calculated by densitometric analysis of Coomassie stained 2-DE gels. Each value is an average from three repeated gels from a single pooled sample from 4-10 lenses from each age group. [‡]Calculated by determining the change in % abundance of each crystallin from newborn to 6-weeks of age divided by the % abundance in newborn lenses X 100.

Developmental changes in crystallin composition

To determine developmental changes in crystallin composition, water-soluble lens proteins from newborn to 6-week-old mice were separated by 2-DE (Fig. 2.2), the percent abundance of each crystallin determined, and percent change from newborn to 6-weeks of age calculated (Table 2.2). The observations of developmental changes in crystallin abundance were limited to the first 6 weeks of life, because post-translational modifications and protein insolubilization in older lenses prevented accurate quantification. The most profound changes occurred in the content of βB2, γS, and αB-crystallins. These proteins increased approximately 50, 6, and 2 fold, respectively, during the first six weeks of life. The fatty acid binding protein also increased 13 fold during this period. In contrast, by 6-weeks of age, βB1, βB3, and γA-crystallins decreased to approximately 1/2 the amounts found in newborn lens. While quantities of αA insert also decreased, inconsistencies in the quantity of this protein between gels prevented any conclusions regarding changes in its abundance with lens growth.

Age-related crystallin modification and insolubilization

To investigate the change in protein profiles of mouse lens during aging, a series of gels of both water-soluble and insoluble lens proteins for mice between 6-51 weeks of age were compared (Fig. 2.3), and new spots appearing with age were identified by LC-MS analysis of in-gel digests. The results of this analysis are shown in Fig. 2.4 that shows enlarged images of 2-DE gels of soluble- and insoluble-protein from 51-week-old mouse lenses with the modified crystallins numbered, and then identified in Table 2.4.

The majority of changes in the relative abundance of soluble crystallins past 6-weeks of age (Table 2.3) were due to post-translational modifications and insolubilization. This conclusion as based on the observation that the total protein content of the lens only increased by 38% from 6-weeks to 51-weeks of age, but

Figure 2.3. Accumulation of modified crystallins in mouse lens during aging. Lens proteins from 6, 10, 31, and 51-week-old mice were separated into (a)soluble and (b) insoluble fractions and analyzed by 2-DE. The appearance of modified crystallins with age can be followed by reference to the identities of unmodified crystallins indicated in the 2-DE gels of proteins from 6-week-old lens. Age-induced changes in the abundance of unmodified crystallins was determined by image analysis as shown in Table 3. The identities of the major modified crystallin subunits appearing with age are shown in Figure 4. Note that intact αA-crystallin was not present in the insoluble fraction of lens at 6-weeks of age. The approximate location where intact αA-crystallin would be expected to migrate is indicted.

Figure 2.4. Identification of modified crystallins appearing with age in mouse lens. Two-DE gels of soluble (a) and insoluble protein (b) from lenses of 51-week-old mice, as shown in Fig. 2.3, are enlarged so that labels on protein spots can be seen. The major modified crystallin species appearing with age are numbered and identities are indicated by reference to Table 4. The position of unmodified crystallin subunits (underlined labels) are circled in the soluble fraction (a) and marked by a plus sign in the insoluble fraction (b). Note that while many modified crystallins appear in both soluble and insoluble fractions, for clarity they are only labeled with a number in the fraction where they are most abundant.

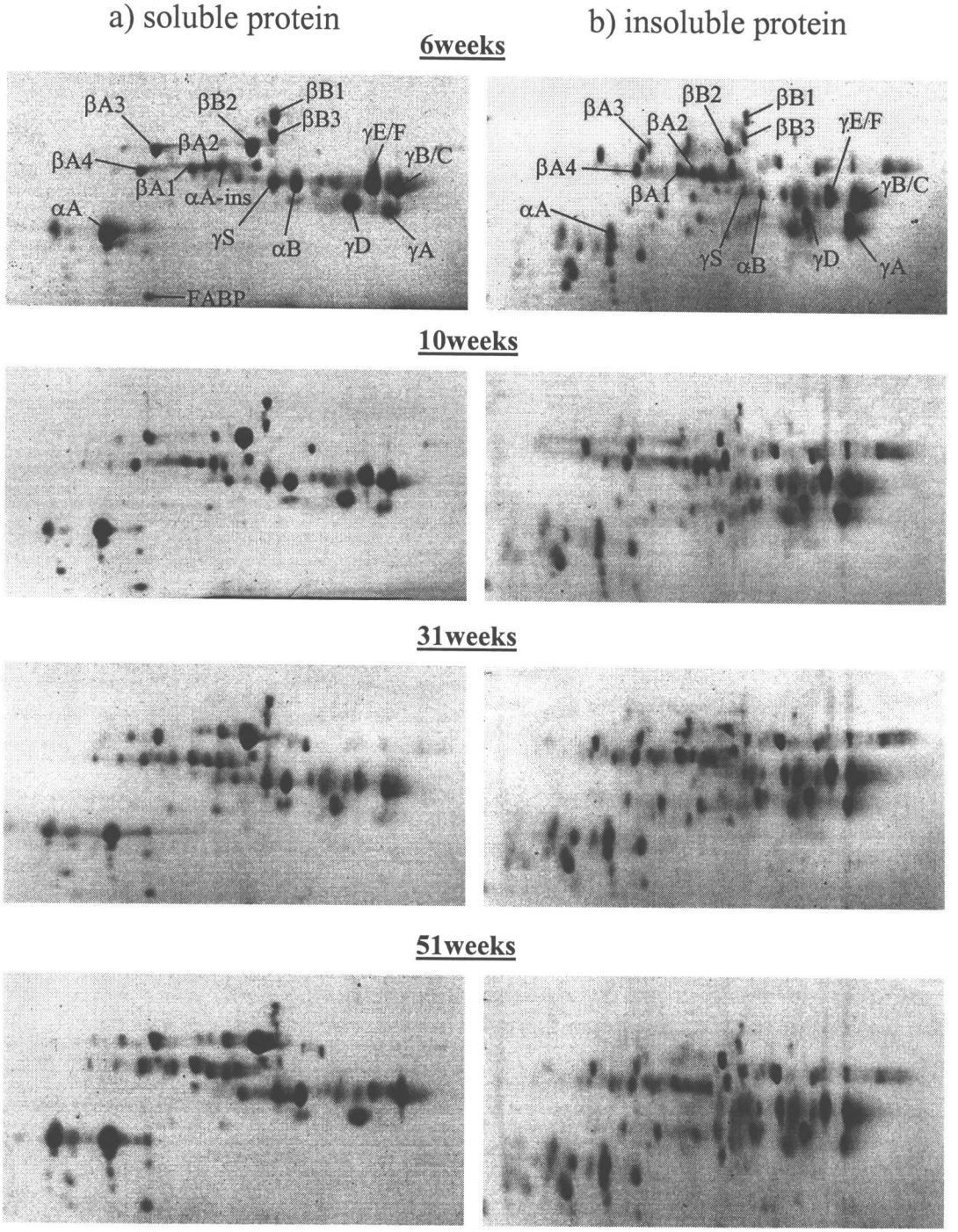
a) soluble protein
b) insoluble protein
6weeks
βA3
βB2
βB1
βB3
βA2
γE/F
γB/C
βA4
βA1
αA-ins
αA
γS
αB
γD
γA
FABP
10weeks
31weeks
51weeks

Figure 2.3

a) Soluble fraction

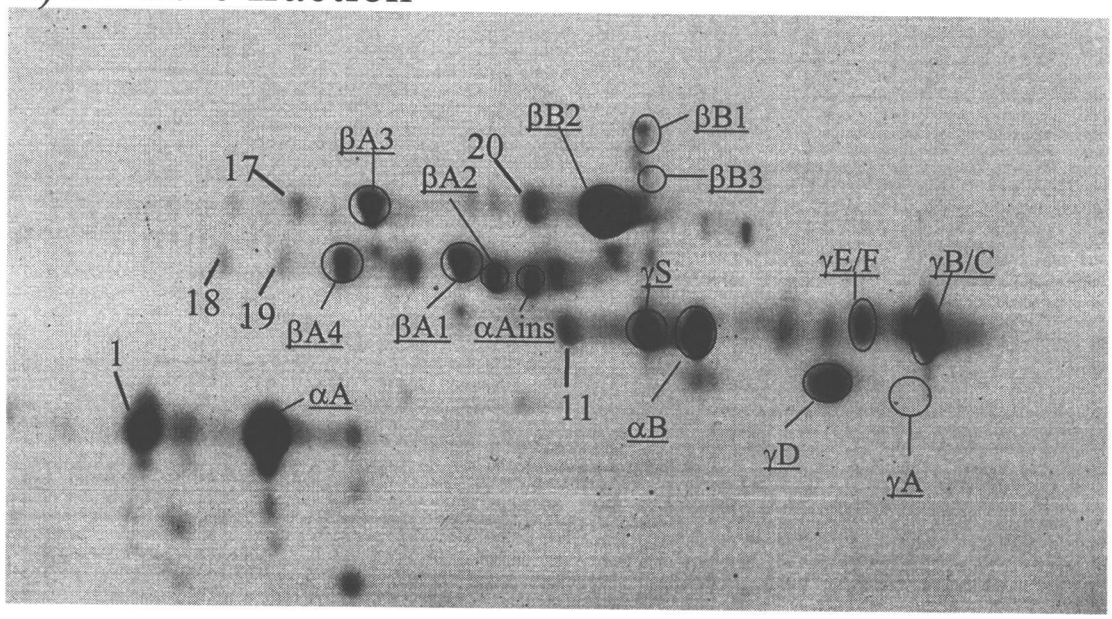

b) Insoluble fraction

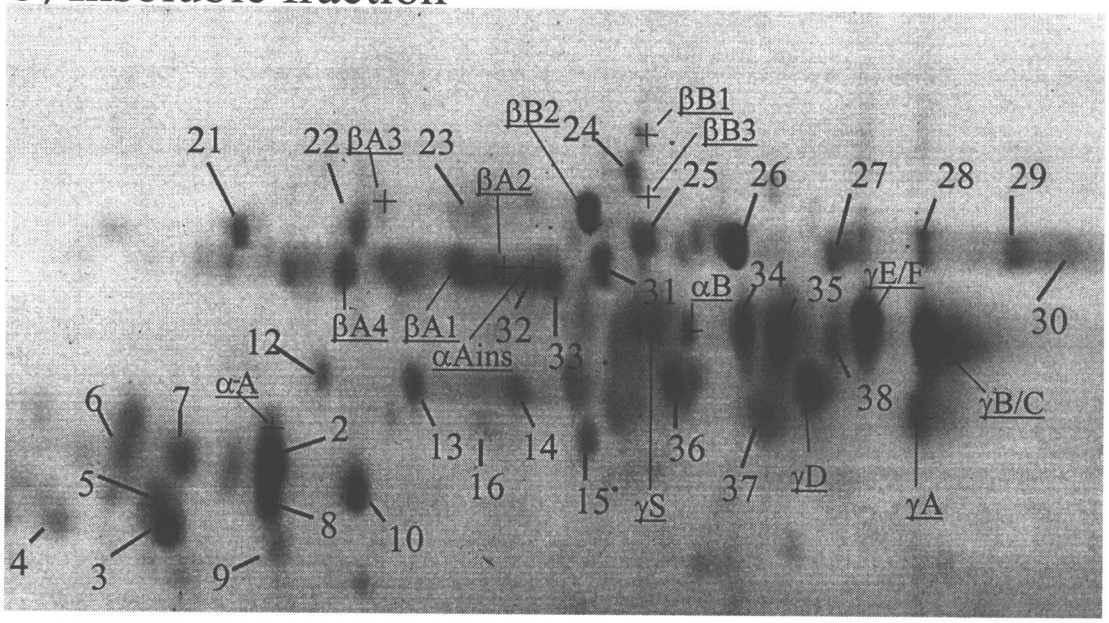

Figure 2.4

Table 2.3. Changes in % abundance of unmodified mouse crystallin subunits during lens aging.

Crystallin*	6 w	10 w	31 w	51 w	% change
βB1	4.4[†]	2.0	1.2	0.3	- 93.[‡]
βB2	10.3	12.3	22.1	20.4	+ 98.
βB3	3.9	1.6	0.5	0.2	- 95.
βA1	1.7	2.3	2.8	2.8	+ 65.
βA2	1.4	1.7	2.0	2.2	+ 57.
βA3	4.3	2.9	3.4	3.3	- 23.
βA4	2.3	2.0	1.7	2.0	- 13.
αAins	1.4	2.3	2.3	1.9	+ 36.
αA	12.9	12.2	12.4	16.6	+ 29.
αB	7.2	7.6	9.1	8.1	+ 12.
γA	3.7	1.5	0.1	0.0	-100.
γB/C	6.3	8.8	2.6	6.1	- 3.
γD	8.5	7.8	5.1	6.0	- 29.
γE/F	14.1	9.8	4.2	2.6	- 82.
γS	4.8	6.3	5.4	4.3	- 10.
(fatty acid binding protein)	1.3	1.1	0.9	0.8	- 38.

*Identified by MS analysis of in-gel digests. [†]% relative abundance of each crystallin subunit calculated by densitometric analysis of Coomassie stained 2-DE gels. Each value is an average from three repeated gels from a single pooled sample from 4-10 lenses from each age group. [‡]Calculated by determining the change in % abundance of each crystallin from 6-weeks to 51-weeks of age divided by the % abundance in 6-week old lenses X 100.

Table 2.4. Identification of modified crystallins in 51-week-old mouse lens*

Spot #	Crystallin	Present in: soluble†	insoluble†	confirmed modification‡	pI§
1	αA	+++	+	phosphorylated (see figure 5a)	5.23
2	αA	+	+++	-5 amino acids, C-terminus	5.52
3	αA	+	++	-22 amino acids, C-terminus	5.28
4	αA	-	+	-	5.02
5	αA	-	+	-	5.25
6	αA	+	+	-	5.17
7	αA	+	++	-	5.31
8	αA	+	++	-	5.52
9	αA	+	+	-	5.54
10	αA	+	++	-	5.72
11	αB	++	-	phosphorylated (see figure 5b)	6.29
12	αB	-	+	-	5.64
13	αB	+	++	-	5.86
14	αB	+	++	-	6.12
15	αB	-	+	-	6.36
16	αB	-	+	-	6.01
17	βA3	+	-	-	5.59
18	βA4	+	+	-	5.41
19	βA4	+	+	-	5.56
20	βB2	++	+	-	6.17
21	βB1	-	++	-	5.44
22	βB1	-	++	-	5.72
23	βB1	-	+	-	6.01
24	βB1	?	+	-	6.51
25	βB2	?	++	-	6.54
26	βB2	+	+++	-8 amino acids, N-terminus	6.86
27	βB3	-	+	-17 amino acids, N-terminus	7.18
28	βB3	-	+	-	7.49
29	βB3	-	+	-	7.79
30	βB3	-	+	-	7.98
31	βA3	+	++	-11 amino acids, N-terminus	6.40
32	βA3	-	+	-	6.15
33	βA3	++	++	-22 amino acids, N-terminus	6.24
34	γE/F	+	++	-	6.88
35	γB/C	+	+++	-	7.00
36	γD	?	++	-	6.64
37	γA	-	+	-	6.95
38	γB/C	+	+	-	7.18

(Table 2.4 legends)
*Identification was based on MS/MS analysis of peptides from in-gel digests. See Fig. 2.4 for position of modified crystallin. The identification was performed on digested protein from gels of either soluble or insoluble protein as indicated in Fig. 2.4. †Presence of the same modified species in both fractions was inferred by a similar migration position in both gels, except for spot 32 (modified βA3) in the insoluble fraction that migrated to the same position as αAinsert in the soluble fraction. ‡Indicated modification confirmed by MS/MS analysis of C- or N-terminally truncated tryptic peptides. §pIs of modified crystallins calculated by Melanie 3 software through comparison to the calculated pIs and relative migration of intact αA, βA2, and γB. The differences in the calculated pIs of similar spots on 4 repeated gels ranged from 0 to 0.11, and averaged 0.027.

crystallins such as βB1, βB3, γA, and γE/F decreased by 80% or more in the soluble fraction during this period (Table 2.3).

Evidence for progressive truncation, acidification, and phosphorylation of crystallins was observed. Furthermore, truncated and acidified forms of crystallins were selectively found in the insoluble fraction of the lens, which increased from 6.2 to 60% of the total lens protein from 6- to 52-weeks of age.

Results for each class of modified crystallin are summarized below.

Age-related changes in α-crystallins

α-crystallin aggregates are composed of αA, αB, and αA insert subunits. αA and αA insert are identical, except for the insertion of 17 extra amino acid in αA insert due to differential mRNA splicing (King and Piatigorsky, 1983). The concentrations of unmodified α-crystallin subunits did not significantly change in the soluble fraction of the adult mouse lens during aging (Table 2.3). The major modification of both αA and αB in the soluble fraction was the age-dependant appearance of acidic forms (Fig 2.4, spots 1 and 11). The isolation of these acidic forms from 2-DE gels, and measurement of their whole masses yielded values of 19,970.5, and 20,190.6 (Fig. 2.5). These masses were each, respectively, approximately 80 mass units greater than the expected masses of alkylated αA, and αB. This indicated that the increased acidity of these species was due to single phosphorylations. The phosphorylated form of αA increased to 38% of unmodified soluble αA by 51-weeks of age. In contrast, the content of phosphorylated αB peaked by 10-weeks of age and the proportion of phosphorylated αB was less extensive than phosphorylated αA.

αA- and αB-crystallins also became progressively truncated with age and were selectively found in the insoluble fraction. In contrast, intact forms of these proteins were only minor components in the insoluble fraction (Fig. 2.4, underlined). Truncated αA and αB spots together accounted for 19% and 4.5% of the total insoluble protein in 51-week-old lenses, respectively.

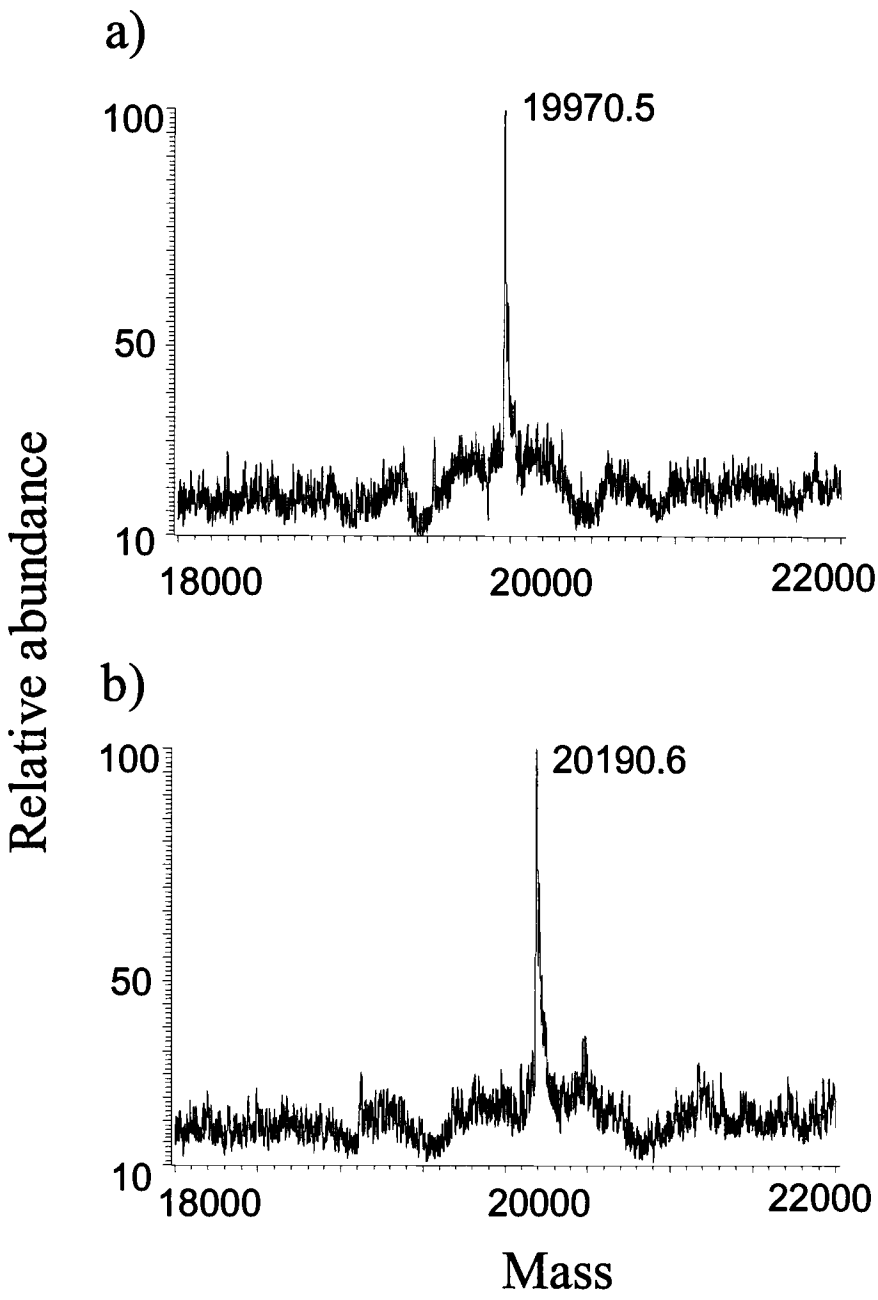

Figure 2.5 Masses of phosphorylated α-crystallins appearing with maturation and increasing age in mouse lens. Deconvoluted mass spectra of phosphorylated αA (a) and phosphorylated αB (b). These proteins were isolated for mass analysis by elution from the soluble fraction of 2-DE gels. The mass of alkylated non-phosphorylated αA- and αB-crystallins are: 19891.2 and 20110.8, respectively. A single phosphorylation increases the mass of proteins by 80 units.

Several pieces of evidence suggested that C-terminal truncation of αA and αB led to their insolubilization. A truncated form of αA (Fig. 2.4, spot 2), just below intact αA, was isolated from 2-DE gels. Its 21,436.7 unit mass indicated that it was missing 5 residues from its C-terminus. Similarly, MS/MS analysis of a tryptic digest from spot 3 yielded peptide 146-151 of αA, indicating that this species was missing 22 residues from its C-terminus. These results suggested that the other numerous species of truncated αA (Fig. 2.4, spots 4 - 10), and αB (Fig. 2.4, spots 12-16) may result from the progressive removal of C-terminal residues. This hypothesis was supported by MS analysis of spots in similar positions from 2-DE gels of insoluble protein from adult rat lens. These modified forms of αA and αB were all C-terminally truncated (Chapter 4). The similar relative molecular weights of spots 12-14 in Fig. 2.4 also suggested that a single truncated species of αB may be phosphorylated. This suggestion was also supported by mass spectral analysis of a similar species of αB in rat lens, which was both C-terminally truncated and phosphorylated (Chapter 4).

Age-related changes in β-crystallins

During aging, soluble forms of βB1and βB3 continued to decrease, such that each comprised less than 0.5% of the total soluble lens protein by 51-weeks of age (Table 2.3). This loss was due to insolubilization following truncation of βB1 (spots 21-24) and βB3 (spots 27-30). βB2 and βA3-crystallins also underwent truncation and insolubilization with increasing age (spots 25-26, and 31-33). However, the accumulation of these insoluble truncated forms did not deplete the soluble fraction of the intact forms of these proteins. In fact, βB2 continued to accumulate in the soluble fraction and became the major species by 51-weeks of age. Unlike other β-crystallin subunits, βA1, βA2, and βA4 were not truncated and did not become selectively insolubilized with age. The stability of these subunits was likely related to their shorter and therefore protease resistant N-terminal extensions.

The truncation of β-crystallins differed from α-crystallin truncation in that N-terminal regions were removed. While specific sites of truncation were not assigned for all modified β-species, truncated βA3, missing either 11 or 22 residues (spots 31 and 33), βB2 missing 8 residues (spot 26), and βB3 missing 17 residues from its N-terminus (spot 27) were identified by MS analysis of peptide digests (Table 2.4). These N-terminal truncation sites were identical to ones previously described in rat lenses, and attributed to activation of a class of calcium-activated proteases called calpains (David et al., 1994a). The truncated forms of βA3 were likely derived from sequential degradation of βA3, and not βA1. The abundance of βA3 missing 11 residues from its N-terminus (spot 31) peaked at 6 - 10 weeks, and then decreased as the more extensively degraded forms increased (spots 32 and 33).

The analysis of spots with similar positions in 2-DE gels of both soluble and insoluble fractions suggested that caution must be used when identifying proteins based on similar positions. The spot identified as αA insert on the 2-DE gel of soluble protein had a position identical to a spot on the 2-DE gel of insoluble protein identified as a truncated βA3 (spot 32).

While partial degradation was the major modification to β-crystallins in mouse crystallins with age, there was also evidence for either deamidation or phosphorylation. Acidic forms of βB2, βA3, and βA4 appeared with age that underwent no alteration in apparent molecular weight on the 2-DE gels (spots 17 – 20). Unlike truncated forms of β–crystallins, these modified species did not undergo insolubilization.

Age-related changes in γ-crystallins

In contrast to α– and β-crystallins, there was no evidence of γ-crystallin proteolysis during lens maturation. However, large shifts in the relative abundance in these proteins occurred. Following the developmentally related decrease in γA-crystallin (Table 2.1), this protein underwent insolubilization and was entirely lost from the soluble fraction by 51-weeks of age (Fig. 2.4, Table 2.4). γ-E/F also decreased

approximately 80% in the soluble fraction from 6-weeks to 51-weeks of age. Since γA-F all accumulated in the insoluble fraction during aging, the selective loss of soluble γA and γE/F was likely due to decreased synthesis of these proteins.

The age-related insolubilization of γA-F crystallins was associated with progressive acidification, such that a duplicate pattern of 4 spots appeared for these 6 proteins at identical apparent molecular weights, but shifted an average of 0.47 pH units more acidic than the unmodified species (Fig. 2.4, Table 2.4). These acidified forms of γA-F were almost exclusively found in the insoluble fraction. The modification causing this acidification was not determined, but could be due to either deamidation, phosphorylation, or very limited proteolysis. The acidification and insolubilization γA-F was very specific, because the closely related protein γS underwent no acidification and remained for the most part soluble with increasing age.

Protein profile comparison of different strains of mice

To determine if lens proteins from different strains of mice varied in abundance or position on 2-DE gels, proteins from the FVB/N strain used in the above studies were compared to C57BL/6, ICR, and CB6F1 strains. In general, all 4 strains of mice had identical protein profiles, including crystallin modifications in both soluble and insoluble fractions. However, an additional spot was found in the γ-region in the strains C57BL/6 and its hybrid CB6F1. Gels comparing the soluble protein profiles of 10 and 12-week old FVB/N and C57BL/6 strains are shown in Fig. 2.6, respectively. The new spot in the C57BL/6 strain (closed arrow) was identified by MS/MS analysis of tryptic peptides as either γB or γC. The region in the position of γB/C in the FVB/N strain was also less abundant (open arrow). This suggested that a polymorphism may exist in these strains resulting in the presence of a more acidic γB- and/or γC-crystallin.

a) FVB/N (10 w)

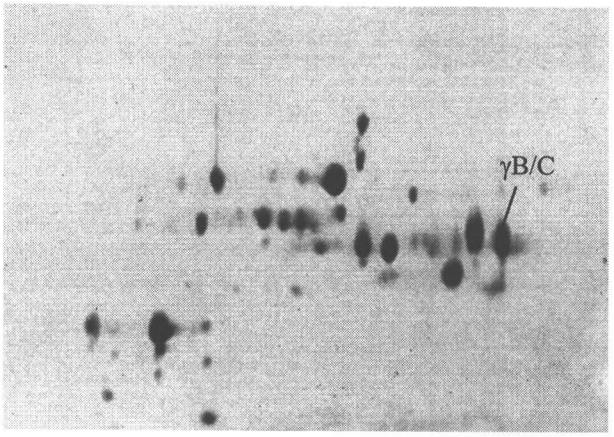

b) C57Bl/6 (12 w)

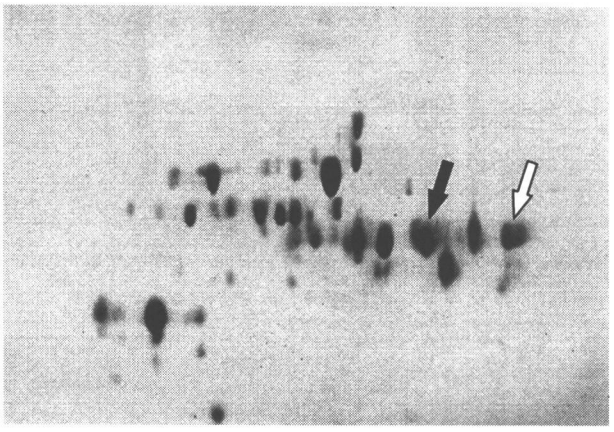

Figure 2.6. Comparison of soluble lens protein profiles from two mouse strains by 2-DE. a) 10-week old FVB/N mouse strain used throughout this study, and b) 12-week-old C57BL/6 strain are shown. The profiles were very similar, except for an altered migration of a γB or γC-crystallin found in the C57BL/6 strain (dark arrow) that was largely absent in the FVB/N strain (white arrow).

Discussion

These studies for the first time investigated the masses of mouse crystallins, and produced a series of 2-DE maps of both soluble and insoluble lens crystallins from mice of increasing age. The accurate mass measurements allowed independent confirmation of reported sequences and facilitated the assignment of post-translational modifications. Analysis of 2-DE gel maps from newborn and mature lenses allowed comparison of earlier measurements of gene expression to actual levels of proteins, and detected the major species of modified crystallins appearing during lens maturation. The 2-DE maps produced in this study complement the earlier 2-DE map produced by Jungblut et al. (Jungblut et al., 1998) by producing maps for lenses of different ages, separately analyzing water-soluble and water-insoluble fractions, and using immobilized pH gradients for isoelectric focusing, which are more easily reproduced in other laboratories.

The masses and measured pIs of mouse crystallins suggested that the previously reported sequences deduced from cDNA were similar to sequences in the FVB/N strain, except for γD, γF, and possibly γE. Similar inconsistencies between the measured masses of rat γ-crystallins (Lampi, 2001) and deduced sequences from cDNAs suggested that many polymorphisms exist in rodent γ-crystallins. This suggestion was also supported in the current study by finding γB or γC in the C57BL/6 strain with an altered pI. While mutations altering critical residues or introducing stop codons in γ-crystallins lead to spontaneous cataracts (Smith et al., 2000; Klopp et al., 1998), polymorphisms, such as in the C57BL/6 stain, may be relatively silent but cause an altered susceptibility to cataract. Mass spectrometry may provide a rapid method to further investigate heterogeneity of crystallin sequences in mice.

Quantification of the relative amounts of each crystallin subunit in lenses from newborn to 6-week-old mice allowed estimation of changes in the relative rates these proteins are synthesized during lens maturation. During development of the mouse lens transcription from the αB gene occurs before transcription from the αA gene (Robinson

and Overbeek, 1996). However, by embryonic day 12.5 transcripts of αA became very abundant and localized to the newly developed primary fibers, while αB expression remained localized in the lens epithelium. Once secondary fibers formed this pattern changed and the site of greatest αB expression shifted from epithelium to secondary fibers. The rapid increase in αB protein content measured in this study from birth to 11-days of age was likely the result of the delayed onset of αB expression in secondary fibers.

The reported post-natal increase in rat βB2 and decrease in rat βB3 gene expression (Aarts et al., 1989) also closely followed changes in βB2 and βB3 proteins in mice. The post-natal accumulation of βB2 was especially dramatic, going from the least to most abundant β-crystallin during the first 6 weeks of life. The age-related increase in mouse lens βB2-crystallin synthesis was also previously demonstrated immunohistochemically using a monoclonal antibody against βB2 (Carper et al., 1986). While changes in βB1 gene expression have not been determined in post-natal rodent lenses, the similar 50% decline in both mouse βB1 and βB3 by 6-weeks of age suggested that the expression of genes coding for both proteins rapidly falls in mice following birth. Human lenses also undergo a rapid loss of βB3, since this protein was only detected in lenses less than three years of age (Ma et al., 1998c). Unlike decreases in βB3, the decrease in βB1 may be restricted to mouse lenses. Similar rates of βB1 protein synthesis were observed in 1-, 2- and 4-month old rats (Voorter et al., 1990).

The increase in γS-crystallin protein also paralleled the reported increase in expression of the lens γS gene during maturation (Sinha et al., 1998). Similarly, the reported post-natal increase in expression of mouse γB and γC genes (Goring et al., 1992) closely matched the increasing abundance of γB and γC proteins during maturation. Expression of γA, E, and F genes were all reported to decrease at similar rates during maturation (Goring et al., 1992). However, levels of γE and F proteins were maintained in 6-week old lenses, while a 50% decrease in γA protein occurred. The rapid loss of soluble γA may be related to its greater tendency to undergo insolubilization during lens maturation than the other γ-crystallins (see Fig. 3, 6-weeks).

These changes in the relative abundance of crystallin subunits would be expected to significantly alter the properties of lens fibers from the center to the periphery of the growing lens. The lower concentrations of αB, βB2, and γB/C/S; and higher concentrations of βB1, βB3, and γA in the older fibers in the lens nucleus may favor dehydration, insolubilization, and a cytosol with a higher index of refraction.

Major post-translational modifications occurred in mice after 6-weeks of age. While numerous modified crystallins were observed in the insoluble fraction in younger lenses, the quantity of insoluble protein did not significantly increase until after 6-weeks. The major modifications were phosphorylation of α-crystallins in the soluble fraction and altered pIs and/or relative molecular weights of α, β and γ-crystallins in the insoluble fraction, due to proteolysis and/or possibly deamidation.

αA-crystallin became progressively phosphorylated with increasing age in the lens soluble fraction, with the phosphorylated form comprising over 1/3 of the total αA by 51-weeks. Phosphorylation of α-crystallins has been well documented in human (Miesbauer et al., 1994; Takemoto, 1996), bovine (Carver et al., 1996), and rat (Wang et al., 2000) lenses. Recent studies by Wang et. al. suggest that αA-crystallin in rat is phosphorylated at a different site than human or bovine αA-crystallins. Furthermore, increased phosphorylation of both αA- and αB-crystallins occurs during oxidative or high calcium stress in rat lens (Wang et al., 2000). The observed pattern of phosphorylation of α-crystallins in mouse lens is consistent with the hypothesis that each subunit is phosphorylated by a different kinase activity. αA became progressively phosphorylated with increasing age, while αB phosphorylation was essentially complete by 10-weeks of age. In this regard αB phosphorylation in mice is more like phosphorylation of αA in man, where it is a maturationally-related rather than age-related (Takemoto, 1996). While cAMP-dependant kinases are likely responsible for at least a portion of α-crystallin phosphorylations, these proteins also exhibit autokinase activity (Kantorow and Piatigorsky, 1998). Further studies are required to determine which mechanism of α-crystallin phosphorylation predominates in mice. These studies

are important, because phosphorylation of α-crystallin may cause dissociation of α-oligomers and reduction of chaperone-like activity (Ito et al., 2000).

α-crystallins also became progressively truncated with increasing age, and these truncated α-crystallins were selectively found in the insoluble fraction. The truncation of α-crystallins occurs mainly at the C-terminus (summarized by Groenen et al., 1994). While the specific sites of all C-terminal truncations in mouse α-crystallins were not determined in this study, identification of αA missing 5 and 22 residues from its C-terminus was consistent with similar forms of these and other C-terminally truncated α-crystallins characterized in rat lens (chapter 4). The loss of C-terminal residues in α-crystallins is physiologically significant, because it reduces chaperone activity (Takemoto et al., 1993; Kelley et al., 1993). The flexible C-terminal extensions of α-crystallins are probably required to maintain the solubility of complexes between α-crystallin and its substrate proteins being chaperoned (Carver, 1999). If truncated α-crystallins become insoluble in mouse lenses during maturation due to the binding of chaperoned proteins, the resulting complexes are compatible with transparency. Perhaps the greatest significance of the C-terminal truncation and insolubilization of α-crystallin during maturation is that it consumes soluble α-crystallins that then become unavailable to chaperone proteins in stressed lenses.

Recent evidence suggests that the proteases causing truncation of α-crystallins during maturation and aging in rodent lenses are a combination of the calpain class proteases m-calpain and Lp82 (Ma et al., 1999). The species of αA-crystallin missing 5-residues from its C-terminus in rodent lenses is specifically produced by Lp82 (Chapter 4). However, the protease(s) removing 5 amino acids from the C-terminus of αA-crystallin in human lenses (Lund et al., 1996) (Takemoto, 1995) remains unknown, since human lenses contain no Lp82 (Fougerousse et al., 2000).

Mouse lenses also underwent extensive truncation of β-crystallin N-terminal extensions during maturation. These truncated β-crystallins were also selectively found in the insoluble fraction of the lens. Similar truncation of β-crystallin N-terminal extensions also occurs during maturation in rat lens, and studies of cleavage site

specificity have implicated calpains as the proteases most likely responsible (David et al., 1994a). Furthermore, similar to β-crystallins in rat lens, mouse lens β-crystallins become insoluble in vitro following removal of portions of their N-terminal extensions by calpains (Fukiage et al., 1997). Analysis of crystallins from mouse lenses with experimentally induced cataracts also suggests that proteolysis of crystallins is accelerated due to a loss of calcium homeostasis and inappropriate activation of calpains (David et al., 1994b). Lenses from transgenic and knockout mice with cataracts will likely exhibit similar accelerated truncation of α and β-crystallins secondary to the primary genetic defect that initiates cataract.

Analysis of insolubilized γ-crystallins suggested that increased acidification of all six γA-F subunits may partially contribute to their insolubilization. The nature of the modification causing the decreased pI was not investigated, but could be deamidation, phosphorylation, or very limited proteolysis. Proteolysis could decrease the pI of γ-crystallins without significantly altering the relative migration on SDS-PAGE, since residue 2 in all γ-crystallins is lysine. Acidification of γS-crystallin may not occur, because unlike the other γ-crystallins it is N-acetylated and resistant to aminopeptidase activity.

In conclusion, these results provide baseline data that will facilitate the analysis of modified crystallins appearing in cataractous mouse lens. The 2-DE maps produced by identification of proteins by LC-MS analysis can be directly compared to similar 2-DE gels run in other laboratories. Two-DE gel separation coupled with LC-MS analysis of in-gel digests or eluted whole proteins was also demonstrated as a useful technique to identify crystallin modifications. A comprehensive analysis of these modifications in cataractous mouse lenses may provide the necessary information to model how these alterations cause insolubilization and light scatter. The information is particularly useful when compared to similar analysis of human crystallins.

Chapter 3

Purification and Characterization of Lens Specific Calpain (Lp82) from Bovine Lens

Yoji Ueda, Thomas R. Shearer, and Larry L. David

Department of Animal Sciences

Summary

Ubiquitous type m-calpain and lens specific Lp82 calpain were separated and partially purified from fetal bovine lens and the enzymatic characteristics were compared. Lens m-calpain required 200 μM calcium for 1/2 maximal activity, while Lp82 required 30 μM. Both types of calpains were inhibited by 0.1 mM E64, and 5 mM iodoacetamide, but not by 1 mM phenylmethylsulfonyl fluoride. Lp82 was insensitive to 1 μM calpastatin peptide while m-calpain was effectively inhibited. In the presence of calcium, m-calpain lost most of its activity within 2 hours, while Lp82 was continually active for 18 hours. Both calpains cleaved the natural substrates βA3 and αB crystallins in a similar manner. However, incubation of αA crystallin with m-calpain removed 10 amino acid residues from its C-terminus, while incubation with Lp82 removed only 5 residues. The latter truncation product of αA was also found *in vivo*. These data suggested that Lp82 may have a more important role than m-calpain in modification of crystallins during lens maturation.

Introduction

Calpains are calcium-dependant cytosolic proteases found in most animal tissues. Ubiquitous type (m- and μ-) calpains are the most common calpain isoforms. Additionally, several tissue specific forms of calpains have been found in the last decade (Sorimachi et al., 1994). One of these tissue specific calpains is muscle p94. While the p94 gene was once believed to be expressed only in muscle tissue, low levels of transcripts are found in other tissues, and a splice variant of p94, called Lp82, was recently described in rodent lenses (Ma et al., 1998a). Lp82 is a prevalent calpain isoform in both young rat and mouse lens (Shearer et al., 1998; Ma et al., 1999). This abundance suggested that Lp82 may be involved in maturation and cataract formation in rodent lens.

In lens, major substrates for calpains are the crystallins. Crystallins are a family of structural proteins responsible for assuring the transparency of the lens. Three main types of crystallins found in mammalian lens are called α-, β-, and γ-crystallins. The major functions of the β- and γ- crystallins may be the maintenance of structural integrity, transparency, and a high index of refraction in lens. An additional role of α-crystallin is the protection of other crystallins from aggregation and precipitation (Horwitz et al., 1999). Truncation of the C-terminus of α-crystallins inhibits their ability to maintain the solubility of other crystallins (Kelley et al., 1993; Takemoto, 1994), and truncation of the N-terminus of β-crystallins alters their interactions and results in precipitation (Shearer et al., 1995). Cleavage of α- and β-crystallins, as described above, occurs during lens maturation, and is accelerated during experimental cataract (Shearer et al., 1997). The similarity of truncation sites in β-crystallins *in vivo* with truncation sites *in vitro* by purified m-calpain suggested that this protease may be responsible for cleaving crystallins (David et al., 1994a). However, the more recent discovery of lens Lp82 suggested that proteolysis of crystallins by Lp82 may also be important.

To investigate whether Lp82 is in fact responsible for crystallin truncation, substrate specificity of the enzyme needed to be clarified. In previous studies, Lp82 was isolated from very small young rat lenses, which limited the amount of the enzyme obtained (Ma et al., 1998b). In this study, we chose to purify Lp82 from fetal bovine lens so that its enzymatic activity and substrate specificity could be compared to m-calpain. Several unique properties of Lp82 were identified that suggested it may be more active *in vivo* than lens m-calpain. Most notably, Lp82 was capable of partially degrading lens αA-crystallin similar to the cleavage occurring *in vivo*.

Experimental Procedures

Purification of bovine calpains

Lenses were obtained from fetal bovine eyes (Pel-Freez Biologicals, Rogers, AR). Decapsulated lenses were homogenized on ice at a ratio of eight lenses/10 ml buffer A containing 20 mM Tris (pH7.5), 1 mM EGTA, 1 mM EDTA, and 10 mM 2-mercaptoethanol. The lens homogenate was centrifuged at 20,000 xg for 1 hour at 4 °C and the supernatants were kept for further enzyme purification. Both m-calpain and Lp82 were purified using three sequential chromatography steps as before (David et al., 1992), with the following modifications. The supernatant was first applied to an 18 x 5 cm column of Macro-Prep DEAE support (BioRad laboratories, Richmond, CA) at 4 °C. The column was washed for 1 hour with buffer A at a flow rate of 4 ml/min. Bound proteins were then eluted with a linear gradient of 0-450 mM NaCl in buffer A over 3 hours. Fractions containing protease activity were determined as described below, and the Lp82 peak eluting at 240 mM NaCl and m-calpain eluting at 390 mM NaCl were collected. Each enzyme fraction was then individually concentrated by ultrafiltration (YM10 filter, Millipore Corporation, Bedford, MA) and applied to a 95 x 2.5 cm gel filtration column of Sephacryl S-300HR (Pharmacia, Piscataway, NJ) equilibrated with buffer A containing 100 mM NaCl. Proteins were eluted at 0.4 ml/min and active fractions pooled and concentrated. The partially purified Lp82 and m-calpain were then diluted 1:3 with buffer A containing 2 M $(NH_4)_2SO_4$ and injected onto a TSK phenyl 5-PW HPLC hydrophobic interaction column (TosoHaas, Montgomery, PA) equilibrated with buffer A containing 0.5 M $(NH_4)_2SO_4$. Proteins were eluted by a 30 minute linear, decreasing gradient of 0.5 – 0 M $(NH_4)_2SO_4$ in buffer A at 1.0 ml/min. The active fractions were again concentrated by ultrafiltration.

As an alternative source of m-calpain, fetal bovine heart was also obtained from Pel-Freez Biologicals and the enzyme was purified as described before (David et al., 1992). Purified m-calpain was aliquoted and stored in –20°C with 20% glycerol.

Identification of purified calpains

The protein composition of the enzyme preparations following each chromatography step was determined by SDS-PAGE using pre-cast 1.0 mm thick, 8 x 8 cm 10% Bis-Tris gels (Novex, San Diego, CA), and staining with Coomassie Blue.

Calpains were identified on immunoblots using m-calpain and Lp82 polyclonal antibodies, produced in rabbits using peptides either against the N-terminus of Lp82 (Ma et al., 1999), or Domain 3 of m-calpain (peptide sequence: DTLTCDSYKKWKLTKMDGNWRRG). Binding of the antibody to the enzyme was visualized with alkaline phosphate conjugated secondary antibody and BCIP/NBT (Bio-Rad, Hercules, CA).

Protease activity assay

Calcium-activated protease activity was identified using BODIP FL labeled casein as a substrate (EnzChek protease assay kit #E-6638, Molecular Probes, Eugene, OR). Casein substrate stock solution was diluted to 0.1 mg/ml in buffer A. The stock solution was diluted 10 times with buffer A to make the working solution. All protease assays were performed in 96 well flat bottom ELISA plates. The following were added to each well: 10 µl casein working solution, 160 µl buffer A (containing only 1 mM chelating agent), and 10 µl of enzyme fraction. Calcium-dependent proteolysis was initiated by adding 20 µl of 21 mM $CaCl_2$ to the well and incubating at 37 °C for 30 minutes. The proteolysis was then stopped by the addition of 30 µl of 50 mM EGTA. Fluorescence of the samples was then determined at 535 nm after excitation at 485 nm. Free BODIP FL dye (10 mM) was dissolved in methanol and was further

diluted serially in buffer A and used as a fluorescent standard to determine the activity of calpains. One unit of activity was defined as the amount of enzyme that increased fluorescence over 30 minutes equal to the fluorescence of 1 nmole free BODIP FL.

Calcium activation, pH optimum, inhibitors, and time assays

All assays for comparison of m-calpain and Lp82 enzymatic activities were performed using the fluorescence casein assay described above. For determination of calcium activation of m-calpain and Lp82, buffer was prepared without EDTA or EGTA, containing 0 to 1000 μM $CaCl_2$. For the pH optimum assay, 20 mM imidazole was added to the standard buffer A. The pH of the Tris/imidazole buffer was then adjusted between 5.8 and 7.8. Inhibition of m-calpain and Lp82 was measured by addition of either 1 μM calpastatin (recombinant, human, Calbiochem Corporation, La Jolla, CA), 0.1 mM E64 (Peptide Institute, Osaka, Japan), 5 mM iodoacetamide, or 1 mM phenylmethylsulfonyl fluoride (PMSF). To compare the time-dependent inactivation of m-calpain and Lp82, proteolytic activity was stopped at 0, 0.5, 1, 2, 6, and 18 h by addition of 5 mM iodoacetamide. Trypsin, known to maintain proteolytic activity for as long as 24 hours under the given assay condition, was incubated in parallel with m-calpain and Lp82 to ensure that the casein substrate was not depleted when the increase in fluorescence reached a plateau.

Lens crystallin cleavage by calpains---Bovine α-crystallin aggregate containing both αA and αB subunits was purified from fetal bovine lenses by gel filtration purification as described before (David and Shearer, 1986). For βA3-crystallin, *E. coli* BL21(DE31) expressing recombinant βA3-crystallin was expressed and purified (Werten et al., 1996). Twenty μg of each of these proteins were incubated in a 50 μl reaction mixture of buffer A containing m-calpain or Lp82, with or without 2 mM free $CaCl_2$ for 6 hours at 37 °C. Ten units of caseinolytic activity of either enzyme was sufficient to cleave βA3-crystallin. For α-crystallins, equal caseinolytic activities of both enzymes were also initially used, however, under these

conditions, α-crystallins were not sufficiently cleaved by m-calpain so the activity of this enzyme was increased by a factor of two in the incubation mixture. Enzyme reaction was stopped by addition of acetonitrile (final 10% concentration).

Bovine lens insoluble protein preparation---The water insoluble fraction of both fetal and adult bovine lens proteins were isolated by centrifugation as above, washed once, then dissolved in buffer containing 20 mM Tris (pH 7.5) and 6 M urea using sonication. The sample was then centrifuged at 20,000 x g for 30 minutes and the urea-solubilized proteins removed in the supernatant.

Mass determination of crystallins

Proteolysis of crystallins was determined by SDS-PAGE and mass spectrometry. The incubation mixture, 15 µl, was mixed with 6 µl of 4x sample buffer and loaded onto pre-cast 10% polyacrylamide mini-gels (NOVEX) and separated by electrophoresis. Digested and undigested crystallins were then visualized using Coomassie Blue. For accurate mass analysis, 10 µg of the digested crystallin or lens insoluble protein fraction was injected onto either a 2.1 x 250 mm C4 column (Vydac, Hesperia, CA) or a 0.5 x 150 mm Targa C18 column (Higgins Analytical, Mountain View, CA) coupled to an electrospray ionization ion trap mass spectrometer (model LCQ, ThermoQuest, San Jose, CA). Proteins were eluted using a 10 – 50% acetonitrile gradient containing either 0.1% acetic acid (Higgins column) or 0.05% TFA (Vydac column). Mass accuracy of the instrument was monitored using horse myoglobin and was better than 0.01%. Mass spectra were deconvoluted and protein masses were calculated using Bioworks software (ThermoQuest).

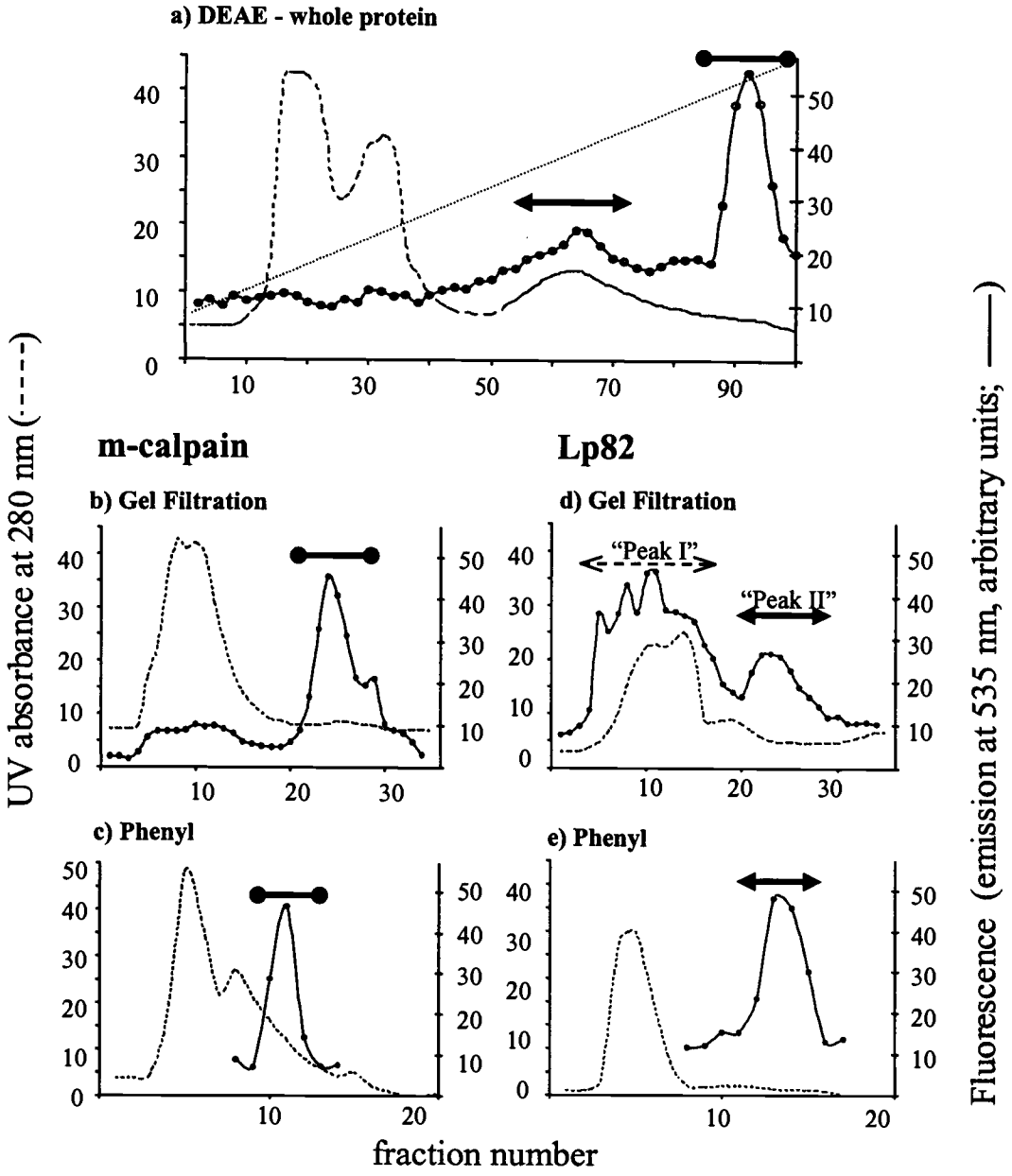

Figure 3.1. Purification of m-calpain and Lp82 from fetal bovine lens. Both protein peaks (dashed line) and proteolytic activity peaks (solid line) are shown on each of the consecutive chromatographs. In each panel the fractions under the bar with solid circles contained m-calpain, and the fractions under the bar with arrows contained Lp82. a) Separation of m-calpain and Lp82 from fetal bovine lens soluble protein by DEAE. DEAE separated m-calpain or Lp82 fractions were further purified by gel filtration (b and d). Note that DEAE purified Lp82 contained two major proteolytic peaks after the gel filtration separation in d. Peak one (dashed bar with arrows) contained leucine aminopetidase activity (see text), and was not further purified, peak II (solid bar with arrows) contained Lp82 activity. A phenyl column was used for the final purification of m-calpain (c) and Lp82 (e).

Figure 3.2. SDS-PAGE of purification steps and immunoblot of purified m-calpain and Lp82. Molecular weight markers are on the left and indicated by "MW", with their corresponding molecular weight in kDa. a) The protein profile following each purification step is shown. Lane 1, whole lens soluble protein; lane 2, m-calpain fraction after DEAE; lane 3, m-calpain fraction after gel filtration; lane 4, m-calpain fraction after phenyl column; lane 5, Lp82 after DEAE separation; lane 6, Lp82 after gel filtration; lane 7, Lp82 after phenyl column. Bands corresponding to the molecular weight of m-calpain (closed arrow) and Lp82 (open arrow) are indicated. Phenyl purified m-calpain and Lp82 were immunoblotted with polyclonal antibody against the third domain of m-calpain (b) or the N-terminus of Lp82 (c).

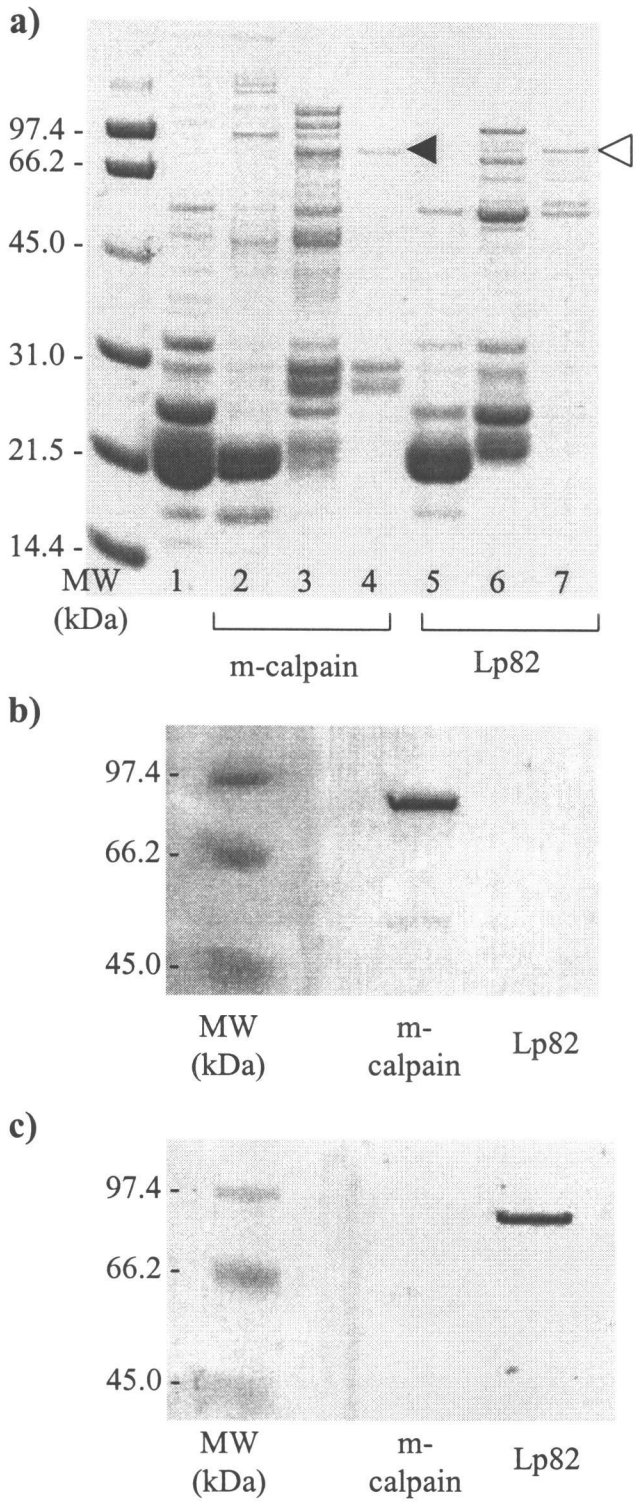
a)
97.4 -
66.2 -
45.0 -
31.0 -
21.5 -
14.4 -
MW (kDa)
1
2
3
4
5
6
7
m-calpain
Lp82
b)
97.4 -
66.2 -
45.0 -
MW (kDa)
m-calpain
Lp82
c)
97.4 -
66.2 -
45.0 -
MW (kDa)
m-calpain
Lp82

Figure 3.2

Results

Purification of bovine lens calpains

The chromatograms and relative proteolytic activities during sequential purification of m-calpain and Lp82 of bovine lens are shown in Fig. 3.1. Two major proteolytic activities were found in DEAE separated fetal bovine lens fractions (Fig. 3.1a). These proteolytic activities appeared only when calcium was added to the incubation mixture. Based on the elution positions of m-calpain and Lp82 in rat lens (Ma et al., 1998a), the first peak contained Lp82 activity and the second peak contained m-calpain activity. The m-calpain peak isolated during DEAE chromatography produced single proteolytic peaks during gel filtration and phenyl hydrophobic interaction chromatography (Fig. 3.1b,c). Following the three purification steps, the 80 kDa band of the catalytic subunit of m-calpain was visible by SDS-PAGE (Fig. 3.2a lane 4). The identity of the copurifying bands at approximately 27 kDa were unknown, but could be the regulatory subunit of m-calpain. The identity of the 80 kDa catalytic subunit of m-calpain was confirmed by immunoreaction with a m-calpain antibody (Fig. 3.2b), and by mass spectrometric analysis of in-gel trypsin digests (data not shown).

When the peak containing Lp82 from the DEAE column was further separated by gel filtration, two proteolytic peaks were observed (assigned as peak I and peak II; Fig 3.1d). Peak I eluted from the gel filtration column with α-crystallin. The protease in this peak did not react with antibody against m-calpain or Lp82, and mass spectrometric analysis of an in-gel trypsin digest of a minor 50 kD band in the preparation identified leucine aminopeptidase (data not shown). Therefore, Lp82 and leucine aminopeptidase coelute during DEAE chromatography of bovine lens soluble protein. Peak II containing the Lp82 activity was further purified by phenyl hydrophobic interaction chromatography (Fig. 3.1e). The identity of Lp82 in the final preparation was shown by the immunoblot with Lp82 antibody (Fig. 3.2c), and by

Figure 3.3. Comparison of m-calpain and Lp82 enzymatic properties. Fluorescently labeled casein was incubated with either m-calpain (●), or Lp82 (▲) under various conditions. a) Enzyme activation by different levels (0, 10, 25, 50, 100, 250, 500, and 1000 μM) of calcium. The extent of activation for each enzyme was significantly different ($p<0.05$) at 25 to 250 μM concentrations of calcium. b) Enzymes were incubated under various pH conditions (5.8, 6.1, 6.4, 6.7, 7, 7.3, and 7.6). The extent of activation was significantly different ($p<0.05$) at pH 6.7, 7, and 7.2. c) The progress of casein proteolysis was measured over time (0, 0.5, 1, 2, 6, and 18 hours). Unlike the Lp82 sample, the fluorescence of the m-calpain sample did not significantly increase after 2 hours of incubation ($p<0.05$). d) Sensitivity of m-calpain (solid bar) or Lp82 (white bar) to various (1 μM calpastatin, 0.1 mM E64, 5 mM iodoacetamide, or 1 mM PMSF) inhibitors. The extent of inhibition was only significantly different during incubation with calpastatin ($p<0.05$). Error bars indicate standard error of mean (n=4).

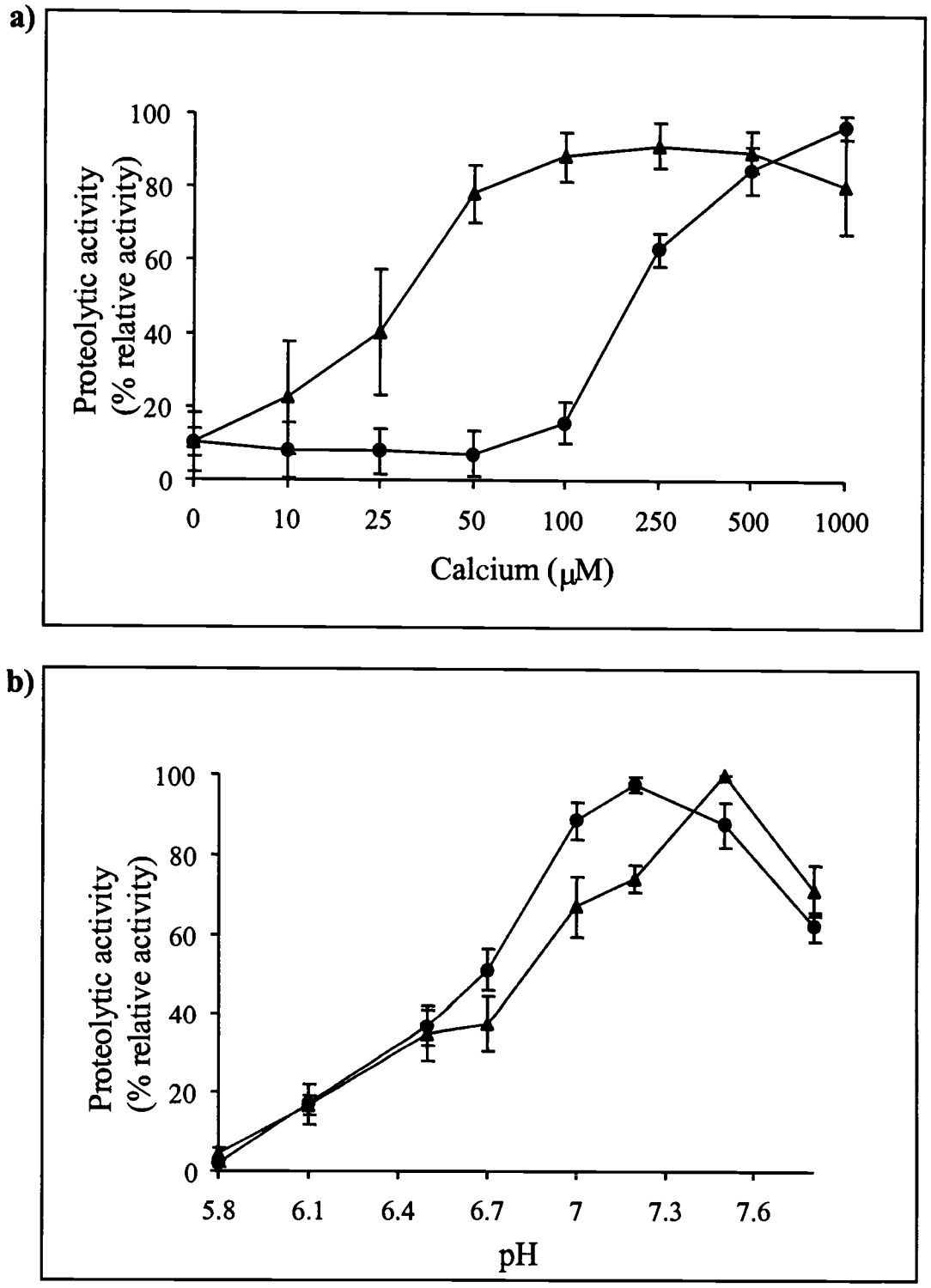
a)
Proteolytic activity (% relative activity)
100
80
60
40
20
0
0
10
25
50
100
250
500
1000
Calcium (μM)
b)
Proteolytic activity (% relative activity)
100
80
60
40
20
0
5.8
6.1
6.4
6.7
7
7.3
7.6
pH

Figure 3.3

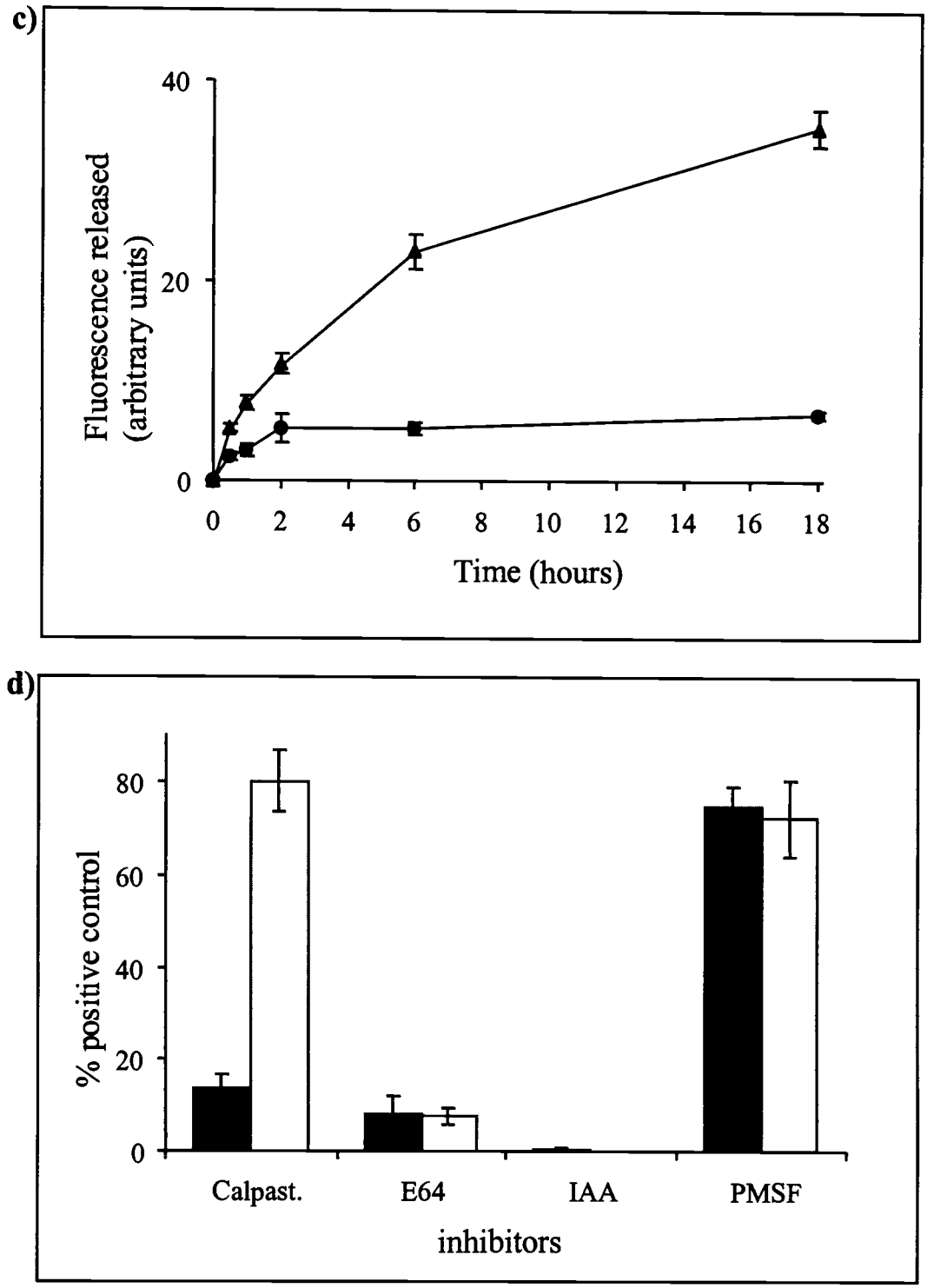

Figure 3.3 - *continued*

mass spectrometric analysis of an in-gel trypsin digest of the 82 kD band belonging to the catalytic subunit of Lp82 (data not shown). The identity of the species directly below the 82 kD band of Lp82 (Fig. 3.2, lane 7) are unknown, but may be autolytic breakdown products of the enzyme (Nakamura et al., 1999b). The presence of other proteases in the final enzyme preparations were negligible because all proteolytic activity against casein was calcium-dependent. Furthermore, the Lp82 fraction contained little or no μ-calpain, because the calcium-dependency of this fraction was too high (Fig. 3.3a), and μ-calpain elutes from DEAE columns much earlier at 100 mM NaCl (Yoshida, 1985). The activity of μ-calpain was not observed in Fig 1a because this enzyme coeluted with calpastatin, the endogenous inhibitor of calpains. Purified Lp82 and m-calpain were stored at 4°C in the presence of 2 mM DTT and used for the enzymatic studies below.

Properties of m-calpain and Lp82

Activity of m-calpain and Lp82 reached 1/2 maximum at approximately 200 μM and 30 μM calcium, respectively (Fig. 3.3a). Lp82 exhibited proteolytic activity with as low as 10 μM of calcium, whereas, m-calpain required 100 μM to be activated. The pH optimum of m-calpain and Lp82 was 7.2 and 7.5, respectively (Fig. 3.3b). The two enzymes exhibited markedly different rates of inactivation due to autolysis during incubation with calcium. There was very little additional proteolysis of labeled casein by m-calpain following a 2 hour incubation (Fig. 3.3c). In contrast, Lp82 retained significant proteolytic activity against the casein substrate even after 18 hours of incubation.

The effect of various inhibitors on proteolytic activity of m-calpain and Lp82 was also examined (Fig. 3.3d). Both m-calpain and Lp82 showed a decrease in activity to less than 10% of the positive control when treated with 0.1 mM E64 or 5 mM iodoacetamide. Both enzymes were insensitive to 1 mM PMSF, a serine protease inhibitor. However, there was a significant difference in inhibition of m-calpain and

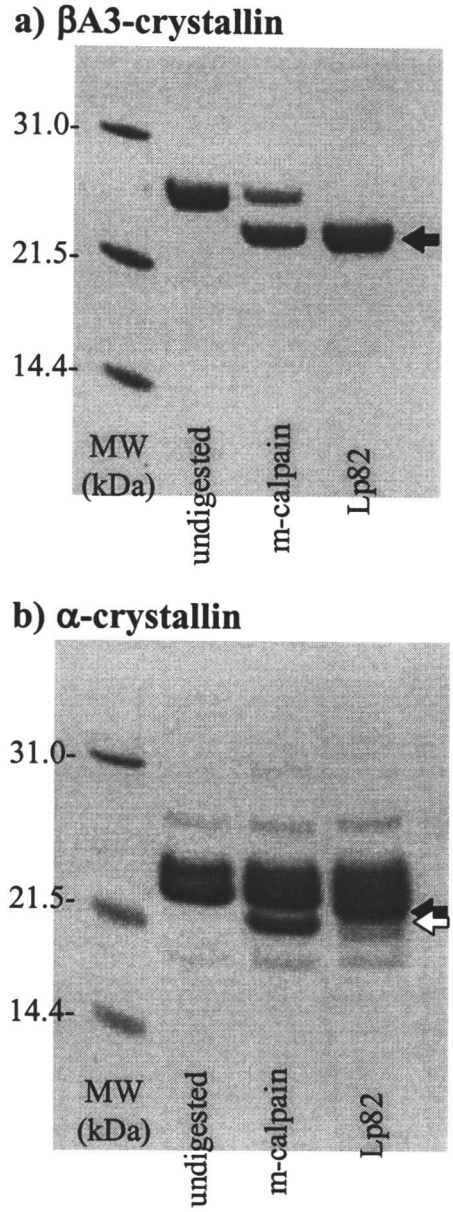

Figure 3.4 SDS-PAGE of lens crystallins incubated with m-calpain or Lp82. Molecular weight markers are on the left lanes indicated by "MW", with their corresponding molecular weight in kDa. Lane 1, undigested crystallin as a negative control; lane 2, m-calpain digestion; lane 3, Lp82 digestion. (a) Recombinant βA3 crystallin was incubated with or without proteases overnight at 37°C in the presence of calcium. The solid arrow indicates the βA3 digestion product. (b) Alpha-crystallins purified from bovine lens were incubated with or without proteases as in (a). The solid arrow indicates the major αA proteolytic product produced by Lp82, and the white arrow indicates the major αA proteolytic product produced by m-calpain. It was impossible to resolve the proteolytic products of αB crystallin by SDS-PAGE due to overlapping bands around 21 to 22 kDa.

Figure 3.5 Mass determination of cleaved crystallins by liquid chromatography/mass spectrometry. Crystallins were incubated overnight in absence (control; top panels) or presence of either m-calpain or Lp82 (middle and bottom panels, respectively). After dilution of the incubation mixture in 10% acetonitrile, samples were separated by a C4 column and analyzed on-line by ESI-MS. a) recombinant βA3, b) αA-crystallin, and c) αB-crystallin. The mass of intact proteins (control) and major proteolytic products of specific calpains are indicated in **bold**. d) Amino acid sequences of cleavage sites of each crystallin. Cleavage sites by m-calpain (solid arrow) and Lp82 (white arrow) are indicated.

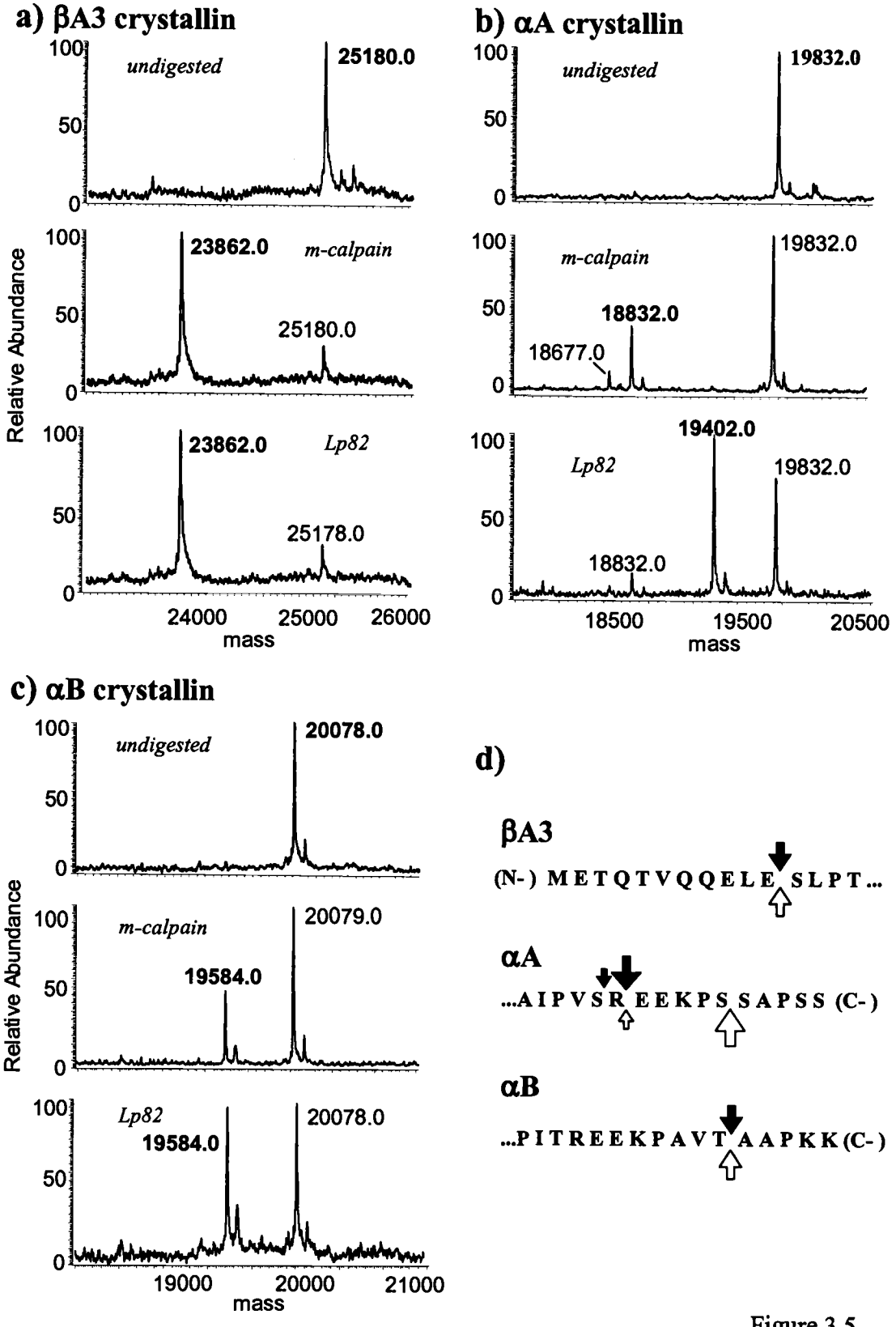
a) βA3 crystallin
undigested
25180.0
23862.0
m-calpain
25180.0
23862.0
Lp82
25178.0
Relative Abundance
24000
25000
26000
mass
b) αA crystallin
undigested
19832.0
m-calpain
19832.0
18832.0
18677.0
19402.0
Lp82
19832.0
18832.0
18500
19500
20500
mass
c) αB crystallin
undigested
20078.0
m-calpain
20079.0
19584.0
Lp82
19584.0
20078.0
Relative Abundance
19000
20000
21000
mass
d)
βA3
(N-) M E T Q T V Q Q E L E S L P T ...
αA
...A I P V S R E E K P S S A P S S (C-)
αB
...P I T R E E K P A V T A A P K K (C-)

Figure 3.5

Lp82 by calpastatin, the endogenous inhibitor of μ- and m-calpains. One μM calpastatin inhibited m-calpain by 85%, while Lp82 was only inhibited by 20%.

Lens crystallin cleavage by calpains

To determine whether bovine m-calpain and Lp82 cleave βA3-, αA- and αB-crystallin differently, 20 μg of each protein was incubated with each enzyme. Both analysis by SDS-PAGE (Fig. 3.4a) and ESI-MS (Fig. 3.5a) indicated that both calpains cleaved βA3 in a similar manner, removing 11 amino acids from the N-terminus, converting the mass of βA3 from 25,180 to 23,862. αB-crystallin was also cleaved similarly by both m-calpain and Lp82. Each enzyme removed 5 amino acid residues from the C-terminus of αB. This cleavage site is consistent with the conversion of αB mass from 20,078 to 19,584 (Fig. 3.5c). The small peaks to the right of each major αB species correspond to the phosphorylated forms of αB (80 mass unit increase; Fig. 3.5c). In contrast to βA3 and αB, m-calpain and Lp82 preferentially cleaved αA at different sites. m-calpain preferentially removed 10 amino acids (major, 18,832) and 11 amino acids (minor, 18,677) from the C-terminus of αA, while Lp82 preferentially removed 5 amino acids (major, 19,402) and 10 amino acids (minor 18,832) from the C-terminus of αA (Fig. 3.5b). The form of αA missing 10 amino acids from its C-terminus was not produced by m-calpain through intermediate removal of 5 amino acid residues. Incubation with less m-calpain did not produce the 19,402 species (data not shown).

The analysis of α-crystallins in the adult bovine lens detected major species with masses of 19,831 and 19,911, corresponding to the unmodified and phosphorylated forms of αA, respectively (Fig. 3.6). Additional minor forms of αA-crystallins were also specifically detected in the insoluble fraction of bovine lens with masses of 19,746, 19,481, and 19,402, corresponding to αA-crystallin missing 1 amino acid, 5 amino acids (phosphorylated form) and 5 amino acids

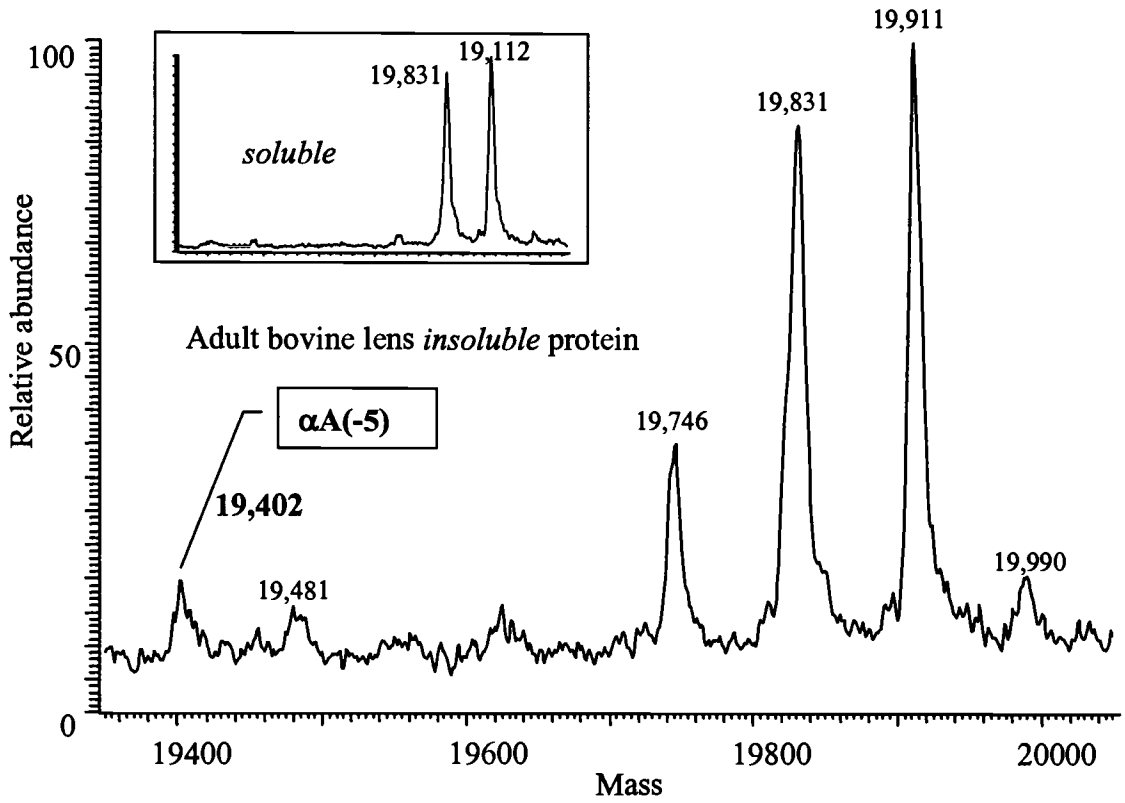

Figure 3.6. Identification of truncated αA-crystallin *in vivo*. The αA-crystallin fraction of insoluble adult bovine lens protein was analyzed by LC/MS. The major peak with mass of 19,911 was intact αA containing a single phosphorylation; the peak at 19,831 was unmodified αA; the peak at 19,746 was αA missing its C-terminal serine; the peak at 19,481 was αA missing 5 residues from its C-terminus and containing a single phosphorylation, and the peak at 19,402 was αA missing 5 residues from its C-terminus, αA(-5). Note that the truncated forms of αA were not present or at very low levels in adult bovine lens soluble protein (inlet), suggesting truncation causes insolubilization of αA-crystallin.

(unphosphorylated form) from the C-terminus, respectively. These truncated forms were absent from the soluble fraction of the same adult bovine lens (Fig. 3.6, insert).

Discussion

The present study identified various differences in the enzymological properties of two calpain family proteases isolated from bovine lens: m-calpain and Lp82. The lower calcium requirement, less sensitivity to inhibition by the endogenous calpain inhibitor calpastatin, and closer similarity of cleavage sites in αA-crystallin to those existing in vivo, suggested that Lp82 was more active in lens than other members of the calpain family. This is the first report describing the purification of Lp82. The methodology may be useful to further characterize the functions of this protease in lens, and by inference, to study p94, an alternate splicing form of Lp82 found in muscle, which due to the inclusion of protease sensitive sites through differential splicing, is too labile to be purified (Sorimachi et al., 1993b).

The relative amounts of Lp82 activity varied greatly between species. In young mouse and rat lens, zymographic assays found nearly equal or greater activities of Lp82 compared to m-calpain (Ma et al., 1999). Activities of Lp82 and m-calpain in young rodent lenses were also at least five fold higher than μ-calpain activities. Compared to young rodent lenses, the fetal calf lenses used in this study contained far lower activities of all calpains. This prevented the direct estimation of the relative activities of Lp82, m-calpain, and μ-calpain in calf lens by zymographic assay. However, due to its size, the calf lens was still a useful source for purification of Lp82. Both m- and μ-calpain have been prepared from this tissue previously (Yoshida, 1985). Unlike rodent and calf lens, human lens contained no Lp82 activity due to a stop codon in exon 1 of the human lens Lp82 transcript (Fougerousse et al., 2000). The differences in the relative activities and presence of Lp82 in lenses of various species may depend on the developmental physiology of the animal, such as the rate of lens maturation or longevity.

Several properties of Lp82 suggested that the enzyme is the major calpain isoform activity in rodent and bovine lenses. The calcium requirement for half-maximal activity of the other major calpain isoform, m-calpain, was approximately 200 μM, a value similar to the findings of previous reports (David and Shearer, 1986). In contrast, Lp82 was half maximally activated by 30 μM calcium, a value between that of μ- and m-calpain requirements (Yoshida, 1985; David and Shearer, 1986). Since free intracellular calcium levels in the 30 μM range have been reported in cataract lens (Hightower et al., 1987), Lp82 would be expected to undergo activation more readily than m-calpain. While this calcium level could also activate μ-calpain, the relative lower activity of this enzyme in lens (Yoshida, 1985; Ma et al., 1999) suggest that Lp82 is more active.

Similar to the results with rodent lens Lp82 (Nakamura et al., 1999b), purified bovine Lp82 was relatively insensitive to inhibition by calpastatin, the endogenous inhibitor of m- and μ-calpains (Maki et al., 1987). Since calpastatin was found in all lenses studied to date (Yoshida, 1985; David et al., 1989; Varnum et al., 1989), this again suggests that Lp82 may be most active *in vivo*.

m- and μ-calpains are known to undergo intermolecular autolysis, which is believed to transitorily activate the enzymes due to a lowering of their calcium requirements, and then cause inactivation due to more extensive degradation (Cong et al., 1989). Although Lp82 does autolyze (Nakamura et al., 1999b), our data showed that it remained active significantly longer than m-calpain. The significantly greater longevity of Lp82 may be due to its resistance to further degradation after its initial autolysis. Again, this finding supports the hypothesis that Lp82 exhibits greater activity *in vivo* than the other forms of calpain. The results also suggest that caution should be used in estimation of relative calpain activities *in vivo* using protease assays that are typically performed over a 30-60 min time period. m- and μ-calpains may exhibit greater activities during the initial time periods, but far less activity than Lp82 if incubations are performed overnight.

The relative insensitivity of lens Lp82 to autolysis is in contrast to its muscle specific spicing variant p94. The presence of additional amino acid sequences in an insert region called IS1 in p94, which is missing in Lp82, cause rapid turnover of p94, such that the protease cannot be purified from muscle (Sorimachi et al., 1993b; Ma et al., 2000). In contrast, the alternate spicing resulting in Lp82 in lens may have evolved to increase the stability of the protease in a tissue that rapidly losses its transcriptional capacity due to loss of organelles following differentiation of lens fiber cells (Bassnett and Beebe, 1992). Due to its greater stability, Lp82 may be useful to investigate the properties of p94, which is similar in sequence to p94 and contains the same cysteine protease domain. These studies are important, because mutations in p94 are a cause of type 2A limb-girdle muscular dystrophy in humans (Richard et al., 1995). Determining the natural substrates for p94 in muscle would greatly increase the understanding of this disease.

The natural substrates for calpains in lens include: cytoskeletal proteins (Yoshida et al., 1984a); membrane proteins, including the lens major intrinsic protein MIP26 (Schey et al., 1999), and connexin 50 (Lin et al., 1997); and crystallins, the major structural proteins of the lens (David and Shearer, 1986). This study focused on comparing the cleavage site specificity of Lp82 and m-calpain using βA3-, αA-, and αB-crystallins as substrates. Such data would be of potential use as markers for *in vivo* activities of Lp82 and m-calpain.

Due to the similarities in Lp82 and m-calpain cleavage sites, proteolyzed βA3- and αB-crystallins were uninformative regarding which protease was responsible for their degradation *in vivo*. Both m-calpain and Lp82 preferentially removed 11 amino acids from the N-terminus of βA3-crystallin *in vitro*. βA3-crystallin missing 11 amino acids from its N-terminus is also found *in vivo* in both young cow (Shih et al., 1998) and rodent lenses (David et al., 1994a), but undergoes removal of an additional 11 residues during further aging (Werten et al., 1999c). While the initial cleavage may be produced by either or both enzymes *in vivo*, the protease responsible for the additional cleavage remains unknown. Similarly, both enzymes removed 5 residues from the C-

terminus of αB-crystallin. This cleavage site was identical to the previously reported major m-calpain cleavage site in bovine αB-crystallin produced in vitro (Yoshida, 1986).

In contrast to βA3- and αB-crystallins, αA-crystallin was differentially cleaved by Lp82 and m-calpain. As previously reported, m-calpain preferentially removed 10 amino acids from the C-terminus of αA-crystallin (Yoshida, 1986), while the present report showed that Lp82 preferentially removed five amino acids from the C-terminus. This αA-crystallin cleavage site was also produced by partially purified rat lens Lp82 (Nakamura et al., 2000). Analysis of αA-crystallin from the water-insoluble protein of adult bovine lens detected a form of αA-crystallin also missing 5 residues from its C-terminus. An identical cleavage site in αA-crystallin was previously reported in various mammals (de Jong et al., 1974), including humans (Takemoto, 1995; Lund et al., 1996). Similar analysis of rat lens also detected the form of αA missing 5 residues from its C-terminus, but at much higher relative concentrations than found in cow or human lens (Chapter 4).

These data suggest that Lp82 is the calpain-family endopeptidase most active in lenses of young rodents and calf. These studies are important to the lens field, because: 1) calpains may play a role in the differentiation of lens epithelium to fiber cells, such as the initiation of apoptotic-like events (Tamada et al., 2000), 2) partial cleavage of β-crystallins by calpains during maturation may be required for dehydration of lens fiber cytosol to increase the refractive index of the lens (David et al., 1994a), and 3) unregulated proteolysis due to loss of calcium homeostasis may contribute to cataract in young lenses. For example, unscheduled proteolysis of β-crystallins causes their insolubilization and contributes to light scatter in experimental cataracts (Shearer et al., 1995), and loss of the C-terminus of α-crystallins disrupts their ability to act as chaperones to maintain the solubility of other lens proteins (Kelley et al., 1993; Takemoto, 1994). While Lp82 may be the major protease responsible for these events in animal lenses, current studies are investigating other

proteases in the calpain family that are expressed in human lens to determine if they play a role analogous to Lp82 in animal lens.

Acknowledgement

The authors thank Dr. Hong Ma for providing antibodies and Dr. Paul Werten for providing recombinant βA3 crystallin. This work was supported by NIH grant EY12016 (LLD) and EY05786 (TRS).

Chapter 4

Comparison of the *In Vitro* and *In Vivo* C-terminal Cleavage Sites Produced by m-Calpain and Lp82 on Rat α-Crystallins

Yoji Ueda, Chiho Fukiage, Marjorie Shih, Thomas R Shearer, and Larry L David

Department of Animal Sciences

Abstract

Molecular chaperone activity of lens α-crystallins is reduced by loss of the C-terminus. The purposes of this experiment were to: 1) determine the cleavage sites produced *in vitro* by ubiquitous m-calpain and lens specific Lp82 on α-crystallins, 2) identify α-crystallin cleavage sites produced *in vivo* during maturation and cataract formation in rat lens, and 3) estimate the relative activities of Lp82 and m-calpain by appearance of protease specific cleavage products *in vivo*.

Total soluble protein from young rat lens was incubated with purified recombinant m-calpain or Lp82 and 2 mM Ca^{2+}. Resulting fragmented α-crystallins were separated by two-dimensional gel electrophoresis. Eluted α-crystallin protein spots were analyzed by mass spectrometry. Cleavage sites on insoluble α-crystallins were similarly determined in maturing rat lens nucleus and in selenite induced nuclear cataract rat lens nucleus.

In vitro proteolysis of α-crystallins by Lp82 produced a unique cleavage site by removing 5 residues from the C-terminus. m-Calpain produced a unique truncation by removing 11 residues from the C-terminus. Other truncation sites common to both calpain isoforms resulted from the removal of: 8, 10, 16, 17, and 22 residues from the C-terminus. *In vivo*, the protease specific truncations removing 5 and 11 residues were both found in maturing lens, while only the truncation removing 5 residues was found in selenite cataract. All other calpain isoform truncation sites were also observed in both cataract and mature rat lens. Lp82 showed a 6 fold lower Ca^{2+} activation requirement than m-calpain.

Using uniquely truncated αA-crystallins as *in vivo* markers, Lp82 and m-calpain were both found to be active during normal maturation of rat lens, while Lp82 seemed especially active during selenite cataract formation. These C-Terminal truncations decrease chaperone activity of α-crystallins, possibly leading to the observed increases in insoluble proteins during aging and cataract.

Introduction

α-Crystallin protein in lens is related to the small heat shock family of proteins (Ingolia and Craig, 1982). Since lens proteins have very little turnover, α-crystallin functions as a molecular chaperone to prevent denaturation of other lens proteins (Horwitz et al., 1992). The C-terminus is essential since loss of 16 amino acid residues of C-terminus from αA-crystallin caused a loss of 50% of its chaperone activity (Takemoto, 1994).

Truncation of lens crystallins is a common feature of both aging and cataract formation. A number of experiments revealed that calcium activated protease (calpain) was involved in formation of cataracts induced by selenite (David et al., 1992), galactose (Azuma et al., 1990), diamide (Azuma and Shearer, 1992), the hypocholesterolemic drug U18666A (Chandrasekher and Cenedella, 1993), and in hereditary Shumiya cataract rat (Inomata et al., 1997). One of the ubiquitous calpains, m-calpain, has been credited with the proteolysis of α-, and β-crystallins during cataractogenesis. Incubation of αA-crystallin with m-calpain reduced chaperone activity and produced truncated forms of αA similar to those observed in cataracteous lenses (Kelley et al., 1993). A recently discovered lens-specific calpain, a splice variant of calpain 3 termed Lp82, has been also shown to have a role in rodent cataract formation (Nakamura et al., 2000).

The primary truncation sites on β-crystallins *in vivo* are at the N-terminus where the cleavage sites can be determined by Edman sequencing (David et al., 1994a). In contrast, determination of the exact α-crystallin truncation sites have not been performed due to the lack of a convenient C-terminal sequencing method. To solve this problem, protein identification and whole mass determination by mass spectrometry has recently become a powerful tool in determination of C-terminal sequence (Cohen and Chait, 1997; Courchesne and Patterson, 1999). Therefore, the purposes of the present report were to use mass spectrometry to: 1) determine *in vitro* cleavage sites produced by m-calpain and Lp82, 2) compare the C-terminal cleavage

sites to those produced *in vivo* during aging and cataract formation, and 3) use this information to determine if the activity of one lens calpain isoform is dominant *in vivo*.

Methods

Preparation of rat lens

Lenses for protein isolation were obtained from normal 12-16 day-old or 6 week-old Sprague-Dawley rats (BK International, Fremont, CA), or cataract lens induced by injection of 30 μmol sodium selenite/kg body weight in 12 day-old rat (David, 1984). Treatment of animals conformed to the ARVO Statement for the Use of Animals in Ophthalmic and Vision Research. The lenses were dissected into cortex and nucleus and homogenized in 20 mM sodium phosphate (pH7.0), and 1.0 mM EGTA containing protease inhibitor (Complete Mini Protease Inhibitor Cocktail, Boehringer Mannheim, Indianapolis, IN) dissolved at 10 ml buffer/tablet (David et al., 1994a). Protein content was then assayed using the BCA method (Pierce Chemical Corp, Rockford, IL). Lens proteins were stored frozen at –80 °C until use.

Expression and purification of recombinant Lp82

The Lp82 cDNA from rat was cloned into a pFASTBAC HTb vector (Life Technologies, Inc., Rockville, MD) with a His tag on the N-terminus. This plasmid was transformed into DH10BAC (Life Technologies, Inc., Rockville, MD) competent cells containing the bacmid and the helper plasmid. Recombinant bacmid DNA containing Lp82 was isolated and used to transfect insect cells.

Transfection of Spodoptera frugiperda 9 (Sf9) insect cells was performed with recombinant Lp82 baculovirus and the titer of this virus was amplified up to 10^8

pfu/ml. The amplified Lp82 virus was infected to Sf9 cells and cells were cultured to express rLp82 protein for 3 days.

Cultured cells were sonicated in buffer containing 20 mM Tris (pH 7.5), 0.5 mM EGTA and 2 mM DTE. The soluble protein was obtained by centrifugation at 13000 g for 30 minutes. The soluble protein was purified with Ni-NTA (QIAGEN Inc, Valencia, CA) metal-affinity chromatography according to the manufacturer's protocol and fractionated by HPLC using a 7.5 mm ID x 7.5 cm DEAE 5PW column (TOSOH, Japan) with a linear 0.0-0.5 M NaCl gradient in buffer A containing 20 mM Tris (pH7.5), 1 mM EDTA, 1 mM EGTA and 2 mM DTE at 1 ml min^{-1} flow rate. ELISA was performed by absorbing 50 µl of each column fraction in 0.1 M $NaHCO_3$ buffer (pH 9.3) overnight onto 96 well flat bottom plates (Corning, New York, USA). The wells were blocked with 5% non-fat dry milk and incubated with Lp82 (1:1000 dilution) antibody for 1 hr (Ma et al., 1998b). rLp82 antigen was visualized using goat anti-rabbit alkaline phosphatase-conjugated secondary antibody and alkaline phosphatase substrate kit (Bio-Rad, Hercules, CA, USA). The rLp82 peak from DEAE fractions was concentrated by ultrafiltration (Microcon 10, Millipore) and then used in the experiments described below.

Incubation of lens proteins with calpains

Soluble proteins from lens cortex of 12-day old rats were diluted to 50 mg/ml in 20 mM Tris (pH 7.4) buffer. Endogeneous cysteine protease activity was inactivated by 5 mM iodoacetamide for 30 minutes at 37 °C, followed by addition of excess dithioerythritol to quench unreacted iodoacetamide. After the inactivation, 400 µg of protein was further diluted to 2.3 mg/ml in Tris buffer, and either 2.3 µg of recombinant rat m-calpain (Calbiochem-Novabiochem Corp., San Diego, CA), or recombinant Lp82 of equal caseinolytic activity were added. m-Calpain and Lp82 were then activated by adding $CaCl_2$ at a final 2 mM concentration, followed by

incubation at 37 °C for 3 hours. The reaction was stopped by addition of 10 mM EDTA and the mixture dried by vacuum centrifugation.

Two-dimensional electrophoresis (2-DE) of lens protein

Proteins were separated by 2-DE using immobilized pH gradient (IPG) gel strips (18 cm, pH 5-9) in the first dimension, followed by 12% SDS-PAGE in the second dimension as previously described (Lampi et. al. 2000). The gels were negatively stained by the imidazole-zinc procedure (Matsui et al., 1999). Immediately after the staining, images were captured using an Expression 1600 flat bed scanner (Epson America, Inc. Long Beach, CA) at a resolution of 200 dpi in 12-bit gray scale. Images were analyzed and protein spots were detected using Melanie 3 software (GeneBio, Geveva, Switzerland). The protein spots were then excised for analysis by mass spectrometry.

Mass measurement of proteins isolated from 2-DE gels

Protein elution from SDS-PAGE gels

For whole mass determination, proteins were eluted directly from 2-DE gels by passive diffusion. Excised gel pieces were pre-incubated twice for 15 minutes at room temperature by rotation in 1.7 ml microcentrifuge tubes containing 1 ml elution buffer (25 mM Tris (pH 8.8), 192 mM glycine, 1 mM thioglycolic acid, and 0.1 % SDS). The protein was then eluted by finely crushing the gel pieces using a modification of the method described by Castellanos-Serra et. al. (1996). Briefly, pre-incubated gel pieces were crushed through a 20 μm frit (Part number A-120X, Upchurch Scientific, Oak Harbor, WA) by removing the plastic rings surrounding the frit, placing it at the bottom of 500 μl glass air tight syringe, and forcing the gel pieces through the frit

using the syringe plunger. The gel particles left in the needle were collected by washing the syringe with additional 50 – 100 µl of elution buffer. After brief vortexing, the gel particles were sonicated in a 37 °C water bath for 30 minutes. The slurry was then filtered through 0.22 µm microcentrifuge filter (Micropure-0.22; Amicon, Beverly, MA) at 13,000 x g for 15 minutes, and the filtrate containing the eluted protein was analyzed by mass spectrometry.

Determination of eluted protein masses

The eluted protein was injected onto a 1.0 x 250 mm C4 column (214 MS C4, Vydac, Hesperia, CA), and masses were determined on-line by electrospray ionization mass spectrometry (ESI-MS) on a model LCQ iontrap (ThermoQuest, San Jose, CA). The flow rate was 25 µl/min with a linear gradient of 18-50% acetonitrile over 40 minutes in a mobile phase containing 0.1% acetic acid and 0.05% trifluoroacetic acid. Samples were autoinjected and concentrated/purified using a micro protein trap cartridge (Michrom Bioresources, Inc., Auburn, CA). Mass spectra of proteins eluted from the C4 column were deconvoluted using Xcalibur software with BioWorks (ThermoQuest). Mass accuracy of better than 0.02% was confirmed using horse myoglobin.

After mass determination, the truncation sites in the proteins were determined using PAWS (version 8.1.1) software to match measured masses with calculated masses of truncated species. The pI of identified truncated species were calculated using GeneWorks 2.5 software (Oxford Molecular Group Inc., Campbell, CA).

Calcium activation assay

For determination of the calcium activation requirements of recombinant m-calpain and Lp82, a fluorescent assay was performed using BODIP FL labeled casein as a substrate (EnzChek protease assay kit #E-6638, Molecular Probes, Eugene, OR).

The working substrate solution contained 0.01 mg/ml labeled casein in water. The assays were performed in 96 well flat bottom ELISA plates. The following were added to each well (200 µl total reaction mixture): 10 µl casein solution, 15 µl of diluted enzyme fraction, and 175 µl 20 mM Tris (pH 7.5) containing 2 mM DTT and CaCl2 to produce a final Ca^{2+} concentration ranging from 0 – 1000 µM. The plate was incubated at 37 °C for 1 hour. Fluorescence of the samples was then determined at 535 nm with excitation at 485 nm. Ten mM Free BODIP FL dye was dissolved in methanol and was further diluted serially in water and used as a fluorescent standard to calculate the enzyme activity. One unit of activity was defined as one nanomole of BODIP FL liberated by proteolysis in one hour.

Results

In vitro hydrolysis of α-crystallins by m-calpain and Lp82

To compare the *in vitro* breakdown patterns of α-crystallins, total soluble lens proteins containing intact α-crystallins were incubated with activated m-calpain and Lp82. m-Calpain and Lp82 readily hydrolyzed α-crystallins to 8 (Fig. 4.1b) and 10 (Fig.4.1c) major fragments, respectively. The general breakdown profile of α-crystallins appeared similar on 2-DE, except Lp82 caused the additional appearance of spot 8 and 9, as well as a triplet of spots marked with an asterisk (Fig. 4.1c).

To examine the specific cleavages producing the truncated α-crystallins, the species described above were isolated from 2-DE gels and analyzed by mass spectrometry. A summary of the measured masses is given in Table 1, along with the indicated missing residues. All Lp82 and m-calpain cleavage sites in α A and α B were at the C-termini. While having very similar positions on 2-DE gels, spot 1 produced by m-calpain (Fig. 4.1b) and spot 2 produced by Lp82 (Fig. 4.1c) were distinct. The m-calpain specific spot 1 (mass = 18,735) was produced by removal of 11 residues from the C-terminus of αA ($\alpha A_{1\text{-}162}$), while the Lp82 specific spot 2 (mass

Figure 4.1. Two-dimensional electrophoresis of soluble α-crystallins from: (a) 12-day-old rat lens cortex (undigested), (b) cortex incubated with m-calpain (m-calpain), and (c) cortex incubated with Lp82 (Lp82). Only the areas of the gels containing αA- and fragmented αB-crystallins are shown. Numbered arrows indicate major species of truncated α-crystallins (>1.5% of total protein added to the gel). The measured masses, predicted truncation sites, calculated masses, and calculated pI's of identified species are listed in Table 1. Species given the same number in b) and c) has similar masses and contained the same C-terminal truncation sites. The spots indicated by an asterisk were additional unique species produced by Lp82, but were not abundant enough for identification by whole mass analysis.

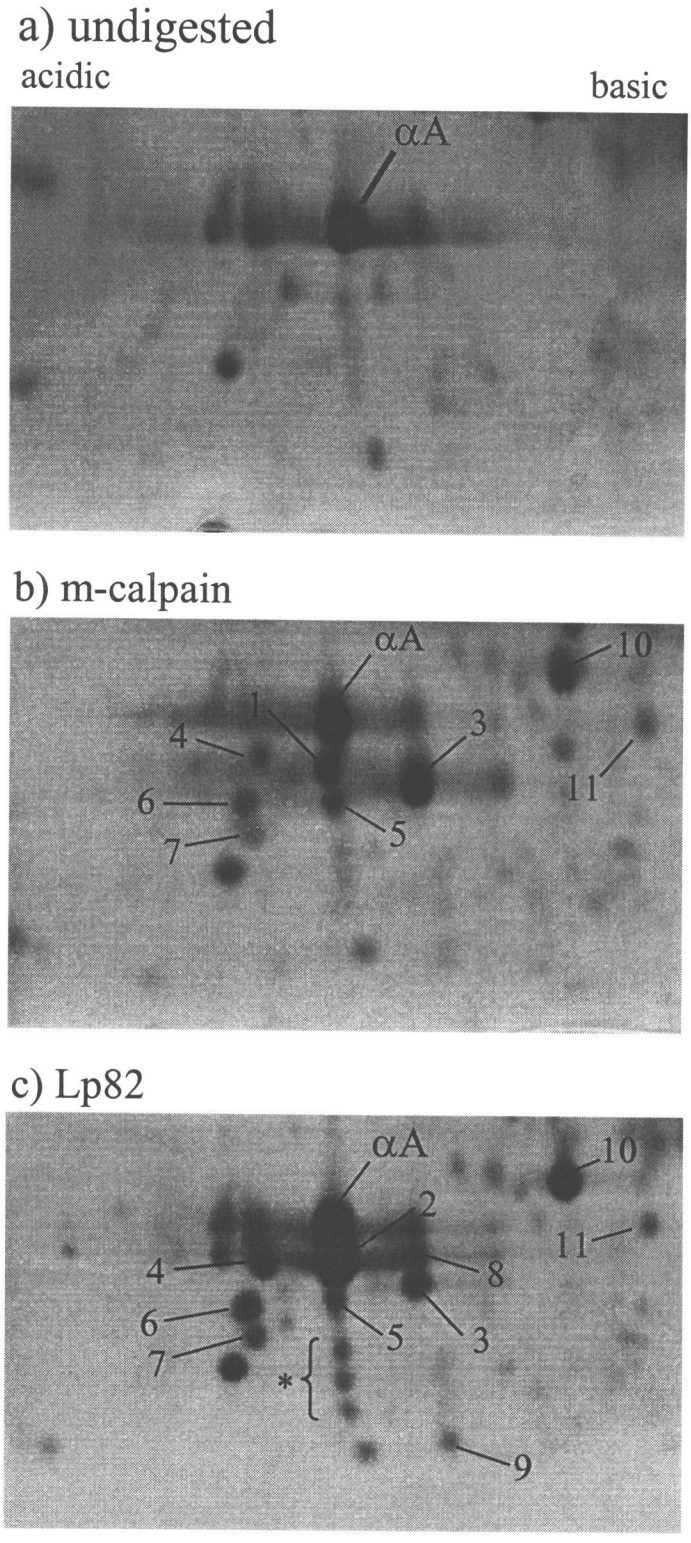
a) undigested
acidic
basic
αA
b) m-calpain
αA
10
1
3
4
11
6
5
7
c) Lp82
αA
10
2
11
4
8
6
5
3
7
*
9

Figure 4.1

Table 4.1. Masses and identities of truncated α-crystallins produced by incubation with Lp82 or m-calpain[a]

Spot No.	α-crystallin[b]	Residues missing from the C-terminus	Measured Mass *(m-calpain incubated)*	Measured Mass *(Lp82 incubated)*	Calculated Mass	Calculated pI
1	**αA_{1-162}**	**11**	**18,735**	**nd[c]**	**18,735**	**5.50**
2	**αA_{1-168}**	**5**	**nd**	**19,461**	**19,462**	**5.52**
3	αA_{1-163}	10	18,891	18,890	18,892	5.72
4	αA_{1-165} (acidic)[d]	8	19,149	19,147	19,149	5.54
5	αA_{1-157}	16	18,267	18,267	18,267	5.50
6	αA_{1-156}	17	18,111	18,112	18,112	5.27
7	αA_{1-151}	22	na[e]	17,629	17,630	5.29
8	αA_{1-168} (basic)[d]	5	nd	19,460	19,462	5.52
9	unknown	unknown	nd	na	-	-
10	αB_{1-170}	5	19,635	19,635	19,635	6.14
11	αB_{1-163}	12	18,880	18,880	18,880	6.33

a) Truncated α-crystallins produced by incubation with Lp82 or m-calpain and numbered in Fig. 1b and 1c were eluted from 2-DE gels of incubated proteins from lens cortex and their masses determined by electrospray ionization mass spectrometry. αA fragments in **bold** were unique in that they were Lp82 or m-calpain specific.

b) The numbers in lower case give the amino acid residues remaining following incubation. Intacat αA contains 173 residues, and intact αB 175 residues.

c) nd: not detected.

d) These species migrated to pIs either more acidic or basic than their predicted pIs (last column).

e) na: not analyzed or insufficient protein recovery for mass determination.

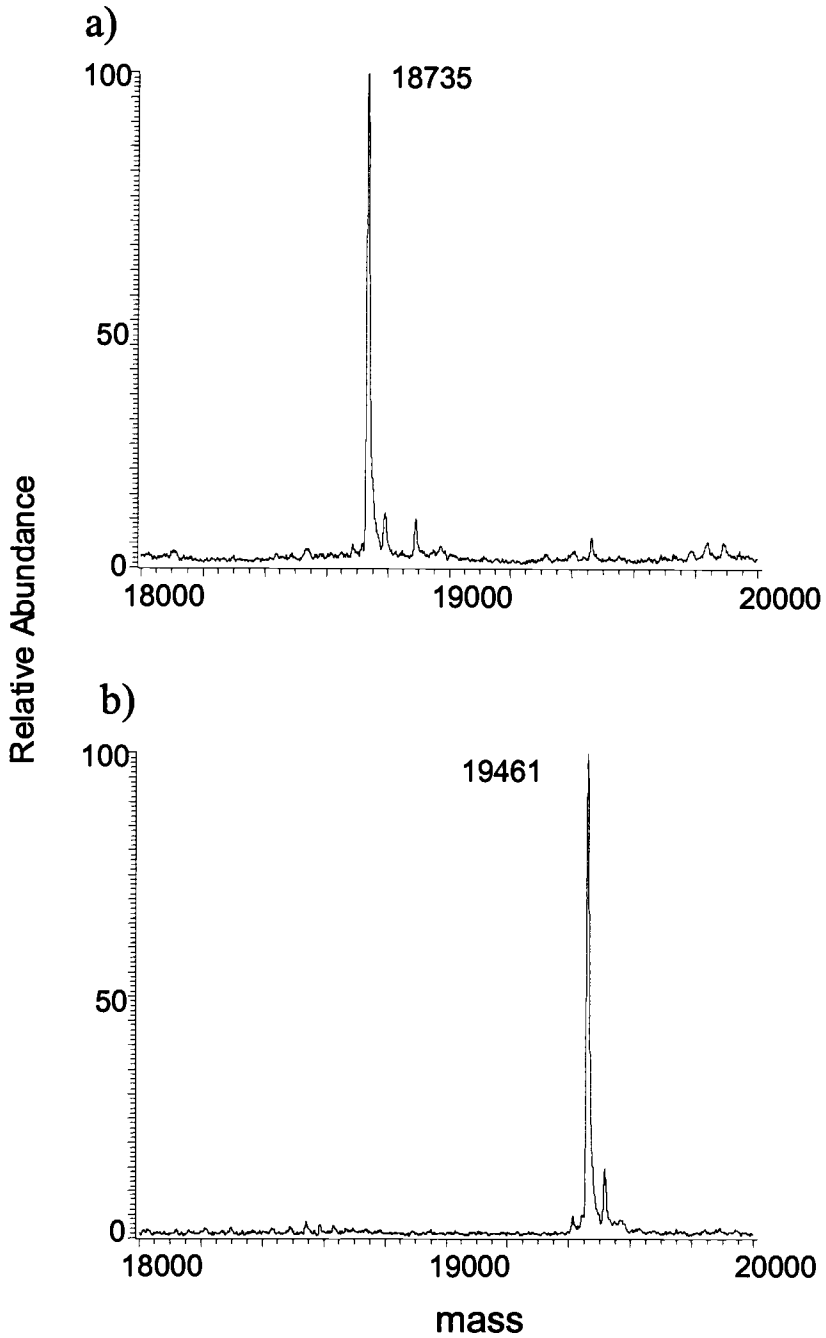

Figure 4.2. Deconvoluted mass spectra of unique αA-crystallin fragments produced *in vitro* by incubation with (a) m-calpain (spot 1, Fig. 1b), and (b) Lp82 (spot 2, Fig. 1c). Proteins in each spot were eluted from 2-DE gels and analyzed by electrospray ionization mass spectrometry. The species in spot 1 with a mass of 18,735 matched the mass of $\alpha A_{1\text{-}162}$, and the species in spot 2 with a mass of 19,461 matched the mass of $\alpha A_{1\text{-}168}$. See Table 1 for the calculated masses of these and other α-crystallin fragments.

= 19,461) was produced by removal of 5 residues ($\alpha A_{1\text{-}168}$). The deconvoluted mass spectra for these truncated αA-crystallins are shown in Fig. 4.2.

Two other potential unique Lp82 markers were observed (spots 8 and 9, Fig. 4.1c). However, the αA fragment in spot 8 was nearly identical in mass to the αA fragment in spot 2. The masses of both these species matched $\alpha A_{1\text{-}168}$ (Table 4.1). While the pI of spot 2 matched the calculated pI for $\alpha A_{1\text{-}168}$, the pI of spot 8 was higher (basic) than expected (Table 4.1). A modification causing an increase in pI, but no significant change in mass is unknown. Spot 9 was also analyzed, but its concentration was too low to determine its mass.

The remaining partially truncated α-crystallins produced by m-calpain and Lp82 were identical. αA-crystallin missing 8, 10, 16, 17, and 22 residues from its C-terminus, and αB-crystallin missing 5 and 12 residues from its C-terminus were produced by both enzymes (Fig. 4.1b and 4.1c, spots 3-7, 10, 11). However, m-calpain and Lp82 differed in their preferred cleavage sites. The major truncation product of m-calpain was $\alpha A_{1\text{-}163}$, followed by $\alpha A_{1\text{-}162}$ and $\alpha A_{1\text{-}157}$. In contrast, $\alpha A_{1\text{-}168}$ was the dominant truncation product produced by Lp82, and $\alpha A_{1\text{-}163}$ was a relatively minor species.

In general, the measured pIs of the partially degraded α-crystallins matched their calculated pIs. The two exceptions were the fragment identified in spot 8 discussed above, and the fragment in spot 4 matching the mass of $\alpha A_{1\text{-}165}$. This fragment was expected to migrate to a pI nearly identical to intact αA, but migrated to a more acidic position. The cause of the pI shifts of these truncated species is unknown. However, minor species of αA were found in the undigested control sample (Fig. 4.1a) with shifts in pI to both basic and acidic sides of the major αA species. This suggested that the truncated αA species in spots 4 and 8 were derived from the pI shifted αA species that existing before incubation. It was also interesting to note that the relative molecular weights estimated for $\alpha A_{1\text{-}163}$ and $\alpha A_{1\text{-}162}$ by SDS-PAGE did not agree with their actual molecular weights determined by mass spectrometry. $\alpha A_{1\text{-}163}$ migrated

faster than αA_{1-162} during SDS-PAGE. This result illustrated the inherent inaccuracy of molecular weight estimation by SDS-PAGE.

Fragmentation of α-Crystallin *in vivo*

Analysis of water-insoluble lens proteins from the nucleus of normal 16-day-old rats by 2-DE indicated that α-crystallins became fragmented at an early age (Fig. 4.3a). This fragmentation was largely absent from the water-soluble fraction (data not shown). Cataract produced by an overdose of selenite in age-matched lenses dramatically increased the concentration of fragmented α-crystallins. Intact αA was largely absent in the insoluble fraction of the nucleus following cataract formation (Fig. 4.3b), the density of most α-fragments increased (Fig. 4.3b, spots 1-17), and the % of total protein that was insoluble increased 2.5 fold (Fig. 4.3d). Aging from 16-days to 6-weeks in normal lenses also increased the abundance of α-crystallin fragments (compare Fig 4.3a and 3c). However, the fragmentation occurring with age was not as extensive as in cataract. Intact αA was still observed in the insoluble fraction of the nucleus of 6-week-old rats, and the amount of insoluble protein only increased by 35% from 16-days to 6-weeks of age (Fig. 4.3d). The correlation between fragmentation of β-crystallins and formation of insoluble protein has been documented in both cataractous lenses from young rats, and mature normal rat lens (David et al., 1994a). The present results indicated that breakdown of αA-crystallin was also associated with accelerated crystallin insolubilization.

The positions of α-crystallin fragments on the 2-DE gels of insoluble protein from the nucleus of 16-day control, 16-day cataractous, and 6-week old normal lenses were very similar (Fig. 4.3). Their positions were also very similar to the α-crystallin fragments produced by Lp82 and m-calpain incubation (Fig. 4.1). All of the α-crystallin fragments produced *in vitro* during incubation with Lp82 and m-calpain were also found *in vivo*. However, the abundance of specific fragments in cataractous and aged lenses suggested that Lp82 activity was more prevalent during maturation

Figure 4.3. Two-dimensional electrophoresis gels of insoluble protein from the nucleus of rat lenses: (a) 16-day-old normal rat lens, (b) 16-day-old lens with selenite-induced cataract, and (c) 6-week-old normal rat lens. Only the areas of the gels containing αA- and fragmented αB-crystallins are shown. Masses and predicted identities of the majority of numbered spots are listed in Table 4.2. The position of intact αA on gel b) is circled, since only trace amounts of this protein remained following cataract formation. (d) The percent of total protein in the nucleus that is water-insoluble in normal 16-day-old rats, 16-day-old rats with selenite cataract, and 6-week-old normal rats is indicated.

a) 16-day-old normal lens nucleus

acidic basic

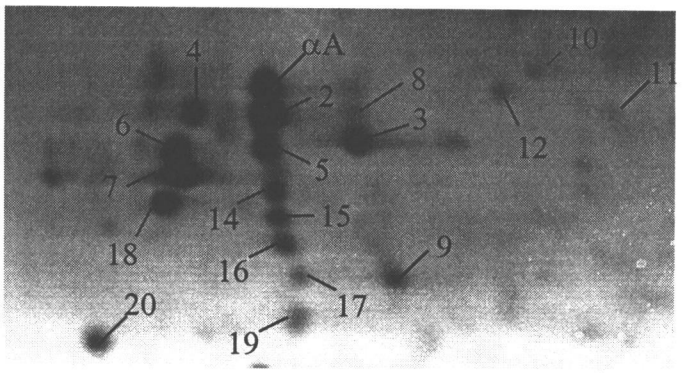

b) 16-day-old lens nucleus with selenite cataract

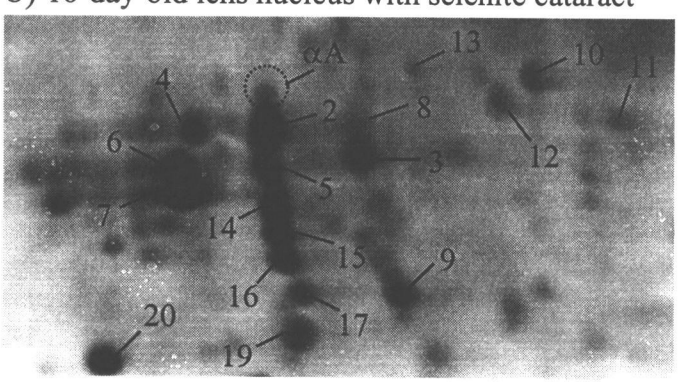

c) 6-week-old normal lens nucleus

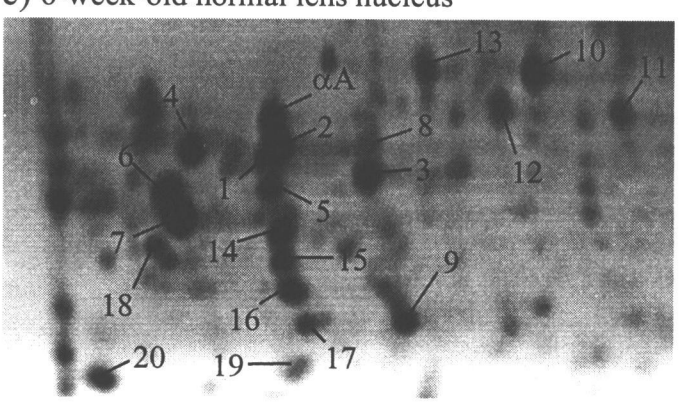

d) % insoluble protein in lens

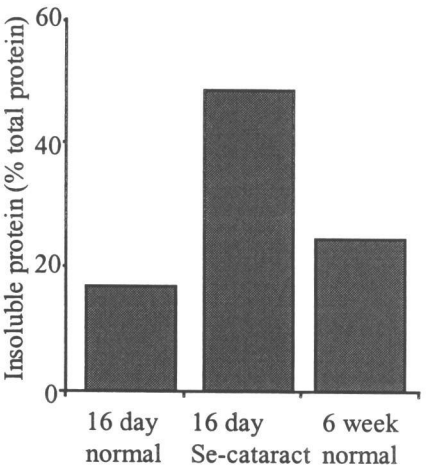

Figure 4.3

Table 4.2. Masses and identities of truncated α-crystallins found in the insoluble fraction of rat lens nucleus.

Spot No.[a]	Identified protein[b]	Residues removed from C-terminus	Measured Mass *(16-day-old normal)*	Measured Mass *(16-day-old cataract)*	Measured Mass *(6-week-old normal)*	Calculated Mass	Calculated pI	Abundance[c] (16-day-old normal)	Abundance[c] (16-day-old cataract)	Abundance[c] (6-week-old normal)
αA	αA_{1-173}	(intact)	19,891	na[d]	19,890	19,891	5.52	+++	+	+++
1	αA_{1-162}	11	nd[e]	nd	18,735	18,735	5.50	-	-	+
2	αA_{1-168}	5	19,461	19,461	19,461	19,462	5.52	+++	+++	+++
3	αA_{1-163}	10	18,890	18,990	18,890	18892	5.72	+++	+++	++
4	αA_{1-165} (acidic)[f]	8	19,149	19,149	19,149	19,150	5.54	++	++	++
5	αA_{1-157}	16	18,267	18,267	18,268	18,268	5.50	++	++	+
6	αA_{1-156}	17	18,111	18,111	18,111	18,112	5.27	++	+++	++
7	αA_{1-151}	22	17,629	17,630	17,629	17,631	5.29	+++	+++	+++
8	na	-	-	-	-	-	-	+	+	+
9	αA_{1-119}	54	na	14,365	na	14,365	5.79	++	++	++
10	αB_{1-170}	5	na	19,635	19,634	19,635	6.14	+	++	+++
11	αB_{1-163}	12	na	na	18,881	18,880	6.33	+	+	++
12	αB_{1-163} (mono-phosphorylated)[g]	12	na	na	18,961	18,960	-	+	++	++
13	αB_{1-170} (mono-phosphorylated)[g]	5	nd	na	19,715	19,715	-	-	+	++
14	αA_{1-147}	26	17,257	17,256	17,256	17,257	5.54	++	++	++
15	αA_{1-130}	43	15,477	15,477	15,477	15,477	5.54	+	++	+
16	αA_{1-126}	47	na	15,119	15,119	15,119	5.54	+	++	++
17	αA_{1-118} (basic)[f]	55	na	14,209	ND	14,209	5.54	+	+	+
18	GRIFIN		15,833	na	15,832	15,896	5.28	++	+	+
19	unknown		na	na	na	-	-	+	++	++
20	unknown		na	11,848	na	-	-	+	+	+

(*Continued*)

(Table 4.2 Legends)

a) Numbers of truncated α-crystallins isolated from 2-DE gels and analyzed by electrospray ionization mass spectrometry correspond to the numbered spots shown in Fig. 4.3.

b) Truncated and modified proteins were identified based on their measured masses, except for GRIFIN, which was identified by analysis of its tryptic fragments. Intact αA contains 173 residues (mass = 19,891), and intact αB contains 175 residues (mass = 20,131).

c) Relative amounts of each species was determined by image analysis of the 2-DE gels: +++ > 10% of protein in the region of the 2-DE gels shown in Fig. 4.3, ++ > 5%, + > 1%, - = below detection limit.

d) na: not analyzed or insufficient protein recovery for mass determination.

e) nd: not detected.

f) These species migrated to pIs either more acidic or basic than their predicted pIs (8^{th} column)

g) Identified by a 80 mass unit shift in the measured mass compared to the unphosphorylated form.

and cataract formation in young rats, and that proteolysis by m-calpain did not become significant until after 6-weeks of age. The extent of proteolysis *in vivo* was also greater. Many of the minor products produced by Lp82 incubation *in vitro*, which were too low in concentration to analyze by mass spectrometry, were present in sufficient quantities *in vivo* for analysis. Several additional species not produced by either enzyme *in vitro* were also observed. Three none α-crystallin species were also detected. The masses and identities of the various spots marked in Fig. 4.3 are summarized in Table 4.2.

The Lp82 specific product $\alpha A_{1\text{-}168}$ was one of the major forms of insoluble αA-crystallin in both normal and cataractous lenses from 16-day-old animals (Fig. 3a and b, spot 2). Figure 4.4a shows the deconvoluted mass spectrum of the protein isolated from spot 2 of the 2-DE gel shown in Fig. 4.3b that was identified as $\alpha A_{1\text{-}168}$. The mass spectrum of the protein from control lenses isolated from spot 2 of Fig. 3a was nearly identical (data not shown). Neither of these spots contained a protein matching the mass of $\alpha A_{1\text{-}162}$, the unique m-calpain produced fragment. In contrast, spot 1, observed in the insoluble protein isolated from normal 6-week old lens nucleus (Fig. 4.3c), contained a major species with a mass of 19,735 (Fig. 4.4b). This matched the mass of $\alpha A_{1\text{-}162}$, the unique m-calpain produced fragment. A second species corresponding to $\alpha A_{1\text{-}168}$ (mass = 19,462) was also observed, due to the incomplete resolution of spots 1 and 2. These data indicated that Lp82 was active in both normal and cataractous lenses of 16-day old rats, and that m-calpain was only appreciably active in older 6-week old lenses.

Additional spots numbered 9, 14, 15, 16, and 17 in Fig. 4.3, corresponding in position to unique species produced by Lp82 *in vitro*, were also analyzed. These were identified as forms of αA missing 54, 26, 43, 47, and 55 residues from its C-terminus, respectively (Table 4.2). Other truncated forms of α-crystallins common to both Lp82 and m-calpain proteolysis were also found (spots 3, 4, 5, 6, 7, 10, 11). αB-crystallin truncation was not as extensive in both 16-day-old normal and cataractous lenses as

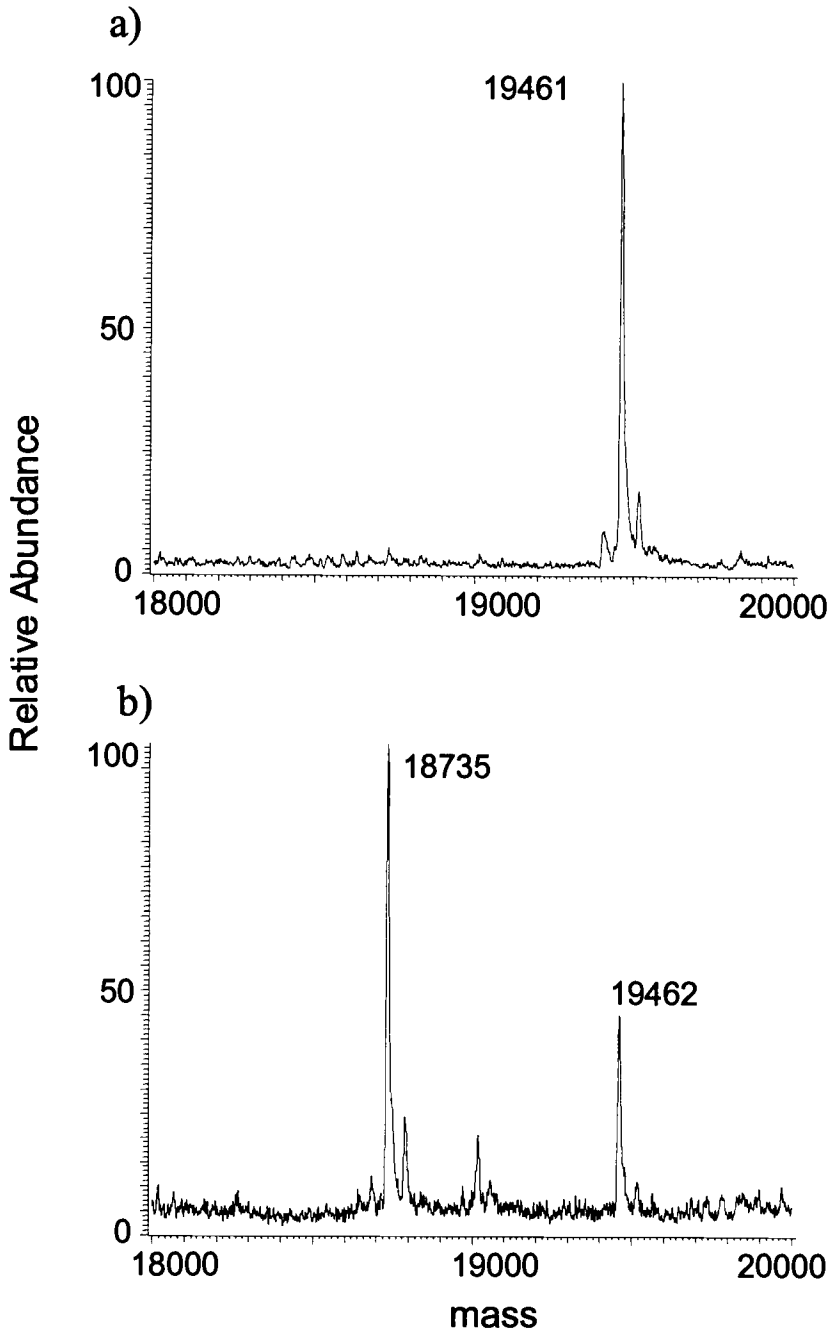

Figure 4.4. Deconvoluted mass spectra of αA-crystallin fragments found in: (a) spot 2 of the 2-DE gel of insoluble protein from the lens nucleus of 16-day-old rats with selenite-induced cataract (Fig. 3b), and (b) spot 1 of the 2-DE gel of insoluble protein from the lens nucleus of 6-week-old normal rats (Fig. 3c).

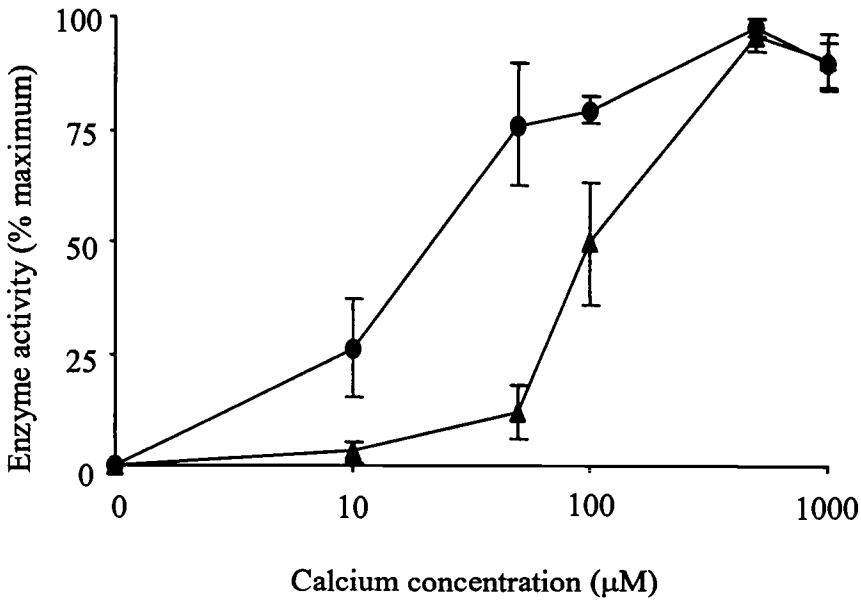

Figure 4.5. Calcium required for proteolysis of casein by recombinant Lp82 (●) and m-calpain (▲). Error bars indicate standard error of mean (n=4). The extent of activation for each enzyme was significantly different ($p > 0.05$) at 10, 50, and 100 μM concentrations of calcium.

was αA-crystallin fragmentation. However, $\alpha B_{1\text{-}170}$, and $\alpha A_{1\text{-}163}$ (spots 10 and 11) and their phosphorylated forms (spots 13 and 12) accumulated in older rat lens (Fig. 4.3c).

The mass of spot 18 did not match the mass of any possible α-crystallin fragment. Therefore, this protein was identified by MS/MS analysis of its peptide fragments as the recently characterized protein GRIFIN (galectin-related inter-fiber protein; Ogden et al., 1998). The identities of the proteins in spots19 and 20 were not determined. However, the mass of spot 20 indicated that this fragment was unlikely to be derived from α-crystallins.

Calcium requirement for m-calpain and Lp82

Calcium requirements of recombinant Lp82 and m-calpain were tested. Activity of m-calpain and Lp82 reached 1/2 of maximum at approximately 120 μM and 20 μM calcium, respectively (Fig. 4.5). Maximum activity of Lp82 was reached at 50 μM calcium, whereas m-calpain required 500 μM calcium for maximum activity.

Discussion

A major findings of this study were: 1) extensive C-terminal truncation of α-crystallins occurred in rat lenses during maturation and cataract formation, 2) these truncated α-crystallins were selectively insolubilized, and 3) the calcium-dependant proteases Lp82 and m-calpain were likely responsible, with the activity of Lp82 predominating over m-calpain in the nucleus of young rat lens. The last finding was based on the detection of unique, truncated αA-crystallin products of both Lp82 and m-calpain in lens, with the predominant accumulation of the Lp82-specific αA products.

m-Calpain has long been implicated as the major protease responsible for the processing of rodent crystallins, during both lens maturation and cataract formation (David and Shearer, 1986; David et al., 1994a). However, due to its abundance and

stability, the more recently discovered lens protease, Lp82, may also play an important role (Ma et al., 1999). Since there was no previous direct evidence that Lp82 was responsible for degradation of endogenous substrates in rat lens, the first goal in the present study was to identify biological markers that could estimate the relative activities of m-calpain and Lp82 *in vivo*. The αA-fragment, $\alpha A_{1\text{-}168}$, missing 5 residues from its C-terminus, was shown to be an Lp82 specific product; while the αA-fragment, $\alpha A_{1\text{-}162}$, missing 11 residues from its C-terminus, was shown to be a m-calpain specific product. This finding agrees with the studies of Yoshida et. al. (Yoshida, 1986), which showed that purified bovine lens m-calpain could remove 10 and 11 residues from the C-terminus of αA-crystallin, but not 5 residues. Similar studies using purified Lp82 and m-calpain from rat (Nakamura et al., 2000) and bovine lens (Chapter 3) also confirmed these m-calpain cleavage sites, and showed that Lp82 uniquely removed 5 residues from the C-terminus of αA. In the present study, using 2-DE gel separation to isolate the various truncated forms of α-crystallins, we were able to demonstrate for the first time that $\alpha A_{1\text{-}168}$ appeared much earlier in lens than did $\alpha A_{1\text{-}162}$. This suggested that Lp82 is activated much earlier than m-calpain during lens maturation, and that Lp82 may be responsible for the majority of excess crystallin proteolysis associated with experimental cataract formation.

There are several findings that may explain the greater activity of Lp82 compared to m-calpain in young rat lens. First, zymographic gels indicated that the amount of Lp82 activity was similar to m-calpain activity in the nucleus of young rodents (Ma et al., 1999). Secondly, unlike m-calpain, Lp82 is relatively insensitive to calpastatin, the endogenous inhibitor of calpains (Nakamura et al., 1999b), (Chapter 3). Thirdly, Lp82 underwent autolytic inactivation more slowly than did Lp82 (Chapter 3). Fourthly, the calcium requirement for activation of Lp82 is much lower than the calcium requirement of m-calpain. The lower calcium requirement of Lp82 compared to m-calpain was demonstrated both for enzymes purified from bovine lens (Chapter 2), and the recombinant forms of Lp82 and m-calpain used in the present study. While, the 108 μM free calcium concentration in the nucleus of young rats

developing selenite-induced cataracts is high enough to activate Lp82, the mechanism for Lp82 activation in normal rat lens containing <1 μM free calcium is unknown (Hightower et al., 1987). One possibility is that Lp82 is activated following association of the enzyme with lens membranes. This hypothesis is supported by the preferential association of Lp82 with the insoluble fraction of the lens (Shearer et al., 1998).

While Lp82 appeared more active in the lenses of both normal and cataractous young rats, evidence for m-calpain was found in the lens nucleus of normal 6-week-old rats. m-calpain may exhibit relatively greater activity in mature lenses, because, unlike Lp82, enzymatic activity and m-RNA for m-calpain are maintained in lens with age (Shearer et al., 1998). m-calpain may function in lens to provide very slow but sustained proteolytic activity in mature lenses, while Lp82 may function only during the period of rapid postnatal growth.

Numerous additional forms of C-terminally truncated αA and αB-crystallins were produced by incubation of crystallins with Lp82 and m-calpain. While the majority of these fragments were produced by both enzymes *in vivo* and could not be used to differentiate between the two proteolytic activities, they were identical to most of the fragmented α-crystallins found *in vivo*. This further confirmed that fragmentation of α-crystallins in rat lens is performed almost entirely by proteases of the calpain family.

While both Lp82 and m-calpain were capable of cleaving β-crystallins, these experiments did not detect any major differences in the migration pattern of β-crystallin fragments on 2-DE following digestion. This was also supported by digestion of recombinantly expressed βA3 by m-calpain and Lp82 (Chapter 3). Thus, fragmented β-crystallins were not analyzed in the present study, because m-calpain cleavage sites in β-crystallins, and the fragmentation of these proteins during maturation and cataract formation have been extensively documented (David et al., 1993; David et al., 1994a). The results of the present study, suggested that attributing β-crystallin fragmentation to m-calpain activation in these earlier studies was in error.

Lp82 is more likely responsible for the majority of both α– and β-crystallin fragmentation in young rat lenses.

Previous studies in this laboratory did not analyze α-crystallins in detail, because, unlike β-crystallins, which all undergo fragmentation within their N-terminal extensions, fragmented α-crystallins in rats remain intact at their N-terminus (Kelley et al., 1993). This prevents the analysis of their cleavage sites by Edman sequencing. The methodology used in the current study avoided these limitations by isolating whole proteins from 2-DE gels and accurately measuring their masses. The methodology represents a significant advance in the analysis of modified crystallins and should greatly enhance the analysis of post-translational modifications in human crystallins.

Except for $\alpha A_{1\text{-}168}$ and $\alpha A_{1\text{-}151}$, missing 5 and 22 C-terminal residues (Chapter 2), respectively, the majority of C-terminal truncated αA-crystallins characterized in this study were previously unreported. $\alpha A_{1\text{-}151}$ missing 22 C-terminal residues was one of the most abundant forms of insoluble αA-crystallins observed in rat lens. $\alpha A_{1\text{-}151}$ was also observed in bovine lenses (van Kleef et al., 1974), however its production was attributed to non-enzymatic spontaneous cleavage due to racemization and isomerization of aspartic acid (Fujii et al., 1997; Fujii et al., 1999). Further investigation is required to clarify if calpains are also involved in truncation of αA-crystallin at this site in bovine lens.

$\alpha A_{1\text{-}168}$, missing 5-residues from its C-terminus, has also been detected in human and bovine lens (de Jong et al., 1974; Takemoto, 1995; Lund et al., 1996). While Lp82 is likely responsible for this cleavage in bovine lens (Chapter 3), the protease causing this cleavage in human lens is unknown, since no Lp82 activity is present in human lens. The $\alpha A_{1\text{-}168}$ species in human lens may be produced by an as yet unidentified calpain isoform. Interestingly, the major αA-crystallin truncation product found in human and bovine lenses, $\alpha A_{1\text{-}172}$, missing the C-terminal serine residue was not found in rat lens (Chapter 3; Ma et al., 1998c; Takemoto, 1995).

The two forms of truncated αB-crystallin observed *in vivo* and produced by both m-calpain and Lp82 *in vitro*, $\alpha B_{1\text{-}170}$ and $\alpha B_{1\text{-}163}$, were both abundant in human lens fiber cells growing in lens capsules following cataract surgery (Colvis et al., 2000). We hypothesize that m-calpain was responsible for these cleavages.

The C-terminal truncation of α-crystallins may have great biological significance in lens. Loss of C-terminal regions of α-crystallins has been previously shown to diminish the chaperone like properties of α-crystallins (Kelley et al., 1993; Takemoto, 1994). The present study also demonstrated that truncated α-crystallins were selectively insolubilized. While β-crystallins readily precipitate *in vitro* following removal of their N-terminal extensions by m-calpain, α-crystallins remain relatively soluble following a similar treatment to remove portions of their C-terminal extensions (David and Shearer, 1993). Carver and Lindner (Carver, 2000) have postulated that the flexible, solvent exposed, hydrophilic C-terminal extensions of α-crystallins may act as solubilizing agents to keep the α-crystallin/denatured protein complexes that form upon chaperone action in solution. Selenite cataract may form due to insolubilization of truncated α/β-crystallin complexes that are unable to stay in solution due to a loss of the solubilizing C-terminal extensions of α-crystallins. Similar complexes of truncated α and β-crystallins may not form opacities during normal aging of lens, because their slow accumulation may allow their ordered packing within the lens cytosol.

During the course of this study, we unexpectedly identified the newly discovered lens specific protein GRIFIN (galectin-related inter-fiber protein) (Ogden et al., 1998). Unlike other members of the galectin family, GRIFIN does not bind β-galactoside sugars and its function is unknown. However, GRIFIN was shown by immunofluorescence to be localized at the interface between lens fiber cells. Since the current study found significant amounts of GRIFIN in the insoluble fraction of the lens, it seemed likely that GRIFIN could function as a peripheral membrane protein. Its function may be similar to another member of the galectin family recently

characterized in lens, galectin-3, which was postulated to act as cell adhesion molecule (Gonen et al., 2000).

In conclusion, analysis of α-crystallin truncation suggested that the recently discovered lens specific member of the calpain family, Lp82, was active in lens, and responsible for the majority of crystallin fragmentation occurring in young rat lens. The differential activation of Lp82 and m-calpain by calcium may allow an ordered truncation and insolubilization of crystallins in rat lens during normal maturation. Loss of calcium homeostasis in young rats may cause cataract by too rapid of activation of Lp82.

Acknowledgments

The authors gratefully thank Dr. Debra A. Brickey and Sean Nygaard (Oregon Health Sciences University) for help in expression of recombinant Lp82. These studies were partially supported by NIH grants EY12016 and EY07755 (LLD); and EY03600 and EY5786 (TRS).

Chapter 5

Conclusions

Yoji Ueda

Department of Animal Sciences

The present study confirmed the accumulation of various post-translational modifications of crystallins during the aging of the lens, and demonstrated that proteolysis of crystallins is closely associated with their insolubilization. We also provided direct evidence for the involvement of the recently discovered protease Lp82 in producing truncated and insolubilized crystallins during normal aging and cataract formation in animal lenses. These results were novel, since hard evidence that this enzyme was active against endogenous substrates in lens was previously lacking.

The data in chapter 2 clearly shows that certain post-translational modifications cause crystallins to accumulate specifically in either the soluble or insoluble fractions. Phosphorylated α-crystallin was found in the soluble fraction, while degraded α-and β-crystallins, and acidified γ-crystallins were mainly found in the insoluble fractions. Protein modifications were first evident between 6- and 10-weeks of age in mice, and the modification pattern did not change thereafter, while the proportion of insoluble proteins continued to increase. By 51-weeks of age, over 60% of the protein of mouse lenses became insoluble. We hypothesized that this major maturational change in lens is essential to maintain proper organization of the lens and transparency. As a result of characterizing these major proteolytic changes in the developing lens, we became interested in determining which proteolytic activities were responsible. The discovery of a lens specific calpain isoform Lp82 by our collaborators led us to hypothesize that this protease may be responsible for the changes we observed in mouse lenses. This hypothesis was provocative, because the accepted dogma was that the ubiquitous calpain isoform m-calpain was the major endopeptidase in lens. We next set out to be the first ones to purify lens Lp82 and determine it properties. The goal was to find if these properties would be consistent with it being more active than m-calpain in lens.

The manuscript in chapter 3 describes the first purification of the lens specific calpain isoform Lp82. This was accomplished using fetal bovine lenses, which, due to their size, provided more starting material than rodent lenses. Although the co-elution of leucine aminopeptidase during the initial purification step interfered with the accurate assessment of specific activity of bovine Lp82, we were able to isolate a

sufficient quantity of Lp82 for characterization studies. There were a number of unique enzymological characteristics of Lp82 identified that distinguished it from m-calpain. First, unlike m-calpain, Lp82 was insensitive to calpastatin, the endogenous calpain inhibitor (Takano et al., 1988). Lp82 was also less susceptible to autolytic inactivation than m-calpain. This was contrary to the Lp82 splice variant p94, which shows rapid auto-degradation and inactivation after translation (Sorimachi et al., 1993). Thus, Lp82 has adapted its physiological characteristics to be able to perform its role in the lens. Insusceptibility of Lp82 to inactivation by auto-degradation favors the activity of this enzyme in lens fibers where protein synthesis is very slow. Another distinguishing characteristic of Lp82 was its lower calcium requirement for activation. All of these findings strongly supported the hypothesis that Lp82 was more active than m-calpain in animal lenses.

Chapter 3 also describes our first analysis of the substrate specificity of Lp82. Isolated Lp82 and m-calpain were compared to determine if they cleave the endogenous substrate lens crystallins differently. Identification of the differential cleavage of α-crystallin provided the first hard evidence that Lp82 was active in lens. The removal of αA-crystallin's five amino acid residues from its C-terminus by Lp82 was especially interesting, since this same cleavage is found *in vivo* in many animals (de Jong et al., 1974). We further confirmed that this cleavage was found in bovine lenses by measuring this truncated form of αA-crystallin in lens of this species. Since α-crystallins act as molecular chaperones in lens, their truncation by Lp82 was further investigated in Chapter 4. The additional purpose of this final manuscript in the thesis was to also more closely examine whether m-calpain or Lp82 was more active in the lens, by comparing the production of isoform specific truncated α-crystallin found *in vivo*.

Two key technological advances were made in our laboratory prior to the study in Chapter 4. First, expression and purification of recombinant Lp82 using insect cells allowed us to obtain a large quantity of Lp82 without resorting to its purification from fetal calf lenses. Second, we developed a method to determine the mass of whole

proteins eluted directly out of 2-DE gels. Without this technique it would have been impossible to determine the cleavage sites in α-crystallins reported in chapter 4. This technique will greatly facilitate the identification of post-translational modifications in lens and other tissues, and it may become a common protocol used in the proteomics field.

The main finding of Chapter 4 was that the α-crystallin breakdown pattern was surprisingly identical between normally maturing lenses and lenses with cataracts. The manuscript in chapter 4 provided the most detailed description of α-crystallin modifications reported to date. Comparison of in vivo breakdown products to those produced in vitro by m-calpain and Lp82 indicated that Lp82 was the major active calpain isoform in lens. The results suggested that only minor amounts of m-calpain activity were present in lenses greater than 6-weeks of age. Analysis of αA-crystallin degradation in lenses with experimental cataracts caused by selenite overdose also suggested the Lp82 was the only calpain isoform that was activated. Thus, over-activation of Lp82 is likely responsible for development of cataract in rat lens.

Thus, proteolysis of crystallins by Lp82 was closely associated with crystallin insolubilization and opacity in rodent lenses. Proteolysis of crystallins is also a key process in normal aging and cataract formation in the human lens as well. However, the absence of Lp82 in the human lens suggests the presence of yet another protease. Interestingly, $\alpha A_{1\text{-}168}$, an Lp82 activity marker, is found in older human lens (Takemoto, 1995), suggesting the possibility that there may be an as yet undiscovered calpain isoform active in human lens. There have been a number of new calpain isoforms identified in the last decade and this trend is likely to continue. It will be important to develop methods to distinguish each calpain activity *in vivo*, and the methods developed in this study will be useful in characterizing the activity of newly discovered calpains. It is also important to keep in mind that proteolysis is one of the key events leading to the formation of cataracts, but it is not the only factor. For example, while the present study was in progress, Nakamura et. al. (Nakamura et al., 1999) showed that oxidation enhanced the light scattering of crystallins following their

degradation by m-calpain. Therefore, further experiments are required to clarify the relationship between other post-translational modifications and proteolysis in the pathways leading to cataract.

The present study not only provided new insights into aging and cataract formation in lens, but the "proteomic" approaches used here represent the new face of research development in this discipline in the post human genome era. By generating a series of 2-DE gels and using the power of mass spectrometric technology, we were able to catalogue a number of changes in the protein profiles that would have previously taken years to compile. For example, we were able to follow the changes in protein expression during mouse development, and determine the various post-translational modifications, including phosphorylation, acidification, and degradation using one series of 2-DE gels (chapter 2). Additionally, the production of a complete mouse lens crystallin proteome map will serve as a master map to assist other lens researchers who are using transgenic and knockout mice to study the mechanisms of cataract formation.

While the research in this thesis was hypothesis driven, the techniques used illustrate how discoveries in proteomics can be data driven. For example, during our characterization of α-crystallin fragmentation in chapter 4, we accidentally discovered the lens specific galectin-related protein GRIFIN in the insoluble fraction of rat lens (chapter 4). The reported localization of this protein with lens membrane, and the strong possibility that it is acting in the lens as a cell adhesion molecule could have profound consequences. While not discussed in the manuscript, the apparent loss of this protein when cataracts formed suggested that it too was acting as a substrate for proteases. Its proteolysis could explain the loss of fiber cell organization accompanying cataract. Thus, the research potential of proteomic approach is not limited to the primary focus, but can be expanded in many other ways. While this thesis was being written, the announcement was made in the news media that the initial analysis of the majority of coding sequences for all human genes is complete. This means that there soon will be no spot on a 2-DE gel produced from a human tissue that cannot be identified.

No animal model perfectly mimics human senile cataract where post-translational modifications have accumulated for decades. However, by putting pieces of information together from these animal cataract models, many key events that are common in both human and animals can be identified. In the present study, we have provided evidence for the involvement of proteolysis during both normal lens maturation and cataract formation in animal lenses, and provided strong evidence for the involvement of Lp82 in the process. The discovery unlocking the mysteries of human cataract is perhaps one small step closer.

Bibliography

Aarts, H. J., E. H. Jacobs, G. van Willigen, N. H. Lubsen and J. G. Schoenmakers (1989). Different evolution rates within the lens-specific beta-crystallin gene family. *J Mol Evol* **28**(4): 313-21.

Andersson, M., J. SjOstrand and J. Karlsson (1998). Proteolytic cleavage of N-Succ-Leu-Leu-Val-Tyr-AMC by the proteasome in lens epithelium from clear and cataractous human lenses. *Exp Eye Res* **67**(2): 231-6.

Augusteyn, R. C. (1998). alpha-Crystallin polymers and polymerization: the view from down under. *Int J Biol Macromol* **22**(3-4): 253-62.

Azuma, M., L. L. David and T. R. Shearer (1991). Cysteine protease inhibitor E64 reduces the rate of formation of selenite cataract in the whole animal. *Curr Eye Res* **10**(7): 657-66.

Azuma, M. and T. R. Shearer (1992). Involvement of calpain in diamide-induced cataract in cultured lenses. *FEBS Letters* **307**(3): 313-7.

Azuma, M., T. R. Shearer, T. Matsumoto, L. L. David and T. Murachi (1990). Calpain II in two in vivo models of sugar cataract. *Exp Eye Res* **51**(4): 393-401.

Barnett, K. C. and F. G. Startup (1985). Hereditary cataract in the standard poodle. *Vet Rec* **117**(1): 15-6.

Bassnett, S. and D. C. Beebe (1992). Coincident loss of mitochondria and nuclei during lens fiber cell differentiation. *Dev Dyn* **194**(2): 85-93.

Bax, B., R. Lapatto, V. Nalini, H. Driessen, P. F. Lindley, D. Mahadevan, T. L. Blundell and C. Slingsby (1990). X-ray analysis of beta B2-crystallin and evolution of oligomeric lens proteins. *Nature* **347**(6295): 776-80.

Beck, J. A., S. Lloyd, M. Hafezparast, M. Lennon-Pierce, J. T. Eppig, M. F. Festing and E. M. Fisher (2000). Genealogies of mouse inbred strains. *Nat Genet* **24**(1): 23-5.

Belloni, E., M. Muenke, E. Roessler, G. Traverso, J. Siegel-Bartelt, A. Frumkin, H. F. Mitchell, H. Donis-Keller, C. Helms, A. V. Hing, H. H. Heng, B. Koop, D. Martindale, J. M. Rommens, L. C. Tsui and S. W. Scherer (1996). Identification of Sonic hedgehog as a candidate gene responsible for holoprosencephaly. *Nat Genet* **14**(3): 353-6.

Berbers, G. A., W. A. Hoekman, H. Bloemendal, W. W. de Jong, T. Kleinschmidt and G. Braunitzer (1984). Homology between the primary structures of the major bovine beta-crystallin chains. *Eur J Biochem* **139**(3): 467-79.

Berti, P. J. and A. C. Storer (1995). Alignment/phylogeny of the papain superfamily of cysteine proteases. *J Mol Biol* **246**(2): 273-83.

Bhat, S. P. and C. N. Nagineni (1989). alpha B subunit of lens-specific protein alpha-crystallin is present in other ocular and non-ocular tissues. *Biochem Biophys Res Commun* **158**(1): 319-25.

Bloemendal, H. (1982). Lens proteins. *CRC Critical Rev Biochem* **12**(1): 1-38.

Bloemendal, H., E. L. Benedetti and I. Dunia (1996). Transgenic mice: models for the study of cataractogenesis. A minireview. *Ophthal Res* **28**(Suppl 1): 1-7.

Blundell, T., P. Lindley, L. Miller, D. Moss, C. Slingsby, I. Tickle, B. Turnell and G. Wistow (1981). The molecular structure and stability of the eye lens: x-ray analysis of gamma-crystallin II. *Nature* **289**(5800): 771-7.

Bova, M. P., L. L. Ding, J. Horwitz and B. K. Fung (1997). Subunit exchange of alphaA-crystallin. *J Biol Chem* **272**(47): 29511-7.

Boyle, D. and L. Takemoto (1994). Characterization of the alpha-gamma and alpha-beta complex: evidence for an in vivo functional role of alpha-crystallin as a molecular chaperone. *Exp Eye Res* **58**(1): 9-15.

Brady, J. P., D. Garland, Y. Duglas-Tabor, W. G. Robison, Jr., A. Groome and E. F. Wawrousek (1997). Targeted disruption of the mouse alpha A-crystallin gene induces cataract and cytoplasmic inclusion bodies containing the small heat shock protein alpha B-crystallin. *Proc Natl Acad Sci USA* **94**(3): 884-9.

Cai, H., I. Singh and B. J. Wagner (1998). Gene expression of the proteasome in rat lens development. *Exp Eye Res* **66**(3): 339-46.

Calvin, H. I., J.-X. Wu, K. Viswanadhan and S.-C. J. Fu (1996). Modifications in lens protein biosynthesis signal the initiation of cataracts induced by buthionine sulfoximine in mice. *Exp Eye Res* **63**(4): 357-368.

Carper, D., S. J. Smith-Gill and J. H. Kinoshita (1986). Immunocytochemical localization of the 27K beta-crystallin polypeptide in the mouse lens during development using a specific monoclonal antibody: implications for cataract formation in the Philly mouse. *Dev Biol* **113**(1): 104-9.

Carver, J. A. (1999). Probing the structure and interactions of crystallin proteins by NMR spectroscopy. *Prog Retin Eye Res* **18**(4): 431-62.

Carver, J. A., J. A. Aquilina, R. J. Truscott and G. B. Ralston (1992). Identification by 1H NMR spectroscopy of flexible C-terminal extensions in bovine lens alpha-crystallin. *FEBS Lett* **311**(2): 143-9.

Carver, J. A., K. A. Nicholls, J. A. Aquilina and R. J. Truscott (1996). Age-related changes in bovine alpha-crystallin and high-molecular-weight protein. *Exp Eye Res* **63**(6): 639-47.

Castellanos-Serra, L. R., C. Fernandez-Patron, E. Hardy and V. Huerta (1996). A procedure for protein elution from reverse-stained polyarcylamide gels applicable at the low picomole level: An alternative route to the preparation of low abundance proteins for microanalysis. *Electrophoresis* **17**(10): 1564-72.

Chambers, C. and P. Russell (1991). Deletion mutation in an eye lens beta-crystallin. An animal model for inherited cataracts. *J Biol Chem* **266**(11): 6742-6.

Chandrasekher, G. and R. J. Cenedella (1993). Calcium activated proteolysis and protein modification in the U18666A cataract. *Exp Eye Res* **57**(6): 737-45.

Chang, B., N. L. Hawes, T. H. Roderick, R. S. Smith, J. R. Heckenlively, J. Horwitz and M. T. Davisson (1999). Identification of a missense mutation in the alphaA-crystallin gene of the lop18 mouse. *Mol Vis* **5**: 21.

Colvis, C. M., Y. Duglas-Tabor, K. B. Werth, N. E. Vieira, J. A. Kowalak, A. Janjani, A. L. Yergey and D. L. Garland (2000). Tracking pathology with proteomics: identification of in vivo degradation products of alphaB-crystallin. *Electrophoresis* **21**(11): 2219-27.

Cong, J., D. E. Goll, A. M. Peterson and H. P. Kapprell (1989). The role of autolysis in activity of the Ca2+-dependent proteinases (mu- calpain and m-calpain). *J Biol Chem* **264**(17): 10096-103.

Courchesne, P. L. and S. D. Patterson (1999). Identification of proteins by matrix-assisted laser desorption/ionization mass spectrometry using peptide and fragment ion masses. *Methods Mol Biol* **112**: 487-511.

Dada, V. K. and N. Sindhu (2000). Cataract in enucleated goat eyes: training model for phacoemulsification. *J Cataract Refract Surg* **26**(8): 1114-6.

Datiles, M. B., D. J. Schumer, J. S. Zigler, Jr., P. Russell, L. Anderson and D. Garland (1992). Two-dimensional gel electrophoretic analysis of human lens proteins. *Curr Eye Res* **11**(7): 669-77.

David, L. L., M. Azuma and T. R. Shearer (1994a). Cataract and the acceleration of calpain-induced beta-crystallin insolubilization occurring during normal maturation of rat lens. *Invest Ophthal Vis Sci* **35**(3): 785-93.

David, L. L., H. I. Calvin and S. C. Fu (1994b). Buthionine sulfoximine induced cataracts in mice contain insolubilized crystallins with calpain II cleavage sites [letter]. *Exp Eye Res* **59**(4): 501-4.

David, L. L., K. J. Lampi, A. L. Lund and J. B. Smith (1996). The sequence of human betaB1-crystallin cDNA allows mass spectrometric detection of betaB1 protein missing portions of its N-terminal extension. *J Biol Chem* **271**(8): 4273-9.

David, L. L. and T. R. Shearer (1986). Purification of calpain II from rat lens and determination of endogenous substrates. *Exp Eye Res* **42**(3): 227-38.

David, L. L. and T. R. Shearer (1993a). Beta-crystallins insolubilized by calpain II in vitro contain cleavage sites similar to beta-crystallins insolubilized during cataract. *FEBS Letters* **324**(3): 265-70.

David, L. L., T. R. Shearer and M. Shih (1993b). Sequence analysis of lens beta-crystallins suggests involvement of calpain in cataract formation. *Journal of Biol Chem* **268**(3): 1937-40.

David, L. L., M. D. Varnum, K. J. Lampi and T. R. Shearer (1989). Calpain II in human lens. *Investigative Ophthal Vis Sci* **30**(2): 269-75.

David, L. L., J. W. Wright and T. R. Shearer (1992). Calpain II induced insolubilization of lens beta-crystallin polypeptides may induce cataract. *Biochim Biophys Acta* **1139**(3): 210-6.

de Jong, W. W., F. S. van Kleef and H. Bloemendal (1974). Intracellular carboxy-terminal degradation of the alpha A chain of alpha-crystallin. *Eur J Biochem* **48**(1): 271-6.

Delamere, N. A., R. E. Manning, Jr., L. Liu, A. E. Moseley and W. L. Dean (1998). Na,K-ATPase polypeptide upregulation responses in lens epithelium. *Invest Ophthalmol Vis Sci* **39**(5): 763-8.

Duncan, M. K., Z. Kozmik, K. Cveklova, J. Piatigorsky and A. Cvekl (2000). Overexpression of PAX6(5a) in lens fiber cells results in cataract and upregulation of (&agr;)5(&bgr;)1 integrin expression. *J Cell Sci* **113**(Pt): 3173-3185.

Fichmann, J. (1999). Advantages of immobilized pH gradients. *Methods Mol Biol* **112**: 173-4.

Fougerousse, F., P. Bullen, M. Herasse, S. Lindsay, I. Richard, D. Wilson, L. Suel, M. Durand, S. Robson, M. Abitbol, J. S. Beckmann and T. Strachan (2000). Human-mouse differences in the embryonic expression patterns of developmental control genes and disease genes [published erratum appears in Hum Mol Genet 2000 Mar 1;9(4):659]. *Hum Mol Genet* **9**(2): 165-73.

Fukiage, C., M. Azuma, Y. Nakamura, Y. Tamada and T. R. Shearer (1997). Calpain-induced light scattering by crystallins from three rodent species. *Exp Eye Res* **65**(6): 757-70.

Fukiage, C., M. Azuma, Y. Nakamura, Y. Tamada and T. R. Shearer (1998). Nuclear cataract and light scattering in cultured lenses from guinea pig and rabbit. *Curr Eye Res* **17**(6): 623-35.

Garber, A. T., D. Goring and R. J. Gold (1984). Characterization of abnormal proteins in the soluble lens proteins of CatFraser mice. *J Biol Chem* **259**(16): 10376-9.

Gilmour, D. T., G. J. Lyon, M. B. Carlton, J. R. Sanes, J. M. Cunningham, J. R. Anderson, B. L. Hogan, M. J. Evans and W. H. Colledge (1998). Mice deficient for the secreted glycoprotein SPARC/osteonectin/BM40 develop normally but show severe age-onset cataract formation and disruption of the lens. *Embo J* **17**(7): 1860-70.

Gong, X., K. Agopian, N. M. Kumar and N. B. Gilula (1999). Genetic factors influence cataract formation in alpha 3 connexin knockout mice. *Dev Genet* **24**(1-2): 27-32.

Goring, D. R., M. L. Breitman and L. C. Tsui (1992). Temporal regulation of six crystallin transcripts during mouse lens development. *Exp Eye Res* **54**(5): 785-95.

Graw, J. (1999). Mouse models of congenital cataract. *Eye* **13**(Pt 3b): 438-44.

Groenen, P. J., K. B. Merck, W. W. de Jong and H. Bloemendal (1994). Structure and modifications of the junior chaperone alpha-crystallin. From lens transparency to molecular pathology. *Eur J Biochem* **225**(1): 1-19.

Gygi, S. P., Y. Rochon, B. R. Franza and R. Aebersold (1999). Correlation between protein and mRNA abundance in yeast. *Mol Cell Biol* **19**(3): 1720-30.

Harding, J. J., and Crabbe, M.J.C. (1984). *The lens: Development, proteins, metabolism and cataract*. Orland, FL, Academic Press.

Hendriks, W., J. Sanders, L. de Leij, F. Ramaekers, H. Bloemendal and W. W. de Jong (1988). Monoclonal antibodies reveal evolutionary conservation of alternative splicing of the alpha A-crystallin primary transcript. *Eur J Biochem* **174**(1): 133-7.

Hightower, K. R. (1985). Cytotoxic effects of internal calcium on lens physiology: a review. *Curr Eye Res* **4**(4): 453-9.

Hightower, K. R., L. L. David and T. R. Shearer (1987). Regional distribution of free calcium in selenite cataract: relation to calpain II. *Invest Ophthalmol Vis Sci* **28**(10): 1702-6.

Hope, J. N., H. C. Chen and J. F. Hejtmancik (1994). Beta A3/A1-crystallin association: role of the N-terminal arm. *Protein Eng* **7**(3): 445-51.

Horwitz, J. (1992). Alpha-crystallin can function as a molecular chaperone. *Proc Natl Acad Sci U S A* **89**(21): 10449-53.

Horwitz, J., M. P. Bova, L. L. Ding, D. A. Haley and P. L. Stewart (1999). Lens alpha-crystallin: function and structure. *Eye* **13**(Pt 3b): 403-8.

Huang, W. Q., J. P. Zhang and S. C. Fu (1990). Differential effects of galactose-induced cataractogenesis on the soluble crystallins of rat lens. *Exp Eye Res* **51**(1): 79-85.

Imajoh, S., H. Kawasaki and K. Suzuki (1986). The amino-terminal hydrophobic region of the small subunit of calcium- activated neutral protease (CANP) is essential for its activation by phosphatidylinositol. *J Biochem (Tokyo)* **99**(4): 1281-4.

Imajoh, S., H. Kawasaki and K. Suzuki (1987). The COOH-terminal E-F hand structure of calcium-activated neutral protease (CANP) is important for the association of subunits and resulting proteolytic activity. *J Biochem (Tokyo)* **101**(2): 447-52.

Ingolia, T. D. and E. A. Craig (1982). Four small Drosophila heat shock proteins are related to each other and to mammalian alpha-crystallin. *Proc Natl Acad Sci U S A* **79**(7): 2360-4.

Inomata, M., K. Nomura, M. Takehana, T. C. Saido, S. Kawashima and S. Shumiya (1997). Evidence for the involvement of calpain in cataractogenesis in Shumiya cataract rat (SCR). *Biochim Biophys Acta* **1362**(1): 11-23.

Ishizaki, Y., M. D. Jacobson and M. C. Raff (1998). A role for caspases in lens fiber differentiation. *J Cell Biol* **140**(1): 153-8.

Ito, H., K. Kamei, I. Iwamoto, Y. Inaguma, D. Nohara and K. Kato (2000). Phosphorylation-induced change of the oligomerization state of alphaB- crystallin. *J Biol Chem.*

Jaworski, C. and G. Wistow (1996). LP2, a differentiation-associated lipid-binding protein expressed in bovine lens. *Biochem J* **320**(Pt 1): 49-54.

Jordan, T., I. Hanson, D. Zaletayev, S. Hodgson, J. Prosser, A. Seawright, N. Hastie and V. van Heyningen (1992). The human PAX6 gene is mutated in two patients with aniridia. *Nat Genet* **1**(5): 328-32.

Jungblut, P. R., A. Otto, J. Favor, M. Lowe, E. C. Muller, M. Kastner, K. Sperling and J. Klose (1998). Identification of mouse crystallins in 2D protein patterns by sequencing and mass spectrometry. Application to cataract mutants. *FEBS Lett* **435**(2-3): 131-7.

Kantorow, M. and J. Piatigorsky (1998). Phosphorylations of alpha A- and alpha B-crystallin. *Int J Biol Macromol* **22**(3-4): 307-14.

Kato, K., H. Shinohara, N. Kurobe, S. Goto, Y. Inaguma and K. Ohshima (1991). Immunoreactive alpha A crystallin in rat non-lenticular tissues detected with a sensitive immunoassay method. *Biochim Biophys Acta* **1080**(2): 173-80.

Kelley, M. J., L. L. David, N. Iwasaki, J. Wright and T. R. Shearer (1993). alpha-Crystallin chaperone activity is reduced by calpain II in vitro and in selenite cataract. *J Biol Chem* **268**(25): 18844-9.

Kelz, M. B., J. R. Kuszak, Y. Yang, W. Ma, C. Steffen, K. Al-Ghoul, Y. J. Zhang, J. Chen, E. J. Nestler and A. Spector (2000). DeltaFosB-induced cataract. *Invest Ophthalmol Vis Sci* **41**(11): 3523-38.

King, C. R. and J. Piatigorsky (1983). Alternative RNA splicing of the murine alpha A-crystallin gene: protein- coding information within an intron. *Cell* **32**(3): 707-12.

Klopp, N., J. Favor, J. Loster, R. B. Lutz, A. Neuhauser-Klaus, A. Prescott, W. Pretsch, R. A. Quinlan, A. Sandilands, G. F. Vrensen and J. Graw (1998). Three murine cataract mutants (Cat2) are defective in different gamma- crystallin genes. *Genomics* **52**(2): 152-8.

Kodama, T. and L. Takemoto (1988). Characterization of disulfide-linked crystallins associated with human cataractous lens membranes. *Invest Ophthalmol Vis Sci* **29**(1): 145-9.

Kono, M., A. C. Sen and B. Chakrabarti (1990). Thermodynamics of thermal and athermal denaturation of gamma- crystallins: changes in conformational stability upon glutathione reaction. *Biochem* **29**(2): 464-70.

Kroone, R. C., G. S. Elliott, A. Ferszt, C. Slingsby, N. H. Lubsen and J. G. Schoenmakers (1994). The role of the sequence extensions in beta-crystallin assembly. *Protein Eng* **7**(11): 1395-9.

Lampi, K. J., Z. Ma, S. R. Hanson, M. Azuma, M. Shih, T. R. Shearer, D. L. Smith, J. B. Smith and L. L. David (1998). Age-related changes in human lens crystallins identified by two- dimensional electrophoresis and mass spectrometry. *Exp Eye Res* **67**(1): 31-43.

Lampi, K. J., Z. Ma, M. Shih, T. R. Shearer, J. B. Smith, D. L. Smith and L. L. David (1997). Sequence analysis of betaA3, betaB3, and betaA4 crystallins completes the identification of the major proteins in young human lens. *J Biol Chem* **272**(4): 2268-75.

Lampi, K. J., Shih, M., Ueda, Y., Shearer, T.R., and David, L.L. (2001). Lens proteomics: analysis of rat crystallin sequences and two-dimensional electrophoresis map. *Invest Ophthalmol Vis Sci* In press.

Lapatto, R., V. Nalini, B. Bax, H. Driessen, P. F. Lindley, T. L. Blundell and C. Slingsby (1991). High resolution structure of an oligomeric eye lens beta-crystallin. Loops, arches, linkers and interfaces in beta B2 dimer compared to a monomeric gamma-crystallin. *J Mol Biol* **222**(4): 1067-83.

le Maire, M., S. Deschamps, J. V. Moller, J. P. Le Caer and J. Rossier (1993). Electrospray ionization mass spectrometry on hydrophobic peptides electroeluted from sodium dodecyl sulfate-polyacrylamide gel electrophoresis application to the topology of the sarcoplasmic reticulum Ca2+ ATPase. *Anal Biochem* **214**(1): 50-7.

Lee, H. J., H. Sorimachi, S. Y. Jeong, S. Ishiura and K. Suzuki (1998). Molecular cloning and characterization of a novel tissue-specific calpain predominantly expressed in the digestive tract. *Biol Chem* **379**(2): 175-83.

Lin, J. S., S. Fitzgerald, Y. Dong, C. Knight, P. Donaldson and J. Kistler (1997). Processing of the gap junction protein connexin50 in the ocular lens is accomplished by calpain. *Eur J Cell Biol* **73**(2): 141-9.

Liu, C., J. Pande, A. Lomakin, O. Ogun and G. B. Benedek (1998). Aggregation in aqueous solutions of bovine lens gamma-crystallins: special role of gamma(s). *Invest Ophthalmol Vis Sci* **39**(9): 1609-19.

Lubsen, N. H., H. J. Aarts and J. G. Schoenmakers (1988). The evolution of lenticular proteins: the beta- and gamma-crystallin super gene family. *Prog Biophys Mol Biol* **51**(1): 47-76.

Lund, A. L., J. B. Smith and D. L. Smith (1996). Modifications of the water-insoluble human lens α-crystallins. *Exp Eye Res* **63**: 661-672.

Ma, H., C. Fukiage, M. Azuma and T. R. Shearer (1998a). Cloning and expression of mRNA for calpain Lp82 from rat lens: splice variant of p94. *Invest Ophthalmol Vis Sci* **39**(2): 454-61.

Ma, H., I. Hata, M. Shih, C. Fukiage, Y. Nakamura, M. Azuma and T. R. Shearer (1999). Lp82 is the dominant form of calpain in young mouse lens. *Exp Eye Res* **68**(4): 447-56.

Ma, H., M. Shih, C. Fukiage, M. Azuma, M. K. Duncan, N. A. Reed, I. Richard, J. S. Beckmann and T. R. Shearer (2000). Influence of specific regions in Lp82 calpain on protein stability, activity, and localization within lens [In Process Citation]. *Invest Ophthalmol Vis Sci* **41**(13): 4232-9.

Ma, H., M. Shih, I. Hata, C. Fukiage, M. Azuma and T. R. Shearer (1998b). Protein for Lp82 calpain is expressed and enzymatically active in young rat lens. *Exp Eye Res* **67**(2): 221-9.

Ma, Z., S. R. Hanson, K. J. Lampi, L. L. David, D. L. Smith and J. B. Smith (1998c). Age-related changes in human lens crystallins identified by HPLC and mass spectrometry. *Exp Eye Res* **67**(1): 21-30.

Maki, M., E. Takano, H. Mori, A. Sato, T. Murachi and M. Hatanaka (1987). All four internally repetitive domains of pig calpastatin possess inhibitory activities against calpains I and II. *FEBS Lett* **223**(1): 174-80.

Matsui, N. M., D. M. Smith-Beckerman and L. B. Epstein (1999). Staining of preparative 2-D gels. Coomassie blue and imidazole-zinc negative staining. *Methods Mol Biol* **112**: 307-11.

McFall-Ngai, M. J., L. L. Ding, L. J. Takemoto and J. Horwitz (1985). Spatial and temporal mapping of the age-related changes in human lens crystallins. *Exp Eye Res* **41**(6): 745-58.

Mellgren, R. L. (1980). Canine cardiac calcium-dependent proteases: Resolution of two forms with different requirements for calcium. *FEBS Lett* **109**(1): 129-33.

Michaeli-Cohen, A., M. Belkin, A. Goldring, M. Rosner and E. I. Assia (1998). Prevention of posterior capsule opacification with the CO2 laser. *Ophthalmic Surg Lasers* **29**(12): 985-90.

Miesbauer, L. R., X. Zhou, Z. Yang, Z. Yang, Y. Sun, D. L. Smith and J. B. Smith (1994). Post-translational modifications of water-soluble human lens crystallins from young adults. *J Biol Chem* **269**(17): 12494-502.

Mitton KP, K. T., Tumminia SJ, Russell P (1996). Cysteine protease activated by expression of HIV-1 protease in transgenic mice.
MIP26 (aquaporin-0) cleavage and cataract formation in vivo and ex vivo. *J Biol Chem* **271**: 31803-31806.

Nakamura, Y., C. Fukiage, M. Azuma and T. R. Shearer (1999a). Oxidation enhances calpain-induced turbidity in young rat lenses. *Curr Eye Res* **19**(1): 33-40.

Nakamura, Y., C. Fukiage, H. Ma, M. Shih, M. Azuma and T. R. Shearer (1999b). Decreased sensitivity of lens-specific calpain Lp82 to calpastatin inhibitor. *Exp Eye Res* **69**(2): 155-62.

Nakamura, Y., C. Fukiage, M. Shih, H. Ma, L. L. David, M. Azuma and T. R. Shearer (2000). Contribution of calpain Lp82-induced proteolysis to experimental cataractogenesis in mice. *Invest Ophthalmol Vis Sci* **41**(6): 1460-6.

Nakayama, H., K. Uchida, F. Shinkai, T. Shinoda, T. Okuyama, K. Seta and T. Isobe (1996). Capillary column high-performance liquid chromatographic-electrospray ionization triple-stage quadrupole mass spectrometric analysis of proteins separated by two-dimensional polyacrylamide gel electrophoresis. Application to cerebellar protein mapping. *J Chromatogr A* **730**(1-2): 279-87.

Narfstrom, K. (1981). Cataract in the West Highland white terrier. *J Small Anim Pract* **22**(7): 467-71.

O'Farrell, P. H. (1975). High resolution two-dimensional electrophoresis of proteins. *J Biol Chem* **250**(10): 4007-21.

Ortwerth, B. J. and P. R. Olesen (1989). Studies on the nature of the water-insoluble fraction from aged bovine lenses. *Exp Eye Res* **48**(5): 605-19.

Pereira, P. C., J. S. Ramalho, C. J. Faro and M. C. Mota (1994). Age-related changes in normal and cataractous human lens crystallins, separated by fast-performance liquid chromatography. *Ophthalmic Res* **26**(3): 149-57.

Piatigorsky, J. (1984). Lens crystallins and their gene families. *Cell* **38**(3): 620-1.

Pierscionek, B. and R. C. Augusteyn (1988). Protein distribution patterns in concentric layers from single bovine lenses: changes with development and ageing. *Curr Eye Res* **7**(1): 11-23.

Rabilloud, T. (1999). Silver staining of 2-D electrophoresis gels. *Methods Mol Biol* **112**: 297-305.

Rao, G. N., B. Sadasivudu and E. Cotlier (1983). Studies on glutathione S-transferase, glutathione peroxidase and glutathione reductase in human normal and cataractous lenses. *Ophthalmic Res* **15**(4): 173-9.

Reneker, L. W., D. W. Silversides, L. Xu and P. A. Overbeek (2000). Formation of corneal endothelium is essential for anterior segment development - a transgenic mouse model of anterior segment dysgenesis. *Development* **127**(3): 533-42.

Richard, I., O. Broux, V. Allamand, F. Fougerousse, N. Chiannilkulchai, N. Bourg, L. Brenguier, C. Devaud, P. Pasturaud, C. Roudaut and et al. (1995). Mutations in the proteolytic enzyme calpain 3 cause limb-girdle muscular dystrophy type 2A. *Cell* **81**(1): 27-40.

Robinson, M. L. and P. A. Overbeek (1996). Differential expression of alpha A- and alpha B-crystallin during murine ocular development. *Invest Ophthalmol Vis Sci* **37**(11): 2276-84.

Russell, P. and C. Chambers (1990). Interaction of an altered beta-crystallin with other proteins in the Philly mouse lens. *Exp Eye Res* **50**(6): 683-7.

Sato, S., K. Mori, M. Wyman and P. F. Kador (1998). Dose-dependent prevention of sugar cataracts in galactose-fed dogs by the aldose reductase inhibitor M79175. *Exp Eye Res* **66**(2): 217-22.

Schey, K. L., J. G. Fowler, T. R. Shearer and L. David (1999). Modifications to rat lens major intrinsic protein in selenite-induced cataract. *Invest Ophthalmol Vis Sci* **40**(3): 657-67.

Sharma, K. K. and K. Kester (1996). Peptide hydrolysis in lens: role of leucine aminopeptidase, aminopeptidase III, prolyloligopeptidase and acylpeptidehydrolase. *Curr Eye Res* **15**(4): 363-9.

Sharma, K. K., K. Kester and N. Elser (1996). Identification of new lens protease(s) using peptide substrates having in vivo cleavage sites. *Biochem Biophys Res Commun* **218**(1): 365-70.

Shearer, T. R., H. Ma, C. Fukiage and M. Azuma (1997). Selenite nuclear cataract: review of the model. *Mol Vis* **3**: 8.

Shearer, T. R., H. Ma, M. Shih, I. Hata, C. Fukiage, Y. Nakamura and M. Azuma (1998). Lp82 calpain during rat lens maturation and cataract formation. *Curr Eye Res* **17**(11): 1037-43.

Shearer, T. R., M. Shih, M. Azuma and L. L. David (1995). Precipitation of crystallins from young rat lens by endogenous calpain. *Exp Eye Res* **61**(2): 141-50.

Shemyakin, M. M., Y. A. Ovchinnikov, A. A. Kiryushkin, E. I. Vinogradova, A. I. Miroshnikov, Y. B. Alakhov, V. M. Lipkin, Y. B. Shvetsov, N. S. Wulfson, B. V. Rosinov, V. N. Bochkarev and V. M. Burikov (1966). Mass spectrometric determination of the amino-acid sequence of peptides. *Nature* **211**(47): 361-6.

Shih, M., K. J. Lampi, T. R. Shearer and L. L. David (1998). Cleavage of beta crystallins during maturation of bovine lens. *Mol Vis* **4**: 4.

Siezen, R. J., M. R. Fisch, C. Slingsby and G. B. Benedek (1985). Opacification of gamma-crystallin solutions from calf lens in relation to cold cataract formation. *Proc Natl Acad Sci U S A* **82**(6): 1701-5.

Siezen, R. J., E. Wu, E. D. Kaplan, J. A. Thomson and G. B. Benedek (1988). Rat lens gamma-crystallins. Characterization of the six gene products and their spatial and temporal distribution resulting from differential synthesis. *J Mol Biol* **199**(3): 475-90.

Sinha, D., N. Esumi, C. Jaworski, C. A. Kozak, E. Pierce and G. Wistow (1998). Cloning and mapping the mouse Crygs gene and non-lens expression of [gamma]S-crystallin. *Mol Vis* **4**: 8.

Slingsby, C. and O. A. Bateman (1990). Quaternary interactions in eye lens beta-crystallins: basic and acidic subunits of beta-crystallins favor heterologous association. *Biochem* **29**(28): 6592-9.

Smith, R. S., N. L. Hawes, B. Chang, T. H. Roderick, E. C. Akeson, J. R. Heckenlively, X. Gong, X. Wang and M. T. Davisson (2000). Lop12, a mutation in mouse Crygd causing lens opacity similar to human Coppock cataract. *Genomics* **63**(3): 314-20.

Sorimachi, H., S. Imajoh-Ohmi, Y. Emori, H. Kawasaki, S. Ohno, Y. Minami and K. Suzuki (1989). Molecular cloning of a novel mammalian calcium-dependent protease distinct from both m- and mu-types. Specific expression of the mRNA in skeletal muscle. *J Biol Chem* **264**(33): 20106-11.

Sorimachi, H., S. Ishiura and K. Suzuki (1993a). A novel tissue-specific calpain species expressed predominantly in the stomach comprises two alternative splicing products with and without Ca(2+)-binding domain. *J Biol Chem* **268**(26): 19476-82.

Sorimachi, H., T. C. Saido and K. Suzuki (1994). New era of calpain research. Discovery of tissue-specific calpains. *FEBS Lett* **343**(1): 1-5.

Sorimachi, H., N. Toyama-Sorimachi, T. C. Saido, H. Kawasaki, H. Sugita, M. Miyasaka, K. Arahata, S. Ishiura and K. Suzuki (1993b). Muscle-specific calpain, p94, is degraded by autolysis immediately after translation, resulting in disappearance from muscle. *J Biol Chem* **268**(14): 10593-605.

Spector, A. and W. H. Garner (1981). Hydrogen peroxide and human cataract. *Exp Eye Res* **33**(6): 673-81.

Srivastava, O. P. and K. Srivastava (1998). Degradation of gamma D- and gamma s-crystallins in human lenses. *Biochem Biophys Res Commun* **253**(2): 288-94.

Srivastava, O. P., K. Srivastava and V. Harrington (1999). Age-related degradation of betaA3/A1-crystallin in human lenses. *Biochem Biophys Res Commun* **258**(3): 632-8.

Srivastava, O. P., K. Srivastava and C. Silney (1996). Levels of crystallin fragments and identification of their origin in water soluble high molecular weight (HMW) proteins of human lenses. *Curr Eye Res* **15**(5): 511-20.

Steinberg, T. H., L. J. Jones, R. P. Haugland and V. L. Singer (1996). SYPRO orange and SYPRO red protein gel stains: one-step fluorescent staining of denaturing gels for detection of nanogram levels of protein. *Anal Biochem* **239**(2): 223-37.

Stolen, C. M. and A. E. Griep (2000). Disruption of lens fiber cell differentiation and survival at multiple stages by region-specific expression of truncated FGF receptors. *Dev Biol* **217**(2): 205-20.

Suzuki, K., S. Tsuji, S. Kubota, Y. Kimura and K. Imahori (1981). Limited autolysis of Ca2+-activated neutral protease (CANP) changes its sensitivity to Ca2+ ions. *J Biochem (Tokyo)* **90**(1): 275-8.

Takano, E., M. Maki, H. Mori, M. Hatanaka, T. Marti, K. Titani, R. Kannagi, T. Ooi and T. Murachi (1988). Pig heart calpastatin: identification of repetitive domain structures and anomalous behavior in polyacrylamide gel electrophoresis. *Biochem* **27**(6): 1964-72.

Takemoto, L. (1994). Release of alpha-A sequence 158-173 correlates with a decrease in the molecular chaperone properties of native alpha-crystallin [letter]. *Exp Eye Res* **59**(2): 239-42.

Takemoto, L., T. Emmons and J. Horwitz (1993). The C-terminal region of alpha-crystallin: involvement in protection against heat-induced denaturation [see comments]. *Biochem J* **294**(Pt 2): 435-8.

Takemoto, L. J. (1995). Identification of the in vivo truncation sites at the C-terminal region of alpha-A crystallin from aged bovine and human lens. *Curr Eye Res* **14**(9): 837-41.

Takemoto, L. J. (1996). Differential phosphorylation of alpha-A crystallin in human lens of different age. *Exp Eye Res* **62**(5): 499-504.

Taketo, M., A. C. Schroeder, L. E. Mobraaten, K. B. Gunning, G. Hanten, R. R. Fox, T. H. Roderick, C. L. Stewart, F. Lilly, C. T. Hansen and et al. (1991). FVB/N: an inbred mouse strain preferable for transgenic analyses. *Proc Natl Acad Sci U S A* **88**(6): 2065-9.

Tamada, Y., C. Fukiage, Y. Nakamura, M. Azuma, Y. H. Kim and T. R. Shearer (2000). Evidence for apoptosis in the selenite rat model of cataract. *Biochem Biophys Res Commun* **275**(2): 300-6.

Taylor, H. R. (1999). Epidemiology of age-related cataract. *Eye* **13**(Pt 3b): 445-8.

Truscott, R. J. (2000). Age-related nuclear cataract: A lens transport problem. *Ophthalmic Res* **32**(5): 185-94.

Tsen, C. C. and A. L. Tappel (1958). Catalytic oxidation of glutathione and other sulfhydryl compunds by selenite. *J Biol Chem* **233**: 1230-32.

van Vreeswijk, H. and J. H. Pameyer (1998). Inducing cataract in postmortem pig eyes for cataract surgery training purposes. *J Cataract Refract Surg* **24**(1): 17-8.

Varnum, M. D., L. L. David and T. R. Shearer (1989). Age-related changes in calpain II and calpastatin in rat lens. *Exp Eye Res* **49**(6): 1053-65.

Voorter, C. E., W. A. De Haard-Hoekman, M. M. Hermans, H. Bloemendal and W. W. De Jong (1990). Differential synthesis of crystallins in the developing rat eye lens. *Exp Eye Res* **50**(4): 429-37.

Wang, K., M. A. Gawinowicz and A. Spector (2000). The effect of stress on the pattern of phosphorylation of alphaA and alphaB crystallin in the rat lens [In Process Citation]. *Exp Eye Res* **71**(4): 385-93.

Wawrousek, E. F., A. B. Chepelinsky, J. B. McDermott and J. Piatigorsky (1990). Regulation of the murine alpha A-crystallin promoter in transgenic mice. *Dev Biol* **137**(1): 68-76.

Wen, Y., G. W. Li, P. Chen, E. Wong and I. Bekhor (1995). Lens epithelial cell mRNA, II. Expression of a mRNA encoding a lipid- binding protein in rat lens epithelial cells. *Gene* **158**(2): 269-74.

Werten, P. J., J. A. Carver, R. Jaenicke and W. W. de Jong (1996). The elusive role of the N-terminal extension of beta A3- and beta A1-crystallin. *Protein Engineering* **9**(11): 1021-8.

Werten, P. J., R. A. Lindner, J. A. Carver and W. W. de Jong (1999). Formation of betaA3/betaB2-crystallin mixed complexes: involvement of N- and C-terminal extensions. *Biochim Biophys Acta* **1432**(2): 286-92.

Werten, P. J., G. J. Stege and W. W. de Jong (1999). The short 5' untranslated region of the betaA3/A1-crystallin mRNA is responsible for leaky ribosomal scanning. *Mol Biol Rep* **26**(3): 201-5.

Werten, P. J., E. Vos and W. W. De Jong (1999). Truncation of betaA3/A1-crystallin during aging of the bovine lens; possible implications for lens optical quality. *Exp Eye Res* **68**(1): 99-103.

Wilkins, M. R., J. C. Sanchez, A. A. Gooley, R. D. Appel, I. Humphery-Smith, D. F. Hochstrasser and K. L. Williams (1996). Progress with proteome projects: why all proteins expressed by a genome should be identified and how to do it. *Biotechnol Genet Eng Rev* **13**: 19-50.

Yoshida, H., T. Murachi and I. Tsukahara (1984a). Degradation of actin and vimentin by calpain II, a Ca2+-dependent cysteine proteinase, in bovine lens. *FEBS Lett* **170**(2): 259-62.

Yoshida, H., T. Murachi and I. Tsukahara (1984b). Limited proteolysis of bovine lens alpha-crystallin by calpain, a Ca2+- dependent cysteine proteinase, isolated from the same tissue. *Biochim Biophys Acta* **798**(2): 252-9.

Yoshida, H., Murachi, T., and Tsukahara, I. (1985). Distribution of calpain I, calpain II, and calpastatin in bovine lens. *Invest Ophthalmol Vis Sci* **26**: 953-956.

Yoshida, H., Yumoto, N., Tsukahara, I., and Murachi, T. (1986). The degradation of α-crystallin at its carboxyl-terminal portion by calpain in bovine lens. *Invest Ophthalmol Vis Sci* **27**: 1269-1273.

Young, R. W. and H. W. Fulhorst (1966). Regional differences in protein synthesis within the lens of the rat. *Invest Ophthalmol* **5**(3): 288-97.

Zhang, W. Z. and R. C. Augusteyn (1994). Ageing of glutathione reductase in the lens. *Exp Eye Res* **59**(1): 91-5.